Carbon TerraVault II

Class VI Permit Application

Narrative Report

Submitted to:

U.S. Environmental Protection Agency Region 9

San Francisco, CA

Prepared by:

27200 Tourney Road, Suite 200
Santa Clarita, CA 91355
(888) 848-4754

Table of Contents

List of Attachments

List of Appendices

Document Version history

Version	Submission Date	File Name	Description of Change
1	5/3/2022	Att A - CTV II Project Narrative	Original submission as part of CTV II storage project
2	8/4/2022	Att A - CTV II Project Narrative V2	Updated submission to address EPA Administrative review request for additional information dated 6/9/2022. Updated document, attachments and appendices to cover requests on additional permits required, Tribes to be consulted, Well Construction, Site characterization & Operational info
3	12/14/2022	Att A – CTV II Project Narrative V3	Updated submission to address EPA Administrative review request for additional information dated 9/21/2022, and for project expansion from two to five injectors
4	2/2/2023	Att A – CTV II Project Narrative V3.1	Updated document to address EPA request.

Class VI Permit Application Narrative
40 CFR 146.82(a)
CTV II

1.0 Project Background and Contact Information

Carbon TerraVault Holdings LLC (CTV), a wholly owned subsidiary of California Resources Corporation (CRC), proposes to construct and operate five CO_2 geologic sequestration wells at CTV II, near the Union Island Field (UIF), located in San Joaquin County, California. This application was prepared in accordance with the U.S. Environmental Protection Agency's (EPA's) Class VI, in Title 40 of the Code of Federal Regulations (40 CFR 146.81) under the Safe Drinking Water Act (SDWA). CTV is not requesting an injection depth waiver or aquifer exemption expansion.

CTV will obtain the required authorizations from applicable local and state agencies, including the associated environmental review process under the California Environmental Quality Act. Appendix 1 outlines potential local, state and federal permits and authorizations. The project wells and facilities will not be located on Indian Lands. Federal act considerations and additional consultation, which includes the Endangered Species Act, the National Historic Preservation Act and consultations with Tribes in the area of review, are presented in "Appendix 2: Applicable Federal Acts and Consultation".

CTV forecasts the potential CO_2 stored in the Winters Formation at 0.97 million tonnes annually for 23 years. The anthropogenic CO_2 will be sourced from direct air capture and / or other CO_2 sources in the CTV II area.

The Carbon TerraVault II (CTV II) storage site is located in the Sacramento Valley, 20 miles southeast of the Rio Vista Field near Stockton, California (**Figure 2.1-1**) within the southern Sacramento Basin. The project will consist of five injectors, surface facilities, and monitoring wells. This supporting documentation applies to the five injection wells.

CTV will actively communicate project details and submitted regulatory documents to County and State agencies:

1. Geologic Energy Management Division (CalGEM)
   Acting District Deputy
   Chris Jones (661)-322-4031

2. CA Assembly District 13
   Assemblyman Carlos Villapudua
   31 East Channel Street – Suite 306
   Stockton, CA 95202
   (209) 948-7479

3. San Joaquin County
   District 3 Supervisor –Tom Patti
   (209) 468-3113
   tpatti@sjgov.org

4. San Joaquin County Community Development
   Director – David Kwong
   1810 East Hazelton Avenue
   Stockton, CA 95205
   (209) 468-3121

5. San Joaquin Council of Governments
   Executive Director – Diane Nguyen
   555 East Weber Avenue
   Stockton, CA 95202
   (209) 235-0600

6. Region 9 Environmental Protection Agency
   75 Hawthorne Street
   San Francisco, CA 94105
   (415) 947-8000

2.0 Site Characterization

2.1 Regional Geology, Hydrogeology, and Local Structural Geology [40 CFR 146.82(a)(3)(vi)]

2.1.1 Field History

The CTV II storage site overlaps the Union Island Gas Field which was discovered in 1972 by Union Oil Company of California. Located in a region of prolific gas production, approximately 20 miles southeast of major gas field Rio Vista, the Union Island Field was one of the largest dry gas fields in California (**Figure 2.1-1**). Commercial production from its gas reservoir, the Winters Formation, began in 1976 until the quick decline in early 1988 (Leong 1994). This formation is now being repurposed for CO_2 storage.

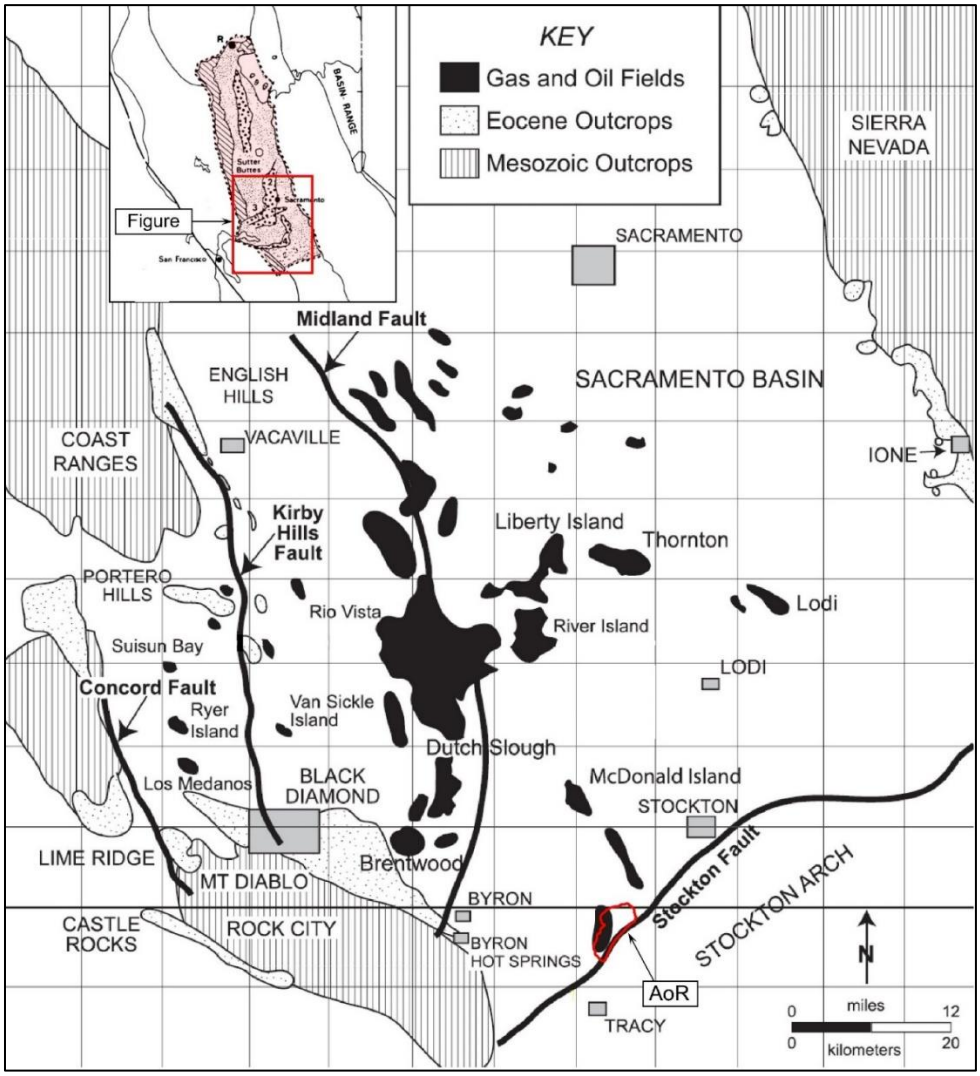

Figure 2.1-1. Location map of the Union Island field with the proposed injection AoR in relation to the Sacramento Basin.

2.1.2 Geology Overview

The Union Island Field lies within the Sacramento Basin in northern California (**Figure 2.1-2**). The Sacramento Basin is the northern, asymmetric sub-basin of the larger, Great Valley Forearc. This portion of the basin, that contains a steep western flank and a broad, shallow eastern flank, spans approximately 240 miles in length and 60 miles wide (Magoon 1995).

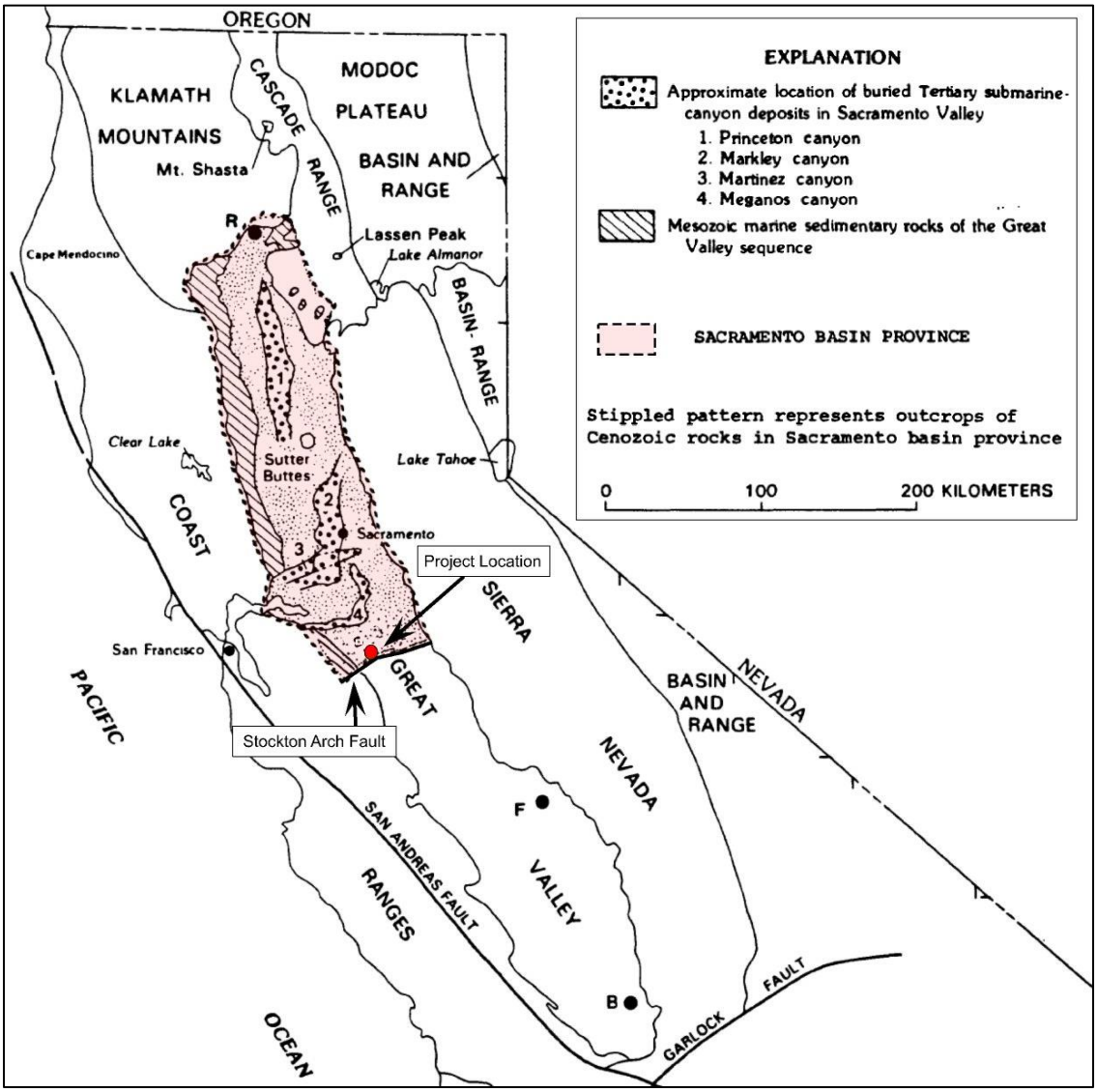

Figure 2.1-2. Location map of California modified from (Beyer, 1988) & (Sullivan, 2012). The Sacramento Basin regional study area is outlined by a dashed black line. B – Bakersfield; F – Fresno; R – Redding.

2.1.2.1 Basin Structure

The Great Valley was developed during mid to late Mesozoic time. The advent of this development occurred under convergent-margin conditions via eastward, Farallon Plate subduction, of oceanic crust

beneath the western edge of North America (Beyer 1988). The convergent, continental margin, that characterized central California during the Late Jurassic through Oligocene time, was later replaced by a transform-margin tectonic system. This occurred as a result of the northward migration of the Mendocino Triple Junction (from Baja California to its present location off the coast of Oregon), located along California's coast (**Figure 2.1-3**). Following this migrational event was the progressive cessation of both subduction and arc volcanism as the progradation of a transform fault system moved in as the primary tectonic environment (Graham 1984). The major current day fault, the San Andreas, intersects most of the Franciscan subduction complex, which consists of the exterior region of the extinct convergent-margin system (Graham 1984).

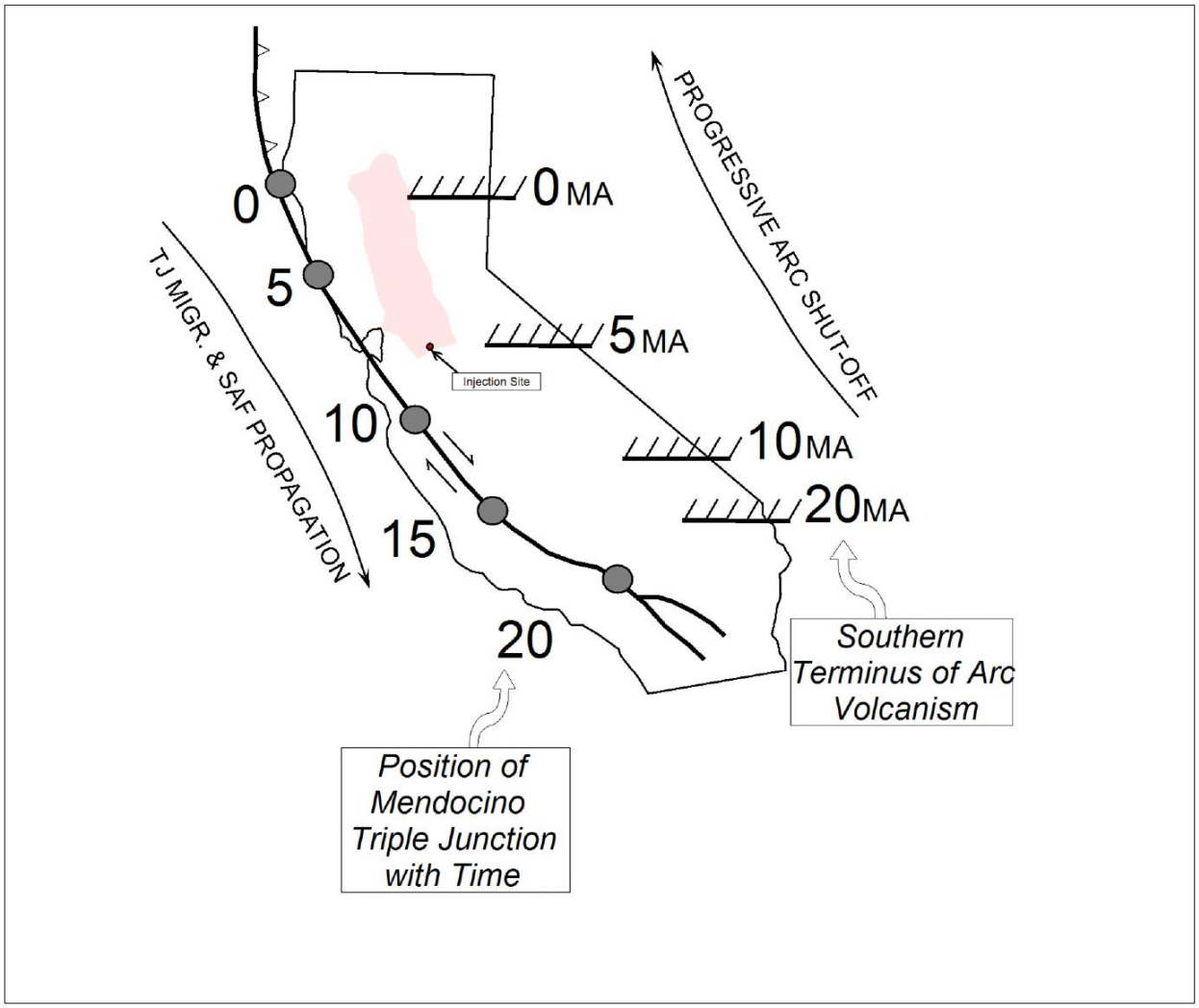

2.1-3. Migrational position of the Mendocino triple junction (Connection point of the Gorda, North American and Pacific plates) on the west and migrational position of Sierran arc volcanism in the east (Graham, 1984). Figure indicates space-time relations of major continental-margin tectonic events in California during Miocene.

2.1.2.2 Basin Stratigraphy

The structural trough that developed subsequent to these tectonic events, that became named the Great Valley, became a depocenter for eroded sediment and thereby currently contains a thick infilled sequence of sedimentary rocks. These sedimentary formations range in age from Jurassic to Holocene. The first deposits occurred as an ancient seaway and through time were built up by the erosion of the surrounding structures. The basin is constrained on the west by the Coast Range Thrust, on the north by the Klamath Mountains, on the east by the Cascade Range and Sierra Nevada and the south by the Stockton Arch Fault (**Figure 2.1-2**). The west, Coastal Range boundary was created by uplifted rocks of the Franciscan Assemblage (**Figure 2.1-3**). The Sierra Nevadas, that make up the eastern boundary, are a result of a chain of ancient volcanos.

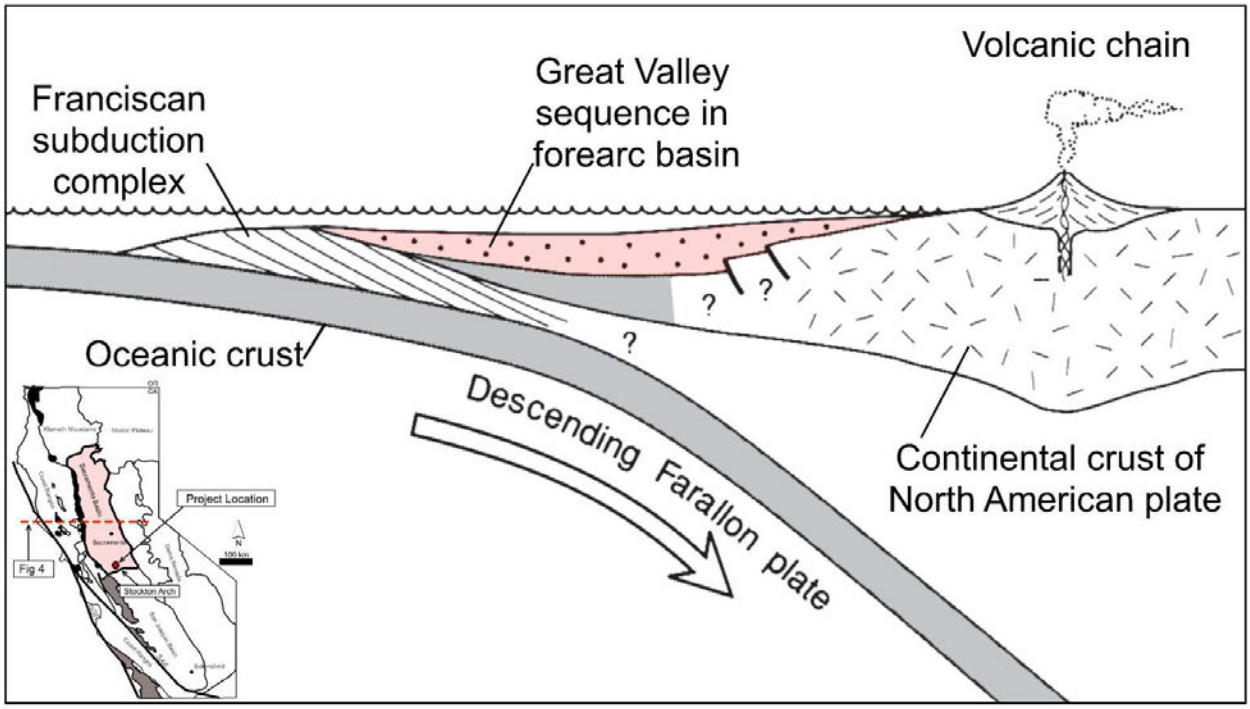

Figure 2.1-4. Schematic W-E cross-section of California, highlighting the Sacramento Basin, as a continental margin during late Mesozoic. The oceanic Farallon plate was forced below the west coast of the North American continental plate.

Basin development is broken out into evolutionary stages at the end of each time-period of the arc-trench system, from Jurassic to Neogene, in **Figure 2.1-5**. As previously stated, sediment infill began as an ancient seaway and was later sourced from the erosion of the surrounding structures. Due to the southward tilt of the basin, sedimentation thickens towards the southern end near the Stockton Arch fault which bounds the SE portion of the Area of Review (AoR), creating sequestration quality sandstones. Sedimentary infill consists of Cretaceous-Paleogene fluvial, deltaic, shelf and slope sediments.

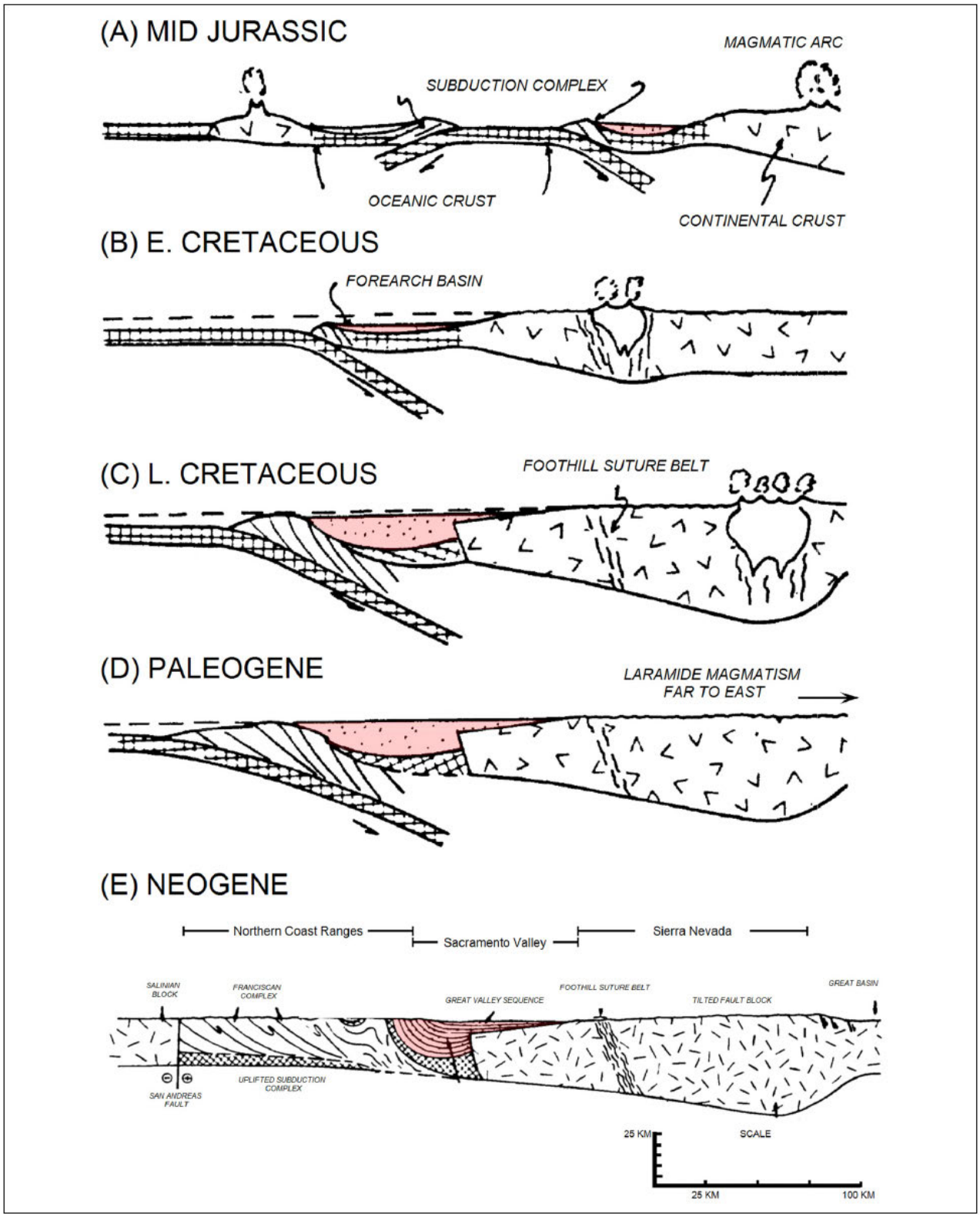
(A) MID JURASSIC
MAGMATIC ARC
SUBDUCTION COMPLEX
OCEANIC CRUST
CONTINENTAL CRUST
(B) E. CRETACEOUS
FOREARCH BASIN
(C) L. CRETACEOUS
FOOTHILL SUTURE BELT
(D) PALEOGENE
LARAMIDE MAGMATISM
FAR TO EAST
(E) NEOGENE
Northern Coast Ranges
Sacramento Valley
Sierra Nevada
SALINIAN BLOCK
FRANCISCAN COMPLEX
GREAT VALLEY SEQUENCE
FOOTHILL SUTURE BELT
TILTED FAULT BLOCK
GREAT BASIN
SAN ANDREAS FAULT
UPLIFTED SUBDUCTION COMPLEX
25 KM
SCALE
25 KM
100 KM

Figure 2.1-5. Evolutionary stages showing the history of the arc-trench system of California from Jurassic (A) to Neogene (E) (modified from Beyer, 1988).

In the southern Sacramento Basin the Winters Formation is a thick-bedded sandstone that creates the principal gas reservoir facies in the project area. This field is a structural-stratigraphic trap set up by both structural closure against the Stockton Arch fault and Winters Formation pinchout to the NE. The Stockton Arch fault is a NE trending thrust fault that dips to the SE and produces from its footwall on the west end of the fault.

2.1.3 Geological Sequence

Figure 2.1-6 is a schematic representing the local stratigraphy of the project area, highlighting the west side of the Stockton Arch fault and proposed zone of injection. The injection wells will inject CO_2 into the Cretaceous aged Winters Formation, located in the Stockton Arch footwall. The footwall injection depth is approximately 9,500 TVD. The injection zone has a known reservoir capacity demonstrated by historic gas production. Cumulative production is 292 (71 North only) BCF of gas and 3.4 (1.4 North only) MMSTB water, lowering reservoir pressure from 5,040 psi to 1,200 psi.

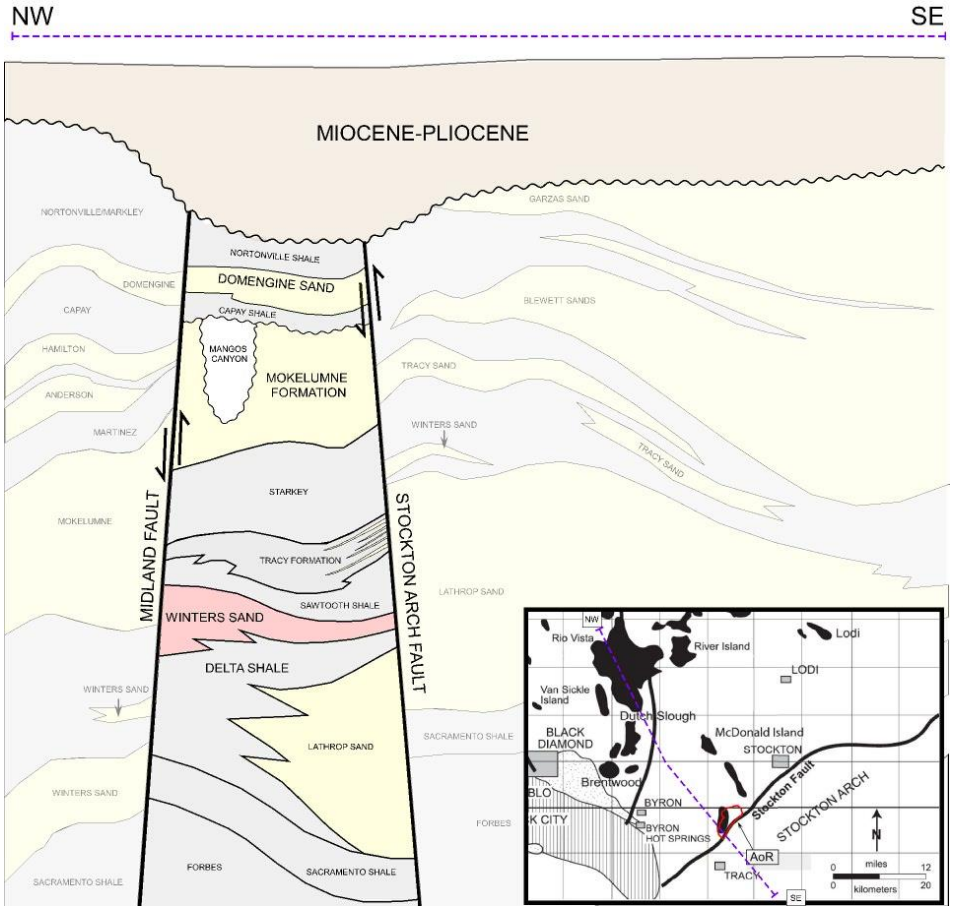

Figure 2.1-6. Schematic northwest to southeast cross section in the Sacramento basin, intersecting the project AoR.

Following its deposition, the Winters Formation was buried under the Sawtooth Shale which carries throughout most of its distribution. This formation, combined with the Starkey formation acts as the upper confining zone for the Winters Reservoir due to its low permeability, thickness, and regional continuity that spans beyond the AoR. Above the Sawtooth Shale are several alternating sand-shale sequences: the Tracy Formation, Starkey Shale, the H&T Shale, Mokelumne River Formation, Capay Shale, Domengine Sandstone and Nortonville Shale.

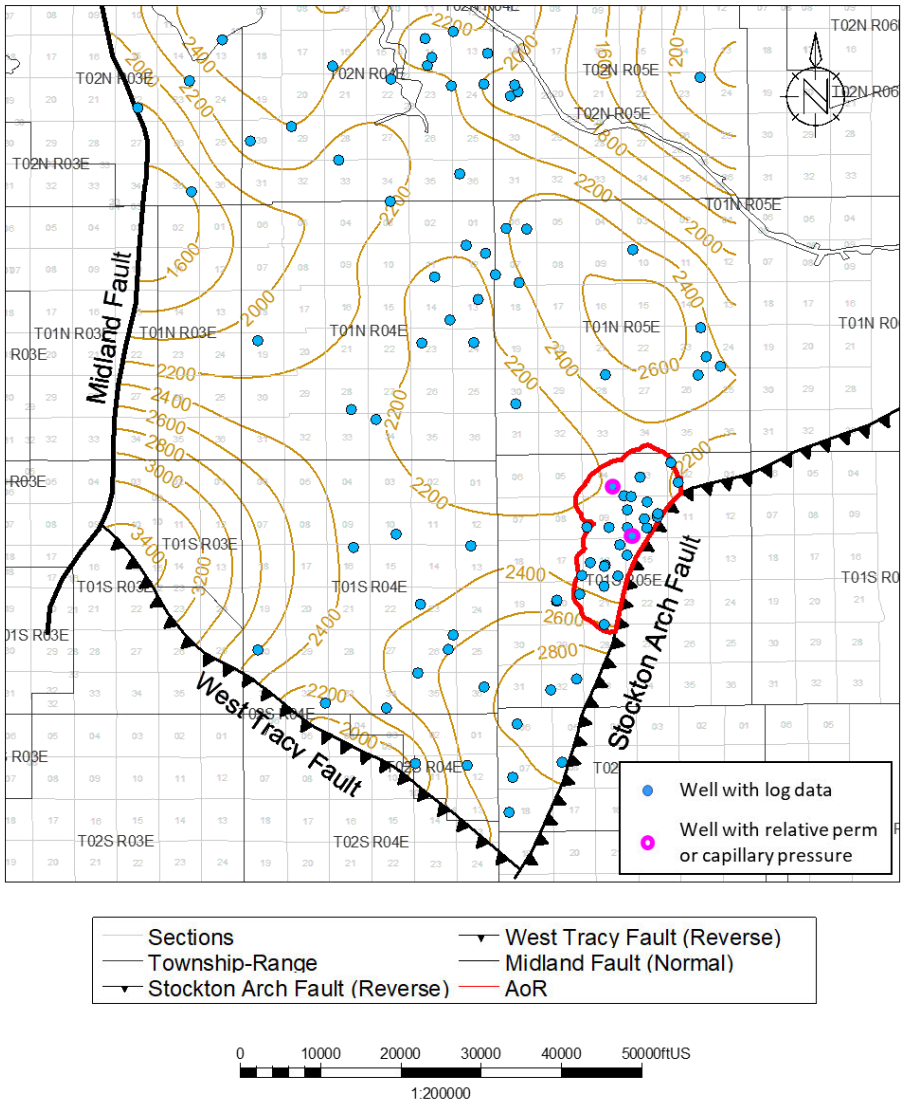

FIGURE 2.1-7. Starkey-Sawtooth Shale isopach map for the greater storage project area. Wells shown as blue dots on the map penetrate the Starkey-Sawtooth Shale and have open-hole logs. Wells with relative permeability or capillary pressure data are shown as magenta circles.

2.2 Maps and Cross Sections of the AoR [40 CFR 146.82(a)(2), 146.82(a)(3)(i)]

2.2.1 Data

To date, 37 wells have been drilled to various depths within the Union Island Field (**Figure 2.2-1**). Although there is not an extensive database of wells in this field, seismic coverage, core and reservoir performance data such as production and pressure give an adequate description of the reservoir.

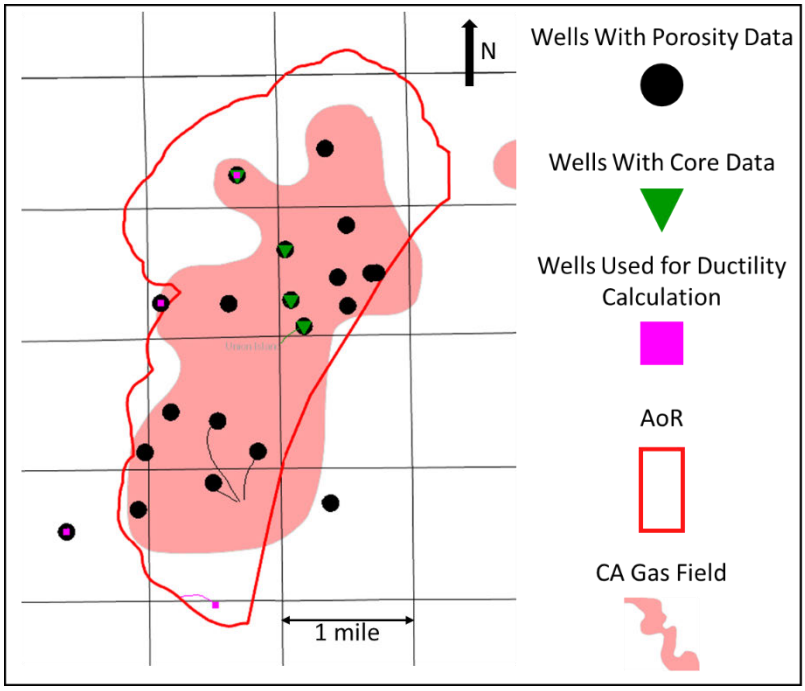

Figure 2.2-1. Wells drilled in the Union Island Field with porosity data are shown in black, wells with core are shown in green and wells used for ductility calculation are shown in pink.

Well data are used in conjunction with three-dimensional (3D) and two-dimensional (2D) seismic to define the structure and stratigraphy of the injection zone and confining zone (**Figure 2.2-2**). **Figure 2.2-3** shows outlines of the seismic data used and the area of the structural framework that was built from these seismic surveys. The 3D data in this area were merged using industry standard pre-stack time migration in 2013, allowing for a seamless interpretation across them. The 2D data used for this model were tied to this 3D merge in both phase and time to create a standardized datum for mapping purposes. The following layers were mapped across the 2D and 3D data:

- A shallow marker to aid in controlling the structure of the velocity field
- The approximate base of the Valley Springs Formation which is unconformable with the Eocene strata below
- Domengine
- Mokelumne River
- H&T Shale
- Winters
- Forbes

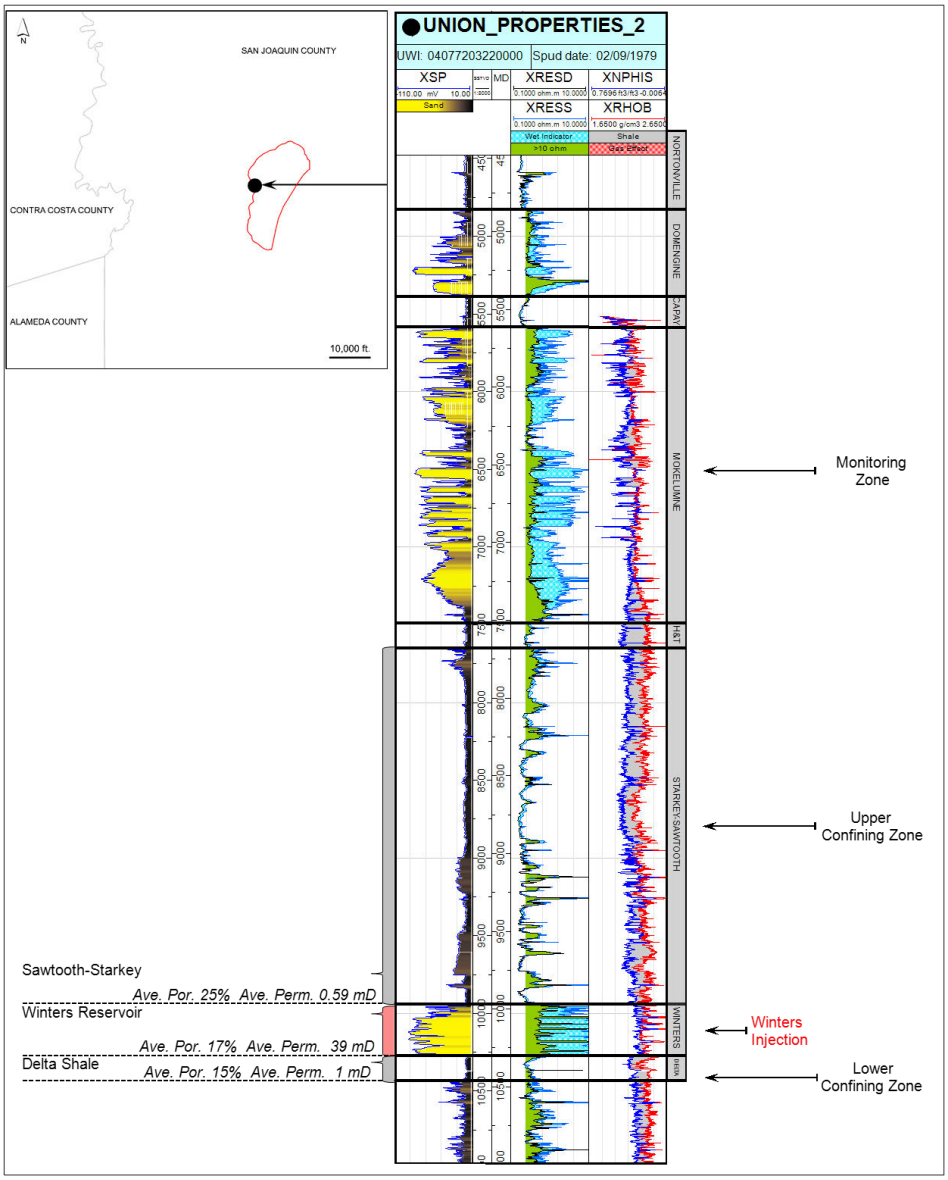

Figure 2.2-2. Type well from the western edge of the AoR boundary showing average rock properties used in the model for confining and injection zones.

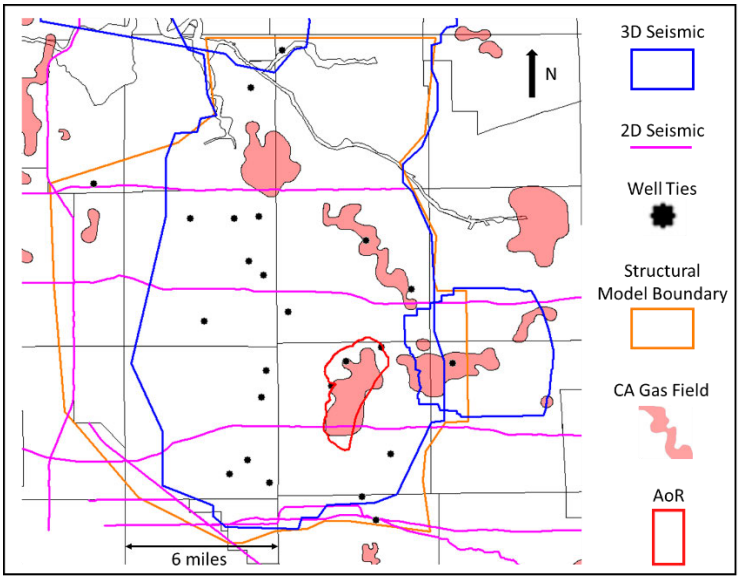

Figure 2.2-3. Summary map and area of seismic data used to build structural model. Both 3D surveys were acquired in 1998 and reprocessed in 2013. The 2D seismic were acquired between 1980 and 1985. California gas fields are shown for reference.

The top of the Cretaceous Forbes Formation was used as the base of this structural model due to the depth and imaging of Basement not being sufficient to create a reliable and accurate surface. Interpretation of these layers began with a series of well ties at well locations shown in **Figure 2.2-3**. These well ties create an accurate relationship between wells which are in depth and the seismic which is in time. The layers listed above were then mapped in time and gridded on a 550 by 550-foot cell basis. Alongside this mapping was the interpretation of any faulting in the area which is discussed further in the Faults and Fracture section of this document.

The gridded time maps and a sub-set of the highest quality well ties and associated velocity data are then used to create a three-dimensional velocity model. This model is guided between well control by the time horizons and is iterated to create an accurate and smooth function. The velocity model is used to convert both the gridded time horizons and interpreted faults into the depth domain. The result is a series of depth grids of the layers listed above which are then used in the next step of this process.

The depth horizons are the basis of a framework which uses conformance relationships to create a series of depth grids that are controlled by formation well tops picked on well logs. The grids are used as structural control between these well tops to incorporate the detailed mapping of the seismic data. These grids incorporate the thickness of zones from well control and the formation strike, dip, and any fault offset from the seismic interpretation. The framework is set up to create the following depth grids for input in to the geologic and plume growth models:

- Nortonville Shale
- Domengine
- Domengine Top Sand
- Capay Shale

- Mokelumne River
- H&T Shale
- Winters
- Delta Shale
- Delta Shale Base

2.2.2 Stratigraphy

Major stratigraphic intervals within the field, from oldest to youngest, include the Delta Shale (L. Cretaceous), Winters Formation (L. Cretaceous), Sawtooth Shale (L. Cretaceous), Tracy Formation (L. Cretaceous), Starkey Shale (L. Cretaceous), H&T Shale (L. Cretaceous), Mokelumne River Formation (L. Cretaceous-E. Paleocene), Capay Shale (E. Eocene), Domengine Sandstone (L. Eocene), and Nortonville Shale (L. Eocene) (**Figure 2.2-4**). Of these formations the regional upper seal rock that partitions the reservoir consists of the Starkey - Sawtooth Shale. These combined formations create an average thickness of ~ 2,240 ft. throughout the AoR. Also shown in **Figure 2.2-4** is a basin-wide unconformity separating overlying Paleocene and younger beds from Cretaceous rocks. This unconformity resides above the Mokelumne River Formation at the base of the Capay shale, creating a secondary seal between reservoir and USDW. During Paleogene time, marine and deltaic deposits continued in the basin until the activity of the Stockton Arch began to separate Sacramento Basin from the San Joaquin basin in late Paleogene time (Downey 2010).

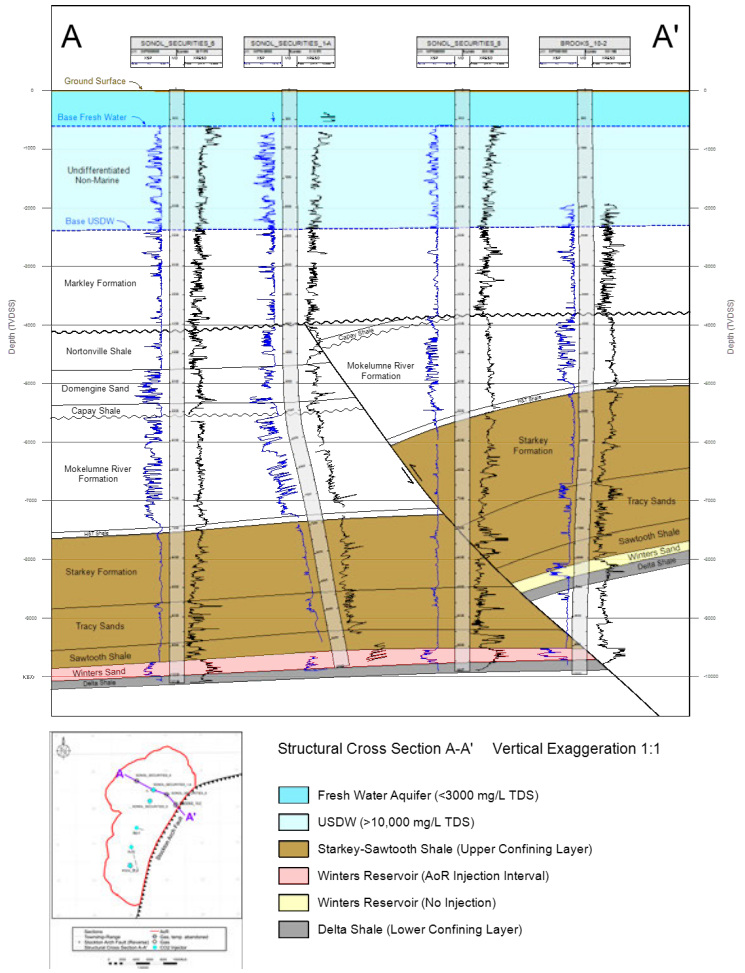

Figure 2.2-4. Dip cross section showing stratigraphy and lateral continuity of major formations across the project area. Section is representative of formations and sand continuity at all five CO2 injector locations.

2.2.2.1 Delta Shale

The underlying Delta Shale Formation serves as the lower confining zone for the Winters Reservoir. This formation consists of approximately 157 feet of shale barrier. This shale has an average permeability of 0.04mD and porosity of 14.7% (as defined in section 2.4.2). Due to the sparse well penetrations and subsequent lack of log data, this formation has been primarily mapped using seismic data as stated above.

2.2.2.2 Winters Reservoir (injection zone)

Within the project area, the Winters Reservoir is a generally upward-fining/thinning sequence that lies perpendicular to the depositional slope and thickens towards the basin. This formation was deposited as coalesced channels which formed at the base of the slope, on the upper channelized portion of a sandy suprafan.

This Upper Cretaceous aged formation is a deep-water sandstone with thinly interbedded sandstone and shale which overlie the Delta shale. These deposits were part of a large deep-sea fan system that were sourced from granitic areas in the Sierra Nevada and fed into the system via submarine canyons and

feeder channels (Williamson 1981). This creates a blocky, sand-rich reservoir that extends to as much as 1,500 ft thick in the center of the basin. Along the basin axis this sandy suprafan stacks up due to the high rate of sand supply relative to the size of the basin as well as the depositional nature of the fans at basin margins (Williamson 1981). Moving towards the upslope portion of the fan system is the Union Island Field where the Winters Formation is closer to 250 ft thick. Core data is supportive of a channelized portion of the suprafan lobe (Williamson 1981). The Winters isochore map (**Figure 2.2-5a**) shows the channel system trending southwest and the 2° dip to the west can be seen on the structure map (**Figure 2.2-5b**). The Winters Formation has a gross thickness of approximately 256 ft. within the model boundary with sand porosity and permeability averages of 18.9% and 13 mD, respectively, as defined in section 2.4.2.

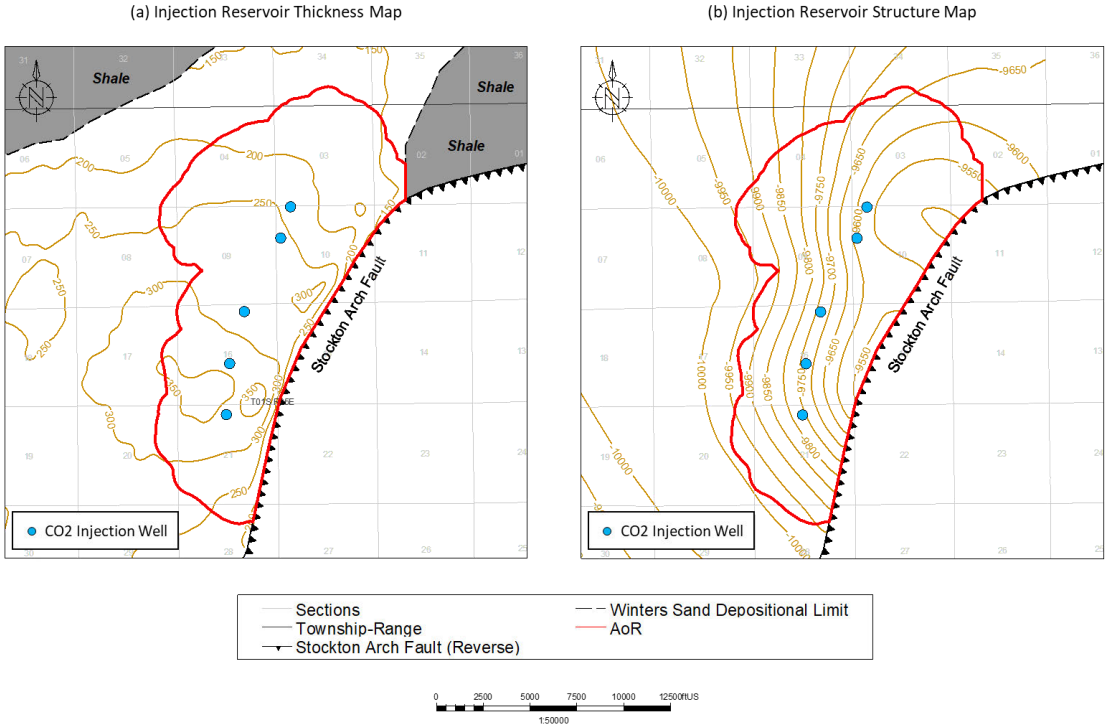

Figure 2.2-5. (a) Injection reservoir thickness map. (b) Injection reservoir structure map. AoR in red.

Outside of the AoR, southwest of the project area, the Winters Formation thickens and fans out, covering a much larger area. Northeast of the AoR, at the base of the slope, the Winters Formation pinches out. This stratigraphic trap along the eastern edge of the Winters Formation where the lobate bodies pinch out upslope contain the best reservoir quality in the system as well as being in upslope position, optimal for hydrocarbon migration or in this case CO_2 storage. The AoR and injectors for this project are shown in **Figure 2.2-6**.

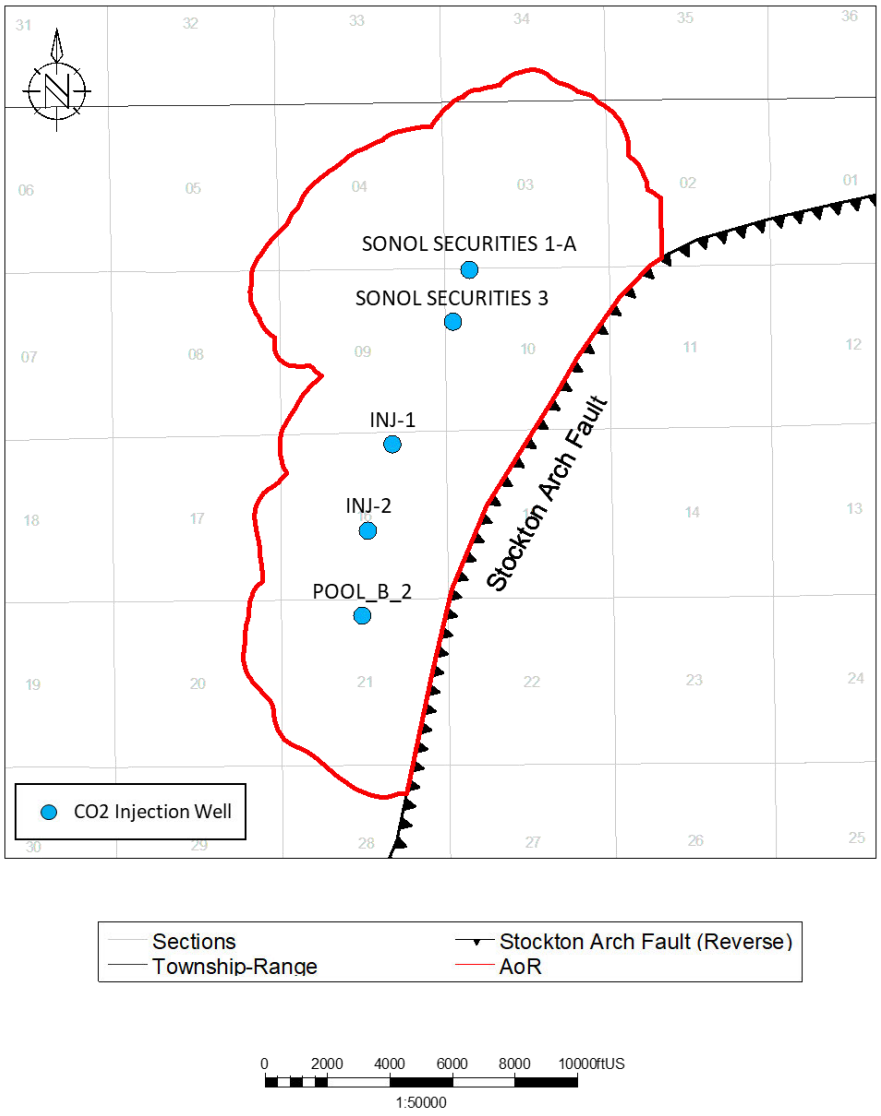

Figure 2.2-6. AoR and injection well location map for the project area. Minimum distance between injection wells is 1,735 ft. and maximum distance is 4,390 ft.

2.2.2.3 Starkey-Sawtooth Confining Zone

- Sawtooth Formation

The Sawtooth Shale overlies the Winters Formation, which provides a regional seal ranging from 100-500 ft. thick. Within the AoR the average gross thickness of the Sawtooth is 100 ft. At the Union Island Field, the Sawtooth Shale is continuous over the field and has a permeability of less than 0.15 mD and 18.5% porosity (as defined in section 2.4.2). This shale has successfully contained gas operations within the Winters for over 50 years and original gas deposits for millions of years.

- Tracy Formation

The Tracy Formation overlies the Sawtooth Shale and thickens southward into the San Joaquin Basin. This formation was deposited as Upper Cretaceous deep-water sandstone as an east-west trending south-facing depositional slope. Sand quality improves on the east side of the Stockton Arch Fault, outside of the AoR. Inside the AoR, on the west side of the fault this formation is very shale rich with minor interlaminations of low-quality sands as shown in **Figure 2.2-2.**

- Starkey Formation

Above the Winters Formation lies another inter-channel shale, the Starkey Formation, which adds to the Sawtooth Shale creating one large confining zone, encasing the reservoir.

2.2.2.4 H&T Shale

The H&T Shale acts as a conformable contact to the Mokelumne River Formation. This shale pinches out and creates an abrupt thickening when it combines with the overlying Capay Shale, moving west. The truncation of the H&T Shale results in a thicker Capay Shale that rests unconformable on the Starkey Sandstone. Moving southwest, the H&T thickens and contains a facies change with the upper marine shale of the Starkey section progressively adds, creating a thicker shale.

2.2.2.5 Mokelumne Monitoring Zone

- Mokelumne River Formation

The Mokelumne River Formation sandstones are excellent reservoir quality sands whose trap types include fault truncations, stratigraphic traps and unconformity traps sealed by intervening shales as well as overlying Menganos submarine canyon mudstone infill (Downey 2006). This formation truncates to the north by the post-Cretaceous angular unconformity until it pinches out in southern Yolo and Sutter counties (Downey 2006). These large sands can be locally eroded or totally gone due to the downcutting by the Menganos submarine canyons, which are located outside of the AoR to the west. This saline reservoir will be monitored and could effectively detect and monitor any possible CO_2 leakage prior to reaching the Markley Formation.

2.2.2.6 Capay Shale

The Capay Shale provides upper confinement to the Mokelumne River Formation as it spans across the basin as a major regional flooding surface. This Eocene aged formation was deposited as a transgressive surface blanketing the shelf with shales. East of the Midland fault zone, the Martinez Shale has been stripped by erosion, and the Mokelumne River Formation sandstones are unconformably overlain by the Capay Shale. Due to its low permeability, this formation acts as a seal to the Mokelumne River Formation monitoring zone and would act as a barrier to any CO_2, from reaching the USDW, if any migration were to occur.

2.2.2.7 Domengine Formation

The Domengine Formation is approximately 800-1200ft thick on the north flank of Mt. Diablo (Nilsen 1975). Prograding across the Capay Shelf in early middle Eocene, this formation is characterized by interbedded sandstones, shales, and coals. This sand ranges from medium to coarse grain silty mudstone and fine sandstone and onlaps the Capay Shale. It is separated from the Capay by a regional unconformity which progressively truncates older units until the Domengine rests on Cretaceous rocks, moving west. The Domengine consists of an upper and lower portion. The lower member is made up of fluvial and

estuarine sandstones. Regionally the lower member is separated from the upper member by an extensive surface of transgression and change in depositional style. This formation acts as a secondary dissipation zone to CO_2 between the injection site and the USDW.

2.2.2.8 Nortonville Shale

Above the Domengine Formation is the Nortonville Shale which is separated by a widespread surface of transgression. The Nortonville Shale is a mudstone member of the Kreyenhagen Formation. It is approximately 500 ft. on the north flank of Mt. Diablo and is considered the upper portion of the Domengine Sandstone (Nilsen 1975). Overlying the Domengine Sandstone, this shale acts as a seal throughout most of the southern Sacramento and northern San Joaquin Basins.

2.2.2.9 Marine Strata "Markley/Valley Springs"

The upper Paleogene and Neogene sequence begin with the Valley Springs Formation which represents fluvial deposits that blanket the entire southern Sacramento Basin. The unconformity at the base of the Valley Springs marks a widespread Oligocene regression and separates the more deformed Mesozoic and lower Paleogene strata below from the less deformed uppermost Paleogene and Neogene strata above. The USDW that resides at the base of the Markley formation is discussed in Section 2.7 of this document.

2.2.3 Map of the Area of Review

As required by 40 CFR 146.82(a)(2), **Figure 2.2-7** shows surface bodies of water, surface features, transportation infrastructure, political boundaries, and cities. Major water bodies in the area are Clifton Court Forebay, Victoria Canals, Grant Line Canal, and the Salmon Slough. The AoR is in San Joaquin County. This figure does not show the surface trace of known and suspected faults because there are no known surface faults in the AoR. There are also no known mines or quarries in the AoR.

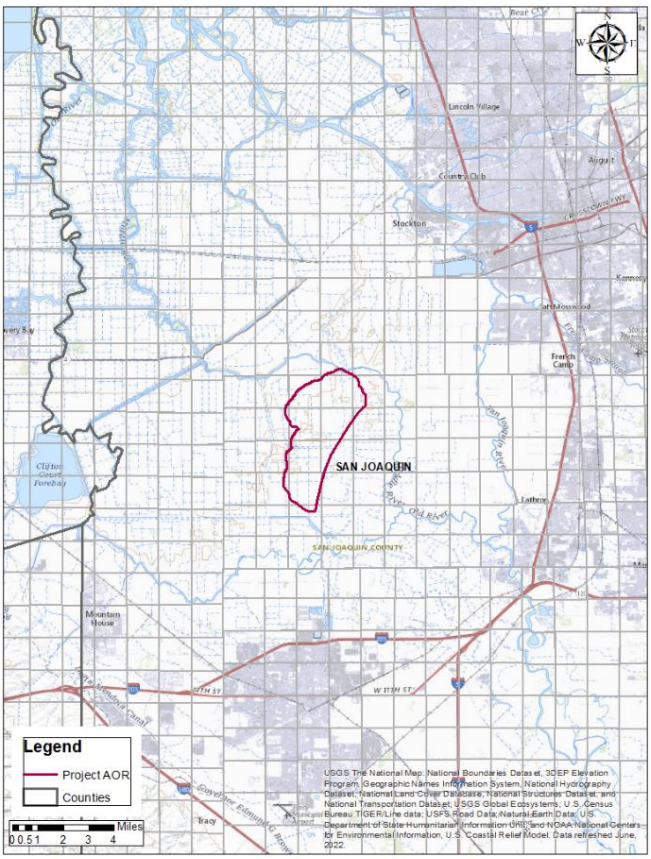

Figure 2.2-7. Surface Features and the AoR

Figure 2.2-8 indicates the locations of State- or EPA-approved subsurface cleanup sites. This cleanup site information was obtained from the State Water Resources Control Board's GeoTracker database, which contains records for sites that impact, or have the potential to impact, groundwater quality. Water wells within and adjacent the AoR are discussed in Section 2.7.7 of this document.

The GeoTracker website indicates that there is a closed clean-up site within the AoR. The site is at a former Union Oil Company Galli Pad Area located within the Union Island Oil Field. The site is listed in GeoTracker as Global ID SLT5S3033339. The case file includes a Mercury Contamination Soil Remediation Closure Report by Unocal Energy Resources Division (Unocal) and a Unocal transmittal letter to Central Valley Water Board staff from Unocal dated March 22,1996. The Unocal report states that Unocal is operating natural gas production wells in the Union Island Field and that there is mercury-contaminated soil in the top six inches of two 3-foot by 3-foot areas where the blow-off valves discharge to the ground surface. Unocal stated that it will excavate the contaminated soil and transport it offsite for disposal. The GeoTracker case file also includes a letter, dated January 18, 2012, from the Central Valley Regional Water Quality Control Board (Central Valley Water Board). The Central Valley Water Board staff determined that: 1) based on the very limited area of impact there was no indication of groundwater contamination and; 2) staff do not consider the site a cleanup site; and 3) staff will not be activating this case and consider it closed.

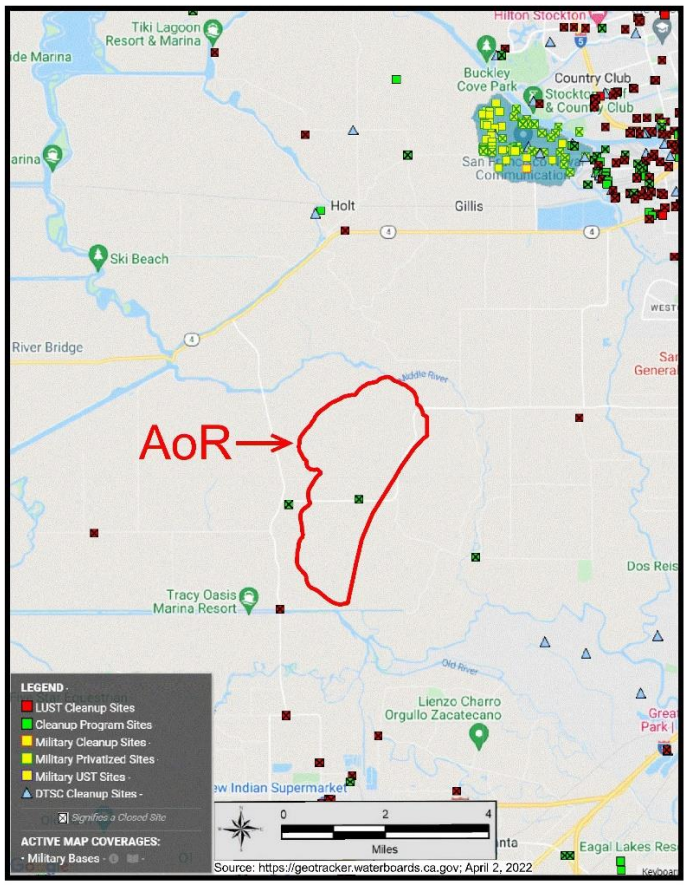

Figure 2.2-8. State or EPA Subsurface Cleanup Sites

2.3 Faults and Fractures [40 CFR 146.82(a)(3)(ii)]

2.3.1 Overview

The Stockton Arch subdivides the Great Valley Forearch into the Sacramento and San Joaquin Basins, bounding the Sacramento Basin in the south. Post-Eocene/Pre-Miocene uplift of the Stockton Arch created a series of high-angle reverse faults known as the Stockton Arch Fault Zone (SFZ). This fault bounds the SE portion of the AoR, trending SW to NE and spanning from Tracy to Linden. The Union Island Field produces from the footwall of this fault-related trap.

The 3D seismic data described in the prior section were used together with well control to define the fault planes within the geologic model boundary. This geologic model is a subset of the larger structural framework that was built using the seismic and well data. Repeat geologic section seen in wells is used to guide the fault pick along with a clear offset and fault plane seen in the modern reprocessing of the 3D seismic data. **Figure 2.3-1** shows the fault at the Winters level along with the location of an example

structural cross-section shown in **Figure 2.3-2**. There is a secondary fault in the hanging wall (east side) of the Stockton Arch fault which may be antithetic to the main fault. Due to the sealing nature of the Stockton Arch Fault and the planned injection in the footwall (west side) of the fault, this secondary fault is not discussed further in this report.

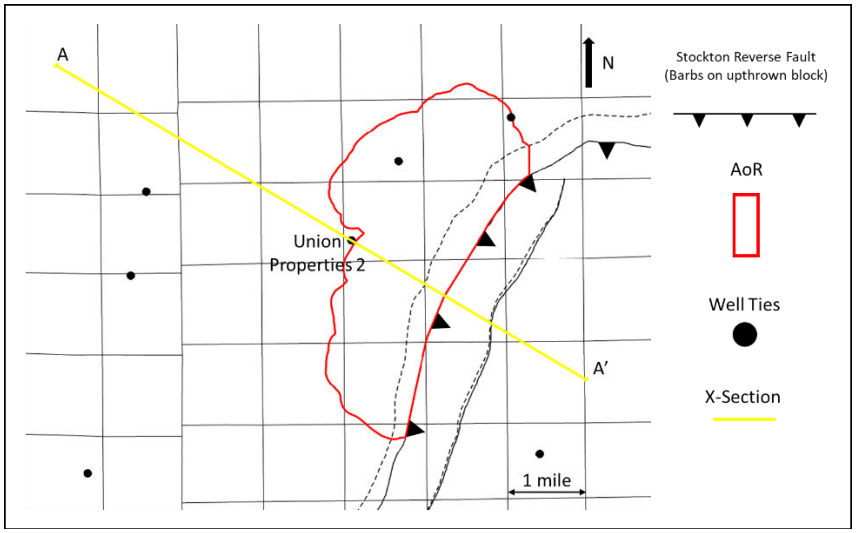

Figure 2.3-1. The two faults within the model are shown at the Winters level. The fault to the east is believed to be antithetic to the main Stockton Arch fault and is dashed into it in cross-section. Yellow line highlights the cross-section shown in **Figure 2.3-2.**

As seen in the cross-section shown in **Figure 2.3-2** the Stockton Arch Fault is cut-off at the Base Valley Springs unconformity. There is some folding in the strata above this which may be related to the structural overprint of the fault beneath the unconformity. The fault appears to have been active through the Eocene section beneath the unconformity due to the missing Domengine section on the east side of it. Further discussion of fault activity is provided in the Seismic History section.

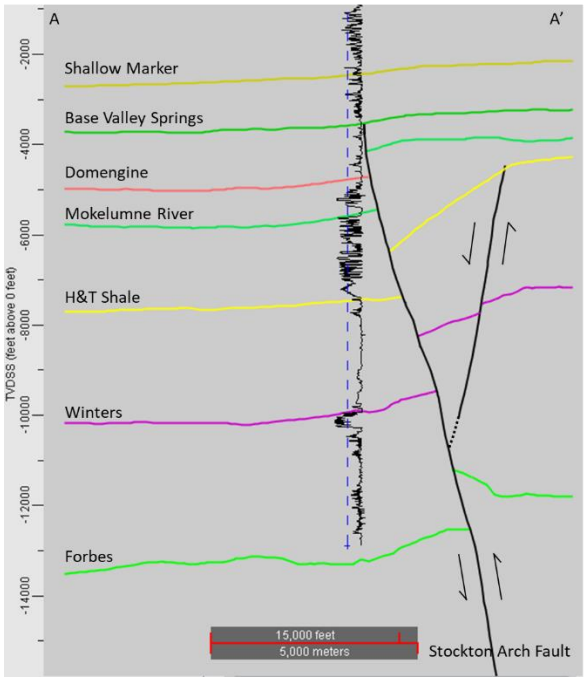

Figure 2.3-2. Structural cross section across the geologic model. Well Union Properties 2 (04077203220000) is shown with SP log (negative values to left) for correlation and geologic packages. Geologic surfaces developed from seismic interpretation. The Stockton Arch Fault is cut-off by the Base Valley Springs. The interpreted antithetic fault to the east is dashed into the Stockton Arch Fault

The Stockton Arch Fault has a sealing capacity adequate to trap natural gas for millions of years, it will also provide a seal to trap injected CO_2. Original reservoir pressure when the field was discovered in 1972 was 5,040 psi. Production of natural gas and water through time has drawn that pressure down to a current pressure of 1,200 psi. Through the injection of CO_2 the proposed final reservoir pressure post-injection will be 4,500 psi. Due to the sealing nature of the fault at higher original pressures and the substantial gas column this held, the fault will continue to seal. Restricting the pressure to below original reservoir pressure is also important for the stability of the fault, and this is discussed further in the Seismic History section of this document.

Secondary information supporting the sealing capacity of the Stockton Arch Fault comes from pressure isolation in the Winters Formation during production. Mudlogs from wells drilled later in field development (late 2000's) indicate normal hydrostatic or lower pressure in the confining and other zones above the Winters. Of the wells reviewed, each were drilled with mud weights overbalanced to hydrostatic pressure and none of them showed any losses above the Winters despite depletion in the Winters Formation. Wells were reviewed that drilled on both sides of the fault. To further confirm pressure isolation within the Winters Formation for injection, pre-operational testing will include taking measured pressures from these shallower zones. The exact intervals to be tested will be based on reservoir properties but should include the Mokelumne River Formation.

2.4 Injection and Confining Zone Details [40 CFR 146.82(a)(3)(iii)]

2.4.1 Mineralogy

No quantitative mineralogy information exists within the AoR boundary. Mineralogy data will be acquired across all the zones of interest as part of pre-operational testing. Several wells outside the AoR have mineralogy over the respective formations of interest, and that data is presented below.

2.4.1.1 Winters Formation

Core descriptions for 3 wells within the AoR mention that the Winters Formation sandstone consists of "quartz, feldspar (plagioclase & K-spar), mica, ferromags, and lithics." Calcite cemented intervals of sandstone are also present within the core, generally as thin "bones" or "sandstone 'shell'" and are confirmed by log data. The exact mineralogic content of these bones is unknown. X-ray diffraction (XRD) data from the GP_Dohrmann_1_RD1 in the Winters Formation confirm this general mineralogy (see **Figure 2.4-1**). Reservoir sand from two samples in this well averages 67% quartz, 14% plagioclase and potassium feldspar, and 12% total clay (**Table 2.4-1**). The primary clay minerals are kaolinite and smectite. Calcite & dolomite make up less than 3% of the samples.

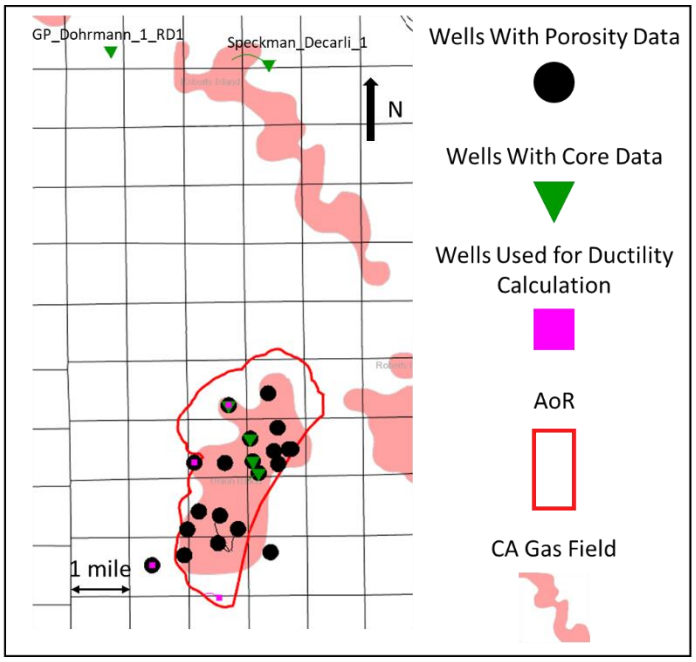

Figure 2.4-1. Map showing location of wells with mineralogy data relative to the AoR.

Table 2.4-1: Formation mineralogy from X-ray diffraction in GP_Dohrmann_1_RD1 and XRD and Fourier transform infrared spectroscopy (FTIR) in the Speckman_Decarli_1 well. Well locations shown in Figure 2.4-1.

Well	Zone	Depth (ft)	Quartz	Plagioclase	K-Feldspar	Calcite	Dolomite	Siderite	Barite	Glauconite	Pyrite	Kaolinite	Chlorite	Illite & Mica	Smectite	MXL I/S	Total Clay
Speckman_Decarli_1	H&TShale	8828.0	23.0	21.0	9.0	3.0	0.0			0.0	1.0	12.0	5.0			26.0	43.0
Speckman_Decarli_1	H&TShale	8830.0	30.0	17.0	11.0	0.0	0.0			0.0	4.0	3.4	14.4	6.1	14.1		38.0
Speckman_Decarli_1	H&TShale	8909.0	20.0	20.0	13.0	0.0	0.0			2.0	2.0	5.0	3.0			35.0	43.0
Speckman_Decarli_1	H&TShale	8937.0	20.0	12.0	8.0	0.0	0.0			0.0	2.0	14.0	6.0			38.0	58.0
Speckman_Decarli_1	H&TShale	8939.0	24.0	18.0	11.0	1.0	0.0			0.0	3.0	3.0	15.5	7.7	16.8		43.0
Speckman_Decarli_1	H&TShale	8940.0	23.0	29.0	12.0	0.0	0.0			0.0	0.0	4.0	5.0			27.0	36.0
Speckman_Decarli_1	H&TShale	8942.0	23.0	15.0	10.0	0.0	0.0			0.0	2.0	12.0	5.0			33.0	50.0
Speckman_Decarli_1	H&TShale	9439.0	20.0	14.0	9.0	0.0	0.0			0.0	1.0	0.0	5.0			51.0	56.0
Speckman_Decarli_1	H&TShale	9441.0	21.0	19.0	12.0	2.0	0.0			0.0	3.0	0.0	0.0			43.0	43.0
GP_Dohrmann_1_RD1	Winters	9755.1	64.0	9.0	2.0		1.0	11.0				5.0			8.0		13.0
GP_Dohrmann_1_RD1	Winters	9758.5	70.0	12.0	4.0		1.0	2.0				5.0			6.0		11.0
GP_Dohrmann_1_RD1	Winters	9762.5	28.0	8.0	3.0		1.0	1.0			1.0	21.0	2.0	2.0	33.0		58.0
GP_Dohrmann_1_RD1	Delta Shale	10073.5	69.0	13.0	5.0		1.0	1.0				3.0	1.0	1.0	6.0		11.0
GP_Dohrmann_1_RD1	Delta Shale	10077.5	30.0	7.0	2.0	1.0		3.0			1.0	17.0	5.0	2.0	32.0		56.0
GP_Dohrmann_1_RD1	Delta Shale	10082.5	70.0	13.0	3.0		1.0	1.0				3.0	2.0	2.0	5.0		12.0
GP_Dohrmann_1_RD1	Delta Shale	10090.5	51.0	8.0	2.0		1.0				2.0	8.0	4.0	3.0	21.0		36.0
GP_Dohrmann_1_RD1	Delta Shale	10096.2	72.0	13.0	3.0		1.0		1.0			3.0	1.0	2.0	4.0		10.0
GP_Dohrmann_1_RD1	Delta Shale	10070.5	69.0	14.0	4.0		1.0	1.0				4.0	1.0		6.0		11.0

2.4.1.2 Upper Confining Zone (Starkey-Sawtooth Shale)

No representative mineralogy data is available for the upper confining zone. Mineralogy data is available for the H&T Shale, a similar Cretaceous age shale directly above the upper confining zone, from the Speckman_Decarli_1 well (see **Figure 2.4-1**) in the form of XRD and FTIR data. Nine samples for this zone show an average of 46% total clay, with mixed layer illite/smectite being the dominant species, with kaolinite and chlorite still prevalent. They also contain 23% quartz, 29% plagioclase and potassium feldspar, 2% pyrite, and 1% calcite & dolomite (**Table 2.4-1**).

2.4.1.3 Delta Shale

X-ray diffraction data is available for the Delta Shale in the GP_Dohrmann_1_RD1, but most of the samples were taken within sandy intervals. Two data points (10077.5 and 10090.5 feet MD) can be classified as shale based on their total clay weight percent. These samples average 46% total clay, with smectite and kaolinite being the major clay species. They also contain 40% quartz, 10% plagioclase and potassium feldspar, and 1% calcite & dolomite.

2.4.2 Porosity and Permeability

2.4.2.1 Winters Formation

Wireline log data was acquired with measurements that include but are not limited to spontaneous potential, natural gamma ray, borehole caliper, compressional sonic, resistivity as well as neutron porosity and bulk density. Formation porosity is determined one of two ways: from bulk density using 2.65 g/cc matrix density as calibrated from core grain density and core porosity data, or from compressional sonic using 55.5 µsec/ft matrix slowness and the Raymer-Hunt equation.

Volume of clay is determined by spontaneous potential and is calibrated to core data.

Log-derived permeability is determined by applying a core-based transform that utilizes capillary pressure porosity and permeability along with clay values from XRD or FTIR. Core data from two wells with 13 data

points was used to develop a permeability transform. An example of the transform from core data is illustrated in **Figure 2.4-2** below.

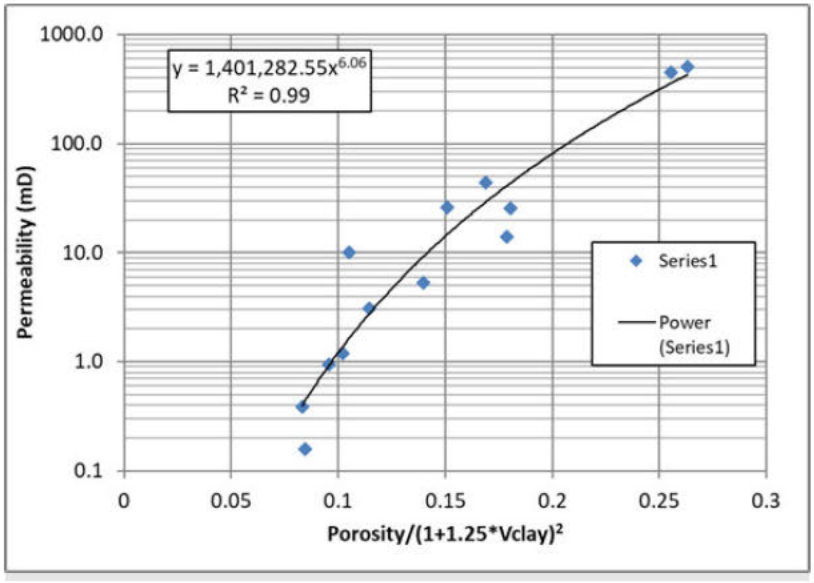

Figure 2.4-2. Permeability transform for Sacramento basin zones.

In the example well below, Sonol_Securities_6, for the Winters Formation, the porosity ranges from 1% - 26% with a mean of 17% (**Figure 2.4-3**). The permeability ranges from 0.0004 mD - 290 mD with a log mean of 5.6 mD (**Figure 2.4-4**).

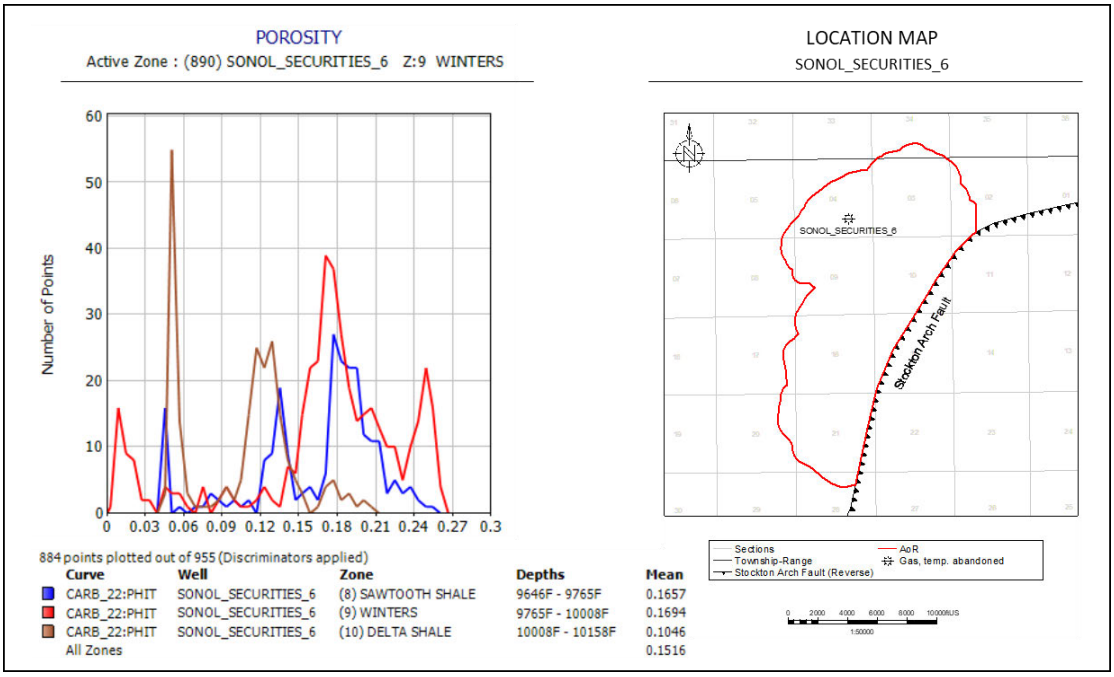

Figure 2.4-3. Porosity histogram for well Sonol_Securities_6. In the histogram, blue represents the Sawtooth Shale, red the Winters Formation, and brown the Delta Shale. For the two shale intervals, only data with VCL>0.25 is shown, and for the Winters only data with VCL<=0.25 is shown.

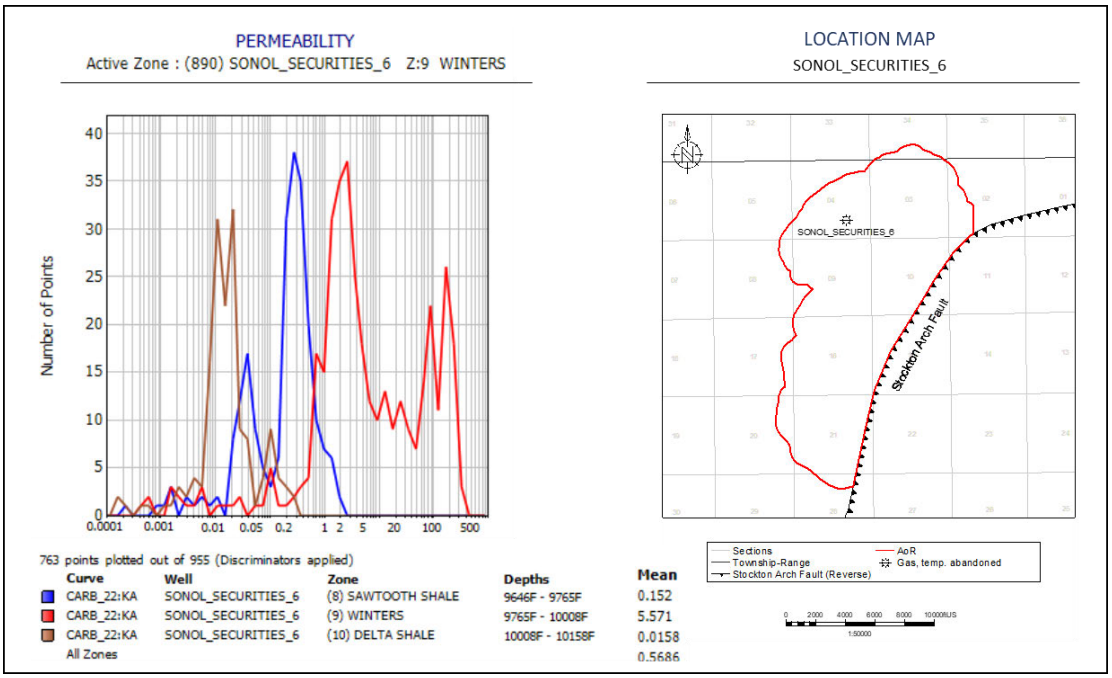

Figure 2.4-4. Permeability histogram for well Sonol_Securities_6. In the histogram, blue represents the Sawtooth Shale, red the Winters Formation, and brown the Delta Shale. For the two shale intervals, only data with VCL>0.25 is shown, and for the Winters only data with VCL<=0.25 is shown.

A log plot for the Sonol_Securities_6 is included in **Figure 2.4-5**. Core porosity and permeability are shown in comparison to log calculated porosity and permeability.

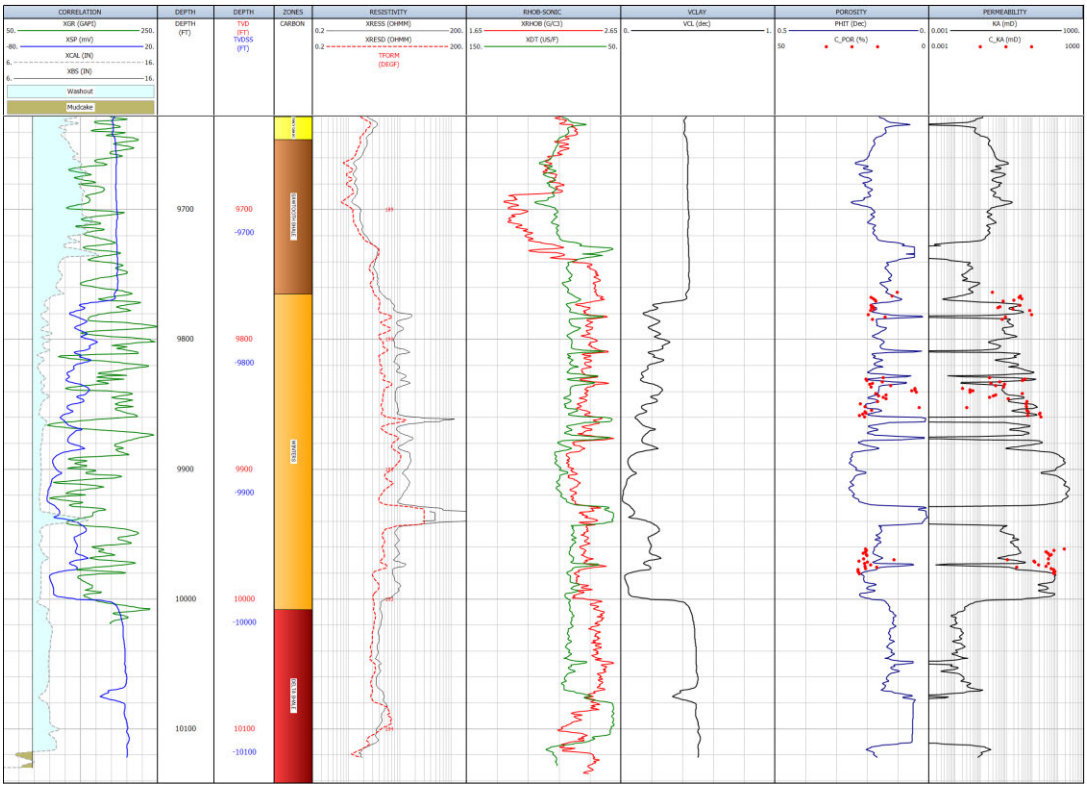

Figure 2.4-5. Log plot for well Sonol_Securities_6, showing the log curves used as inputs into calculations of clay volume, porosity and permeability, and their outputs. Core data for porosity and permeability is shown for comparison to the log model. Track 1: Correlation and caliper logs. Track 2: Measured depth. Track 3: Vertical depth and vertical subsea depth. Track 4: Zones. Track 5: Resistivity. Track 6: Compressional sonic and density logs. Track 7: Volume of clay. Track 8: Porosity calculated from log curves and core porosity. Track 9: Permeability calculated using transform and core permeability.

The average porosity for the Winters Formation is 18.9%, based on 19 wells with porosity logs and 8518 individual logging data points. See **Figure 2.4-6** for location of wells used for porosity and permeability averaging.

The geometric average permeability for the Winters Formation is 13 mD, based on 19 wells with porosity logs and 7993 individual logging data points.

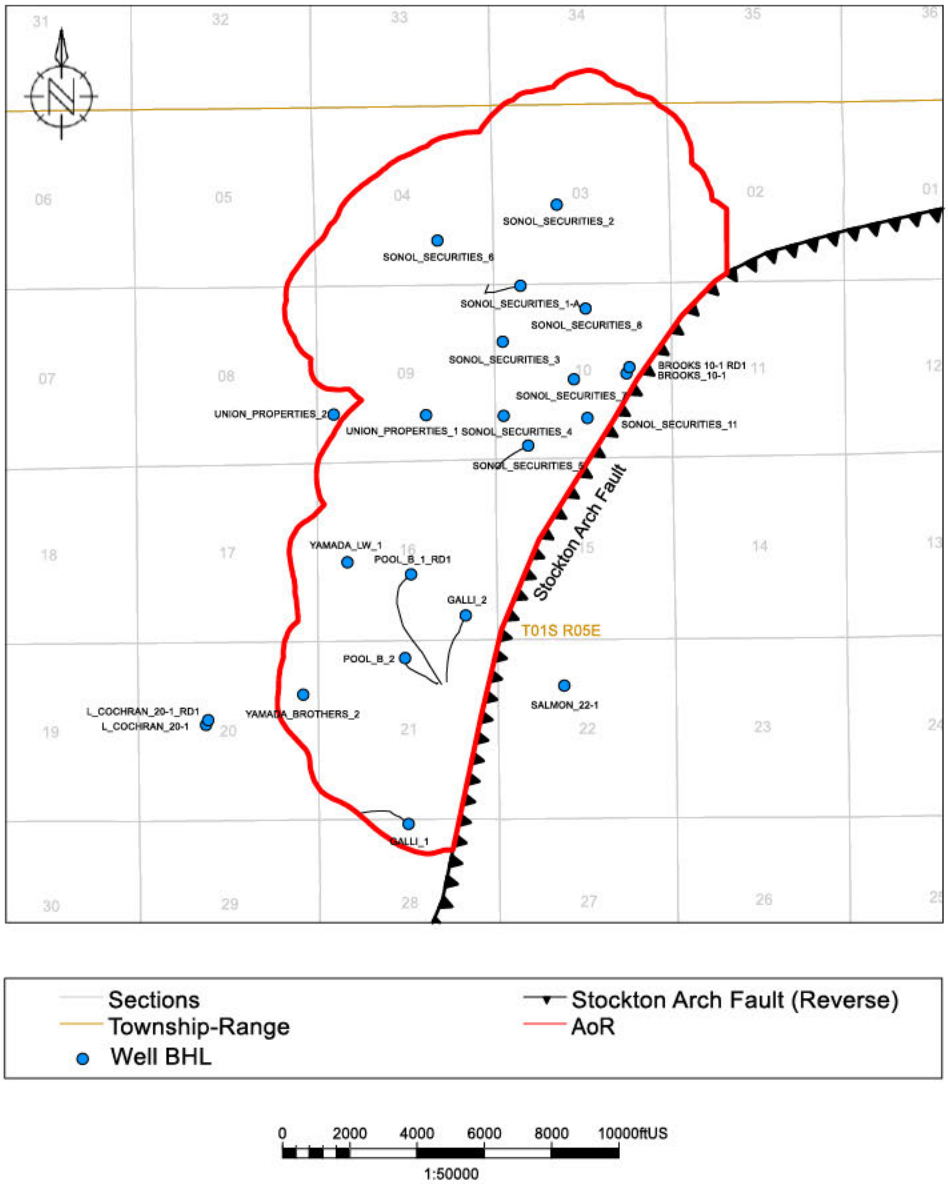

Figure 2.4-6. Map of wells with porosity and permeability data.

2.4.2.2 Upper Confining Zone (Starkey-Sawtooth Shale)

The average porosity of the upper confining zone is 23.0%, based on 16 wells with porosity logs and 50,563 individual logging data points.

The geometric average permeability of the upper confining zone is 0.59 mD, based on 16 wells with porosity logs and 49,662 individual logging data points.

2.4.2.3 Delta Shale

The average porosity of the lower confining zone (Delta Shale) is 14.7%, based on 13 wells with porosity logs and 2983 individual logging data points.

The geometric average permeability of the lower confining zone (Delta Shale) is 0.04 mD, based on 13 wells with porosity logs and 2,906 individual logging data points.

2.4.3 Injection and Confining Zone Capillary Pressure

Capillary pressure is the difference across the interface of two immiscible fluids. Capillary entry pressure is the minimum pressure required for an injected phase to overcome capillary and interfacial forces and enter the pore space containing the wetting phase.

No capillary pressure data was available for the upper confining zone. This data will be acquired as part of pre-operational testing.

For the injection zone, Capillary pressure data obtained from well Sonol Securities 5 in the Union Island Gas field was used. **Figure 2.4-7** shows the Capillary pressure curve for the Injection zone that was used for the Computational modeling. Further details, and location of the well are discussed in Attachment B.

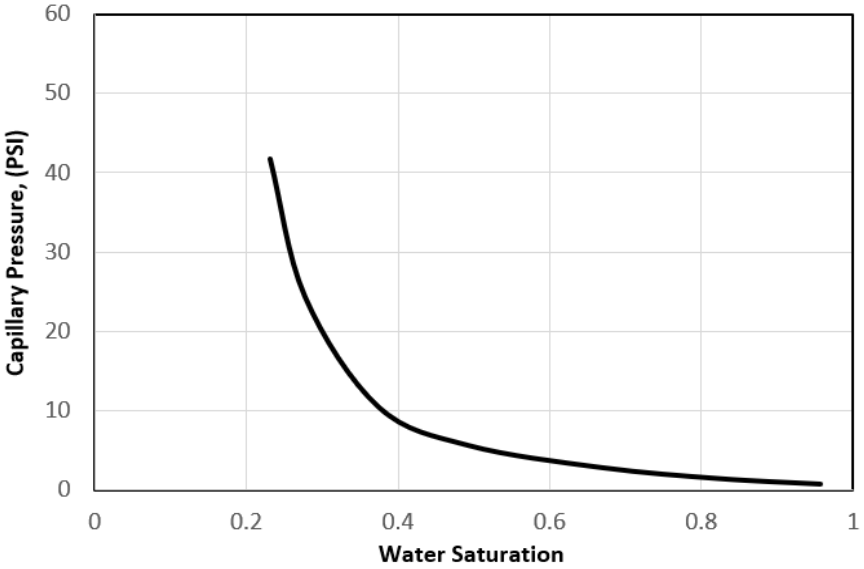

Figure 2.4-7. Injection zone Capillary pressure curve used in Computational modeling. Obtained from Core sample from Sonol Securities 5 in the Union Gas Field.

2.4.4 Depth and Thickness

Depths and thickness of the Winters Formation reservoir and Starkey-Sawtooth confining zone (**Table 2.4-2**) are determined by structural and isopach maps (**Figure 2.4-8**) based on well data (wireline logs). Variability of the thickness and depth measurements is due to:

1. Starkey-Sawtooth Shale and Winters Formation structural variability is due to the slight anticlinal structure.

2. Starkey-Sawtooth Shale thickness variability due to deposition of the Winters Formation. In the AoR, the shale minimum thickness corresponds to a high in Winters Formation sand thickness.

3. Winters Formation thickness variability is from pinch-out of the reservoir in the northeast.

Table 2.4-2: Starkey-Sawtooth Shale and Winters Formation gross thickness and depth within the AoR.

Zone	Property	Low	High	Mean
Upper Confining Zone *Starkey-Sawtooth Shale*	Thickness (feet)	2,158	2,637	2,288
	Depth (feet TVD)	7,208	7,776	7,457
Reservoir *Winters Formation Sandstone*	Thickness (feet)	120	365	256
	Depth (feet TVD)	9,492	9,995	9,713

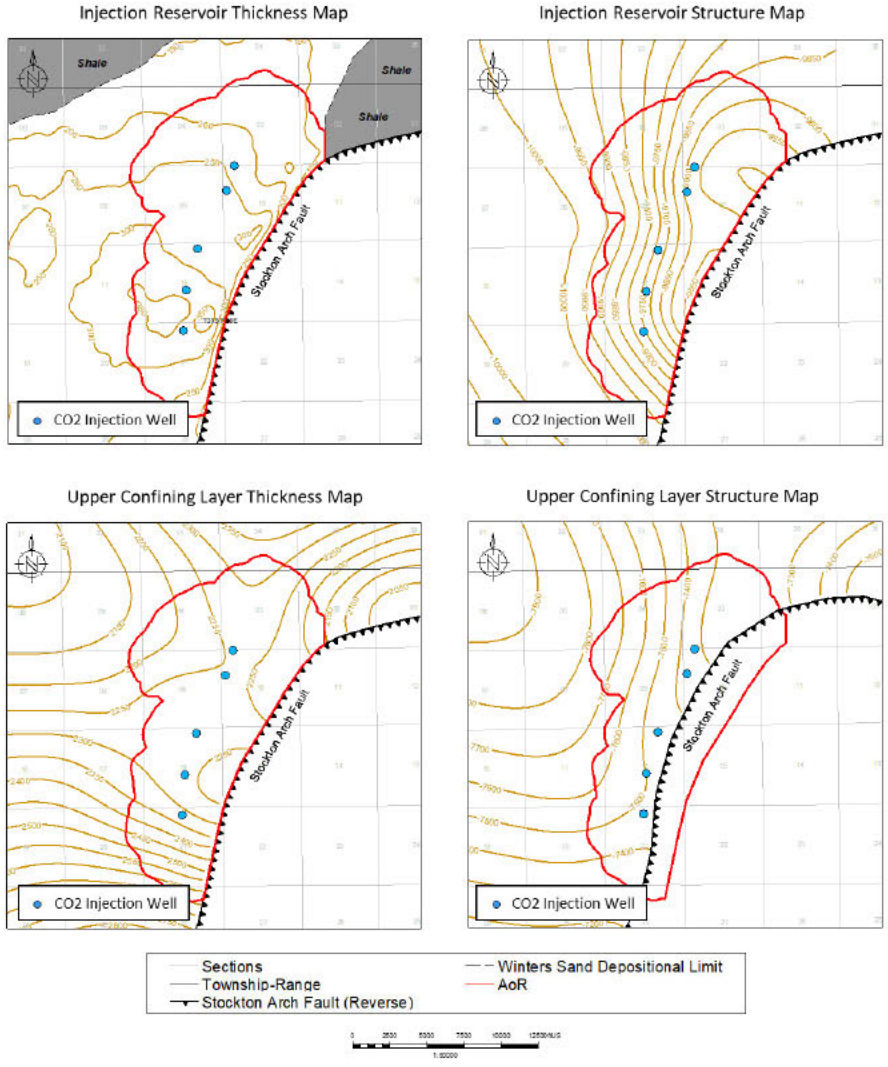

Figure 2.4-8. Gross thickness and depth maps within the AoR for the injection reservoir and upper confining layer.

2.4.5 Structure Maps

Structure maps are provided to indicate a depth to reservoir adequate for supercritical-state injection.

2.4.6 Isopach Maps

Spontaneous potential (SP) logs from surrounding gas wells were used to identify sandstones. Negative millivolt deflections on these logs, relative to a baseline response in the enclosing shales, define the sandstones. These logs were baseline shifted to 0mV. Due to the log vintage variability, there is an effect on quality which creates a degree of subjectivity within the gross sand, however this will not have a material impact on the maps.

Variability in the thickness and depth of either the Starkey-Sawtooth Shale or the Winters Formation sandstone will not impact confinement. CTV will utilize thickness and depth shown when determining operating parameters and assessing project geomechanics.

2.5 Geomechanical and Petrophysical Information [40 CFR 146.82(a)(3)(iv)]

2.5.1 Caprock Ductility

Ductility and the unconfined compressive strength (UCS) of shale are two properties used to describe geomechanical behavior. Ductility refers to how much a rock can be distorted before it fractures, while the UCS is a reference to the resistance of a rock to distortion or fracture. Ductility generally decreases as compressive strength increases.

Ductility and rock strength calculations were performed based on the methodology and equations from Ingram & Urai, 1999 and Ingram et. al., 1997. Brittleness is determined by comparing the log derived unconfined compressive strength (UCS) vs. an empirically derived UCS for a normally consolidated rock (UCS_{NC}).

$$\log UCS = -6.36 + 2.45 \log\left(0.86 V_p - 1172\right) \quad (1)$$

$$\sigma' = OB_{pres} - P_p \quad (2)$$

$$UCS_{NC} = 0.5\sigma' \quad (3)$$

$$BRI = \frac{UCS}{UCS_{NC}} \quad (4)$$

Units for the UCS equation are *UCS* in MPa and V_p (compressional velocity) in m/s. OB_{pres} is overburden pressure, P_p is pore pressure, σ' is effective overburden stress, and *BRI* is brittleness index.

If the value of BRI is less than 2, empirical observation shows that the risk of embrittlement is lessened, and the confining zone is sufficiently ductile to accommodate large amounts of strain without undergoing brittle failure. However, if BRI is greater than 2, the "risk of development of an open fracture

network cutting the whole seal depends on more factors than local seal strength and therefore the BRI criterion is likely to be conservative, so that a seal classified as brittle may still retain hydrocarbons" (Ingram & Urai, 1999).

2.5.1.1 Upper Confining Zone (Starkey-Sawtooth Shale)

Within the AoR, four wells had compressional sonic and bulk density data over the upper confining zone to calculate ductility, comprising 9,633 individual logging data points (see pink squares in **Figure 2.4-1**). 16 wells had compressional sonic data over the upper confining zone to calculate UCS, comprising 59014 individual logging data points (see black circles in **Figure 2.4-1**). The average ductility of the confining zone based on the mean value is 2.0. Additionally, 65% of the shale within the confining layer has a ductility less than 2.The average rock strength of the confining zone, as determined by the log derived UCS equation above, is 4,593 psi.

An example calculation for the well Sonol_Securities_6 is shown below (**Figure 2.5-1**). UCS_CCS_VP is the UCS based on the compressional velocity, UCS_NC is the UCS for a normally consolidated rock, and BRI is the calculated brittleness using this method. Brittleness less than two (representing ductile rock) is shaded red.

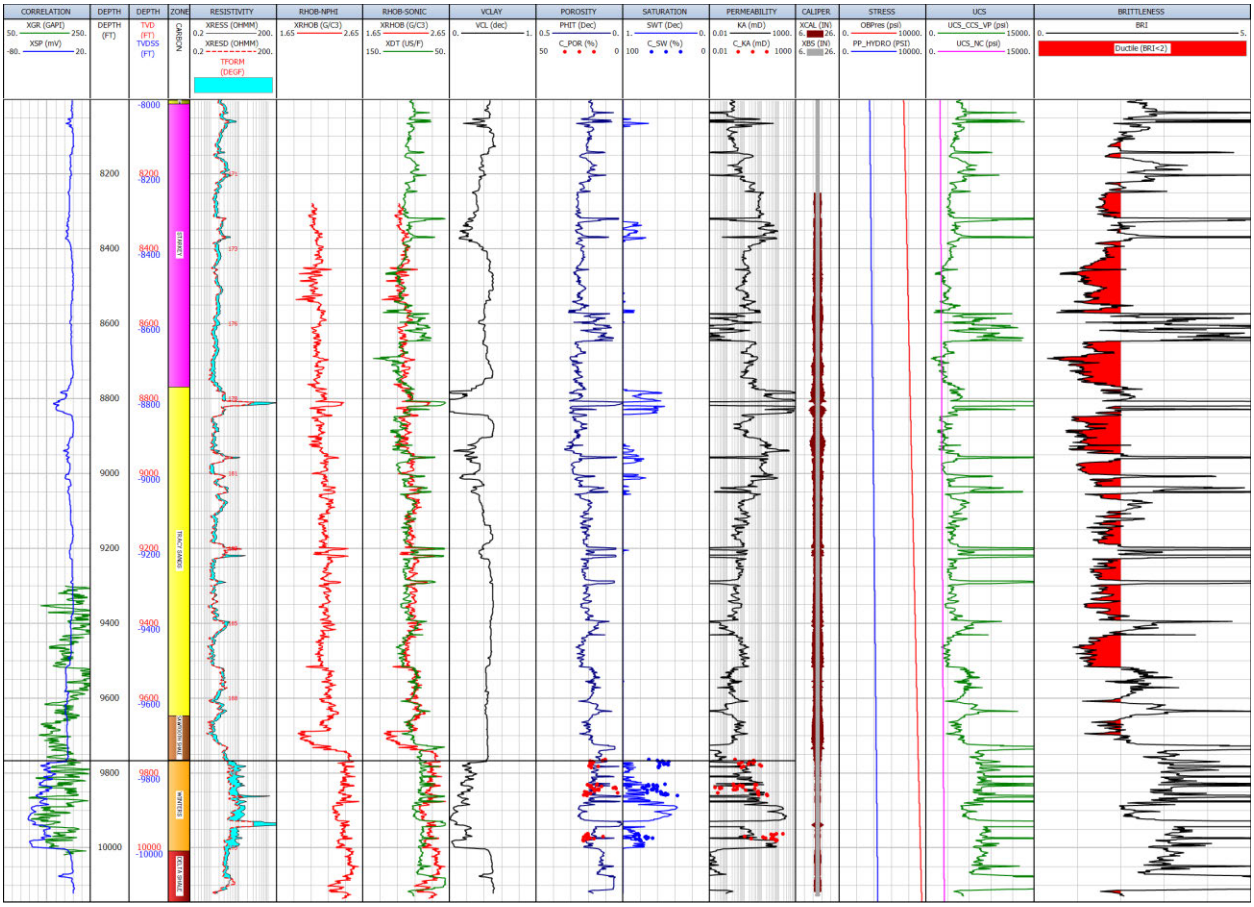

Figure 2.5-1. Unconfined compressive strength and ductility calculations for well Sonol_Securities_6. The upper confining zone ductility is less than two. Track 1: Correlation logs. Track 2: Measured depth. Track 3: Vertical depth and vertical subsea depth. Track 4: Zones. Track 5: Resistivity. Track 6: Density log. Track 7: Density and compressional sonic logs. Track 8: Volume of clay. Track 9: Porosity calculated from sonic and density. Track 10: Water saturation. Track 11: Permeability. Track 12: Caliper. Track 13: Overburden pressure and hydrostatic pore pressure. Track 14: UCS and UCS_NC. Track 15: Brittleness.

Within the upper confining zone, the brittleness calculation drops to a value less than two. As a result of the upper confining zone ductility, there are no fractures that will act as conduits for fluid migration from the Winters Formation. This conclusion is supported by the following:

1. Prior to discovery, the upper confining zone provided a seal to the underlying gas reservoir of the Winters Formation for millions of years.

2.5.2 Stress Field

The stress of a rock can be expressed as three principal stresses. Formation fracturing will occur when the pore pressure exceeds the least of the stresses. in this circumstance, fractures will propagate in the direction perpendicular to the least principal stress (**Figure 2.5-2**).

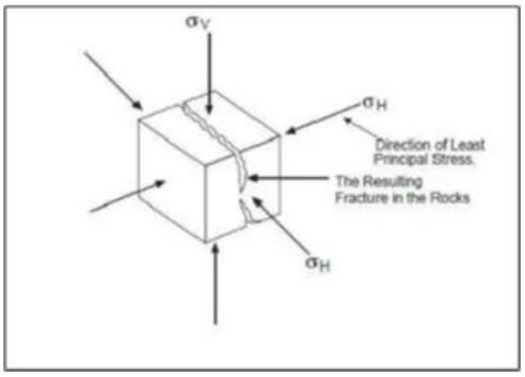

Figure 2.5-2. Stress diagram showing the three principal stresses and the fracturing that will occur perpendicular to the minimum principal stress.

Stress orientations in the Sacramento basin have been studied using both earthquake focal mechanisms and borehole breakouts (Snee and Zoback, 2020, Mount and Suppe, 1992). The azimuth of maximum principal horizontal stress (S_{Hmax}) was estimated at N40ºE ± 10º by Mount and Suppe, 1992. Data from the World Stress Map 2016 release (Heidbach et al., 2016) shows an average S_{Hmax} azimuth of N37.4ºE once several far field earthquakes with radically different S_{Hmax} orientations are removed (**Figure 2.5-3**), which is consistent with Mount and Suppe, 1992. The earthquakes in the area indicate a strike-slip/reverse faulting regime.

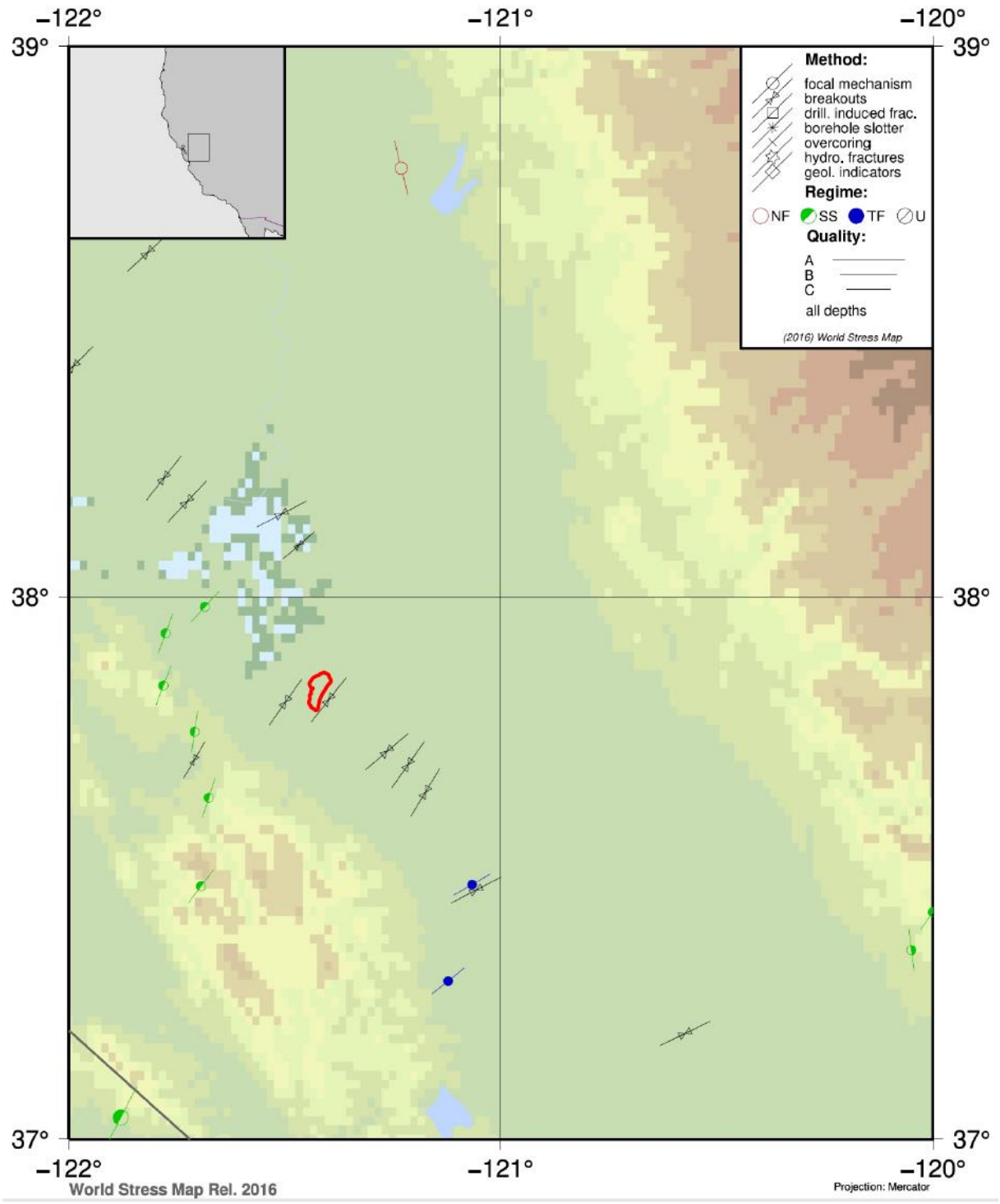

Figure 2.5-3. World Stress Map output showing S_{Hmax} azimuth indicators and earthquake faulting styles in the Sacramento Basin (Heidbach et al., 2016). The red polygon is the project AoR. The background coloring represents topography.

In the project AoR there is no site-specific Winters Formation fracture pressure or fracture gradient. A Winters Formation step rate test will be conducted as per the preoperational testing plan. However, several wells have formation integrity tests (FIT) for shallower formations such as the H&T Shale and Mokelumne River Formation. A FIT performed in the H&T Shale in the Sonol_Securities_8 recorded a minimum fracture gradient of 0.809 psi/ft. Four other wells within the field recorded minimum fracture gradients of 0.75-0.76 psi/ft based on FIT in the H&T Shale and Mokelumne River Formation (Yamada_Line_Well_1, Pool_B_2, Galli_1, and Galli_2). FIT data for three other wells across the Sacramento basin at depths between 8800-10800' TVD averaged 0.84 psi/ft (Transamerica_2-3, Serpa_5, and Wilcox_21). See **Figure 2.5-4** for location of all wells. For computational modeling, a frac gradient of 0.7 psi/ft was used, which should be below the actual frac gradient assuming the Winters Formation frac gradient would be similar to shallower zones.

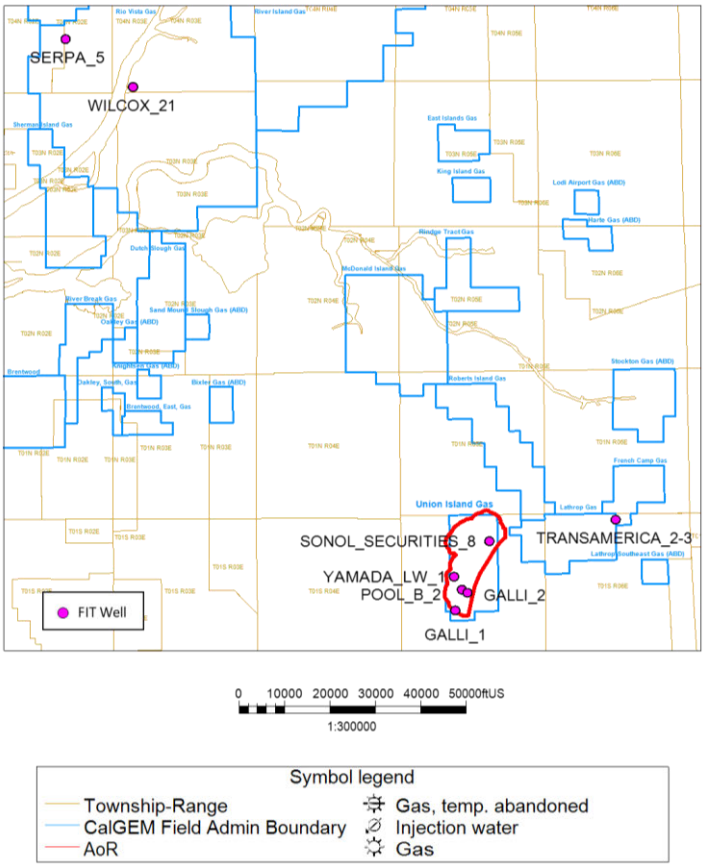

Figure 2.5-4. Location of wells with FIT data.

In the project AoR there is no site-specific fracture pressure or fracture gradient for the upper confining zone. A step rate test will be conducted in the upper confining zone as per the preoperational testing plan.

In the interim, CTV assumes that the upper confining zone will have a similar fracture gradient as the Winters Formation.

The overburden stress gradient in the reservoir and confining zone is 0.94 psi/ft. No data currently exists for the pore pressure of the confining zone. This will be determined as part of the preoperational testing plan.

2.6 Seismic History [40 CFR 146.82(a)(3)(v)]

Due to its lack of surface expression, the Stockton Arch Fault has only been identified via subsurface data. As discussed in the prior Faults and Fractures, three-dimensional seismic and well data were used to create a depth surface for the fault. The trace of this fault generally agrees with that shown by the Fault Activity Map created by the California Geologic Survey and United States Geologic Survey (USGS) (**Figure 2.6-1**). The top of the fault is cut-off by the base of the Valley Springs Formation that unconformably overlays Eocene strata beneath it. The age of the Valley Springs Formation dates back to Early Miocene times approximately 20 to 23 million years ago. While there is some folding of units above this unconformity, it is likely related to remanent structure associated with the fault. The seismic interpretation indicates there is no appreciable offset on the Stockton Arch Fault above this unconformity. The seismic interpretation of the base of the Valley Springs Formation and fault being cut-off agree with the California Department of Conservation of Oil, Gas & Geothermal Resources Oil & Gas Technical Reports Volume III. (https://www.conservation.ca.gov/calgem/pubs_stats/Pages/technical_reports.aspx?msclkid=08d3028aa96811ec886f3c2f6cc3a20a).

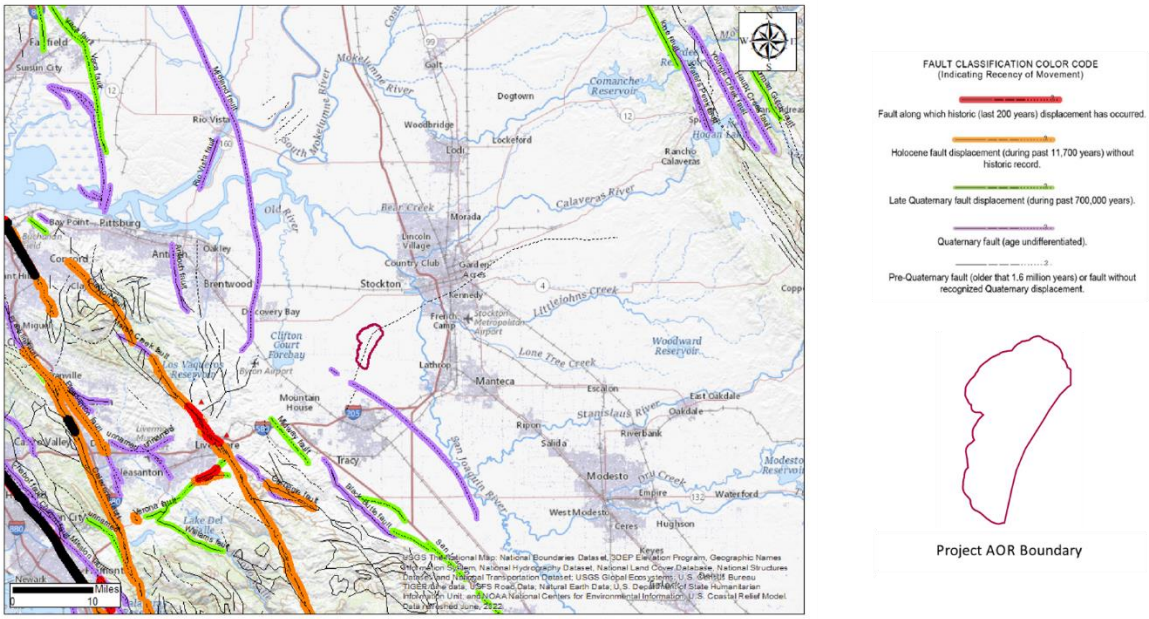

Figure 2.6-1. Fault Activity Map from the California Geologic Survey and United States Geological Survey. The fault trace of the Stockton Fault shown here agrees with the 3D seismic interpretation. The fault trace is not colored indicating it is interpreted as Pre-Quaternary (older than 1.6 million years) by the

California Geologic Survey. This is also in agreement with the seismic and well-based interpretation. (https://maps.conservation.ca.gov/cgs/fam/)

The seismic interpretation provides an estimation of the time when the Stockton Arch Fault was last actively growing. The United States Geologic Survey (USGS) provides an earthquake catalog tool (https://earthquake.usgs.gov/earthquakes/search/) which can be used to search for recent seismicity that could be associated with faults in the area for movement. A search was made for earthquakes in the greater vicinity of the project area from 1850 to modern day with events of a magnitude greater than three. **Figure 2.6-2** shows the results of this search and **Table 2.6-1** summarizes some of the data taken from them.

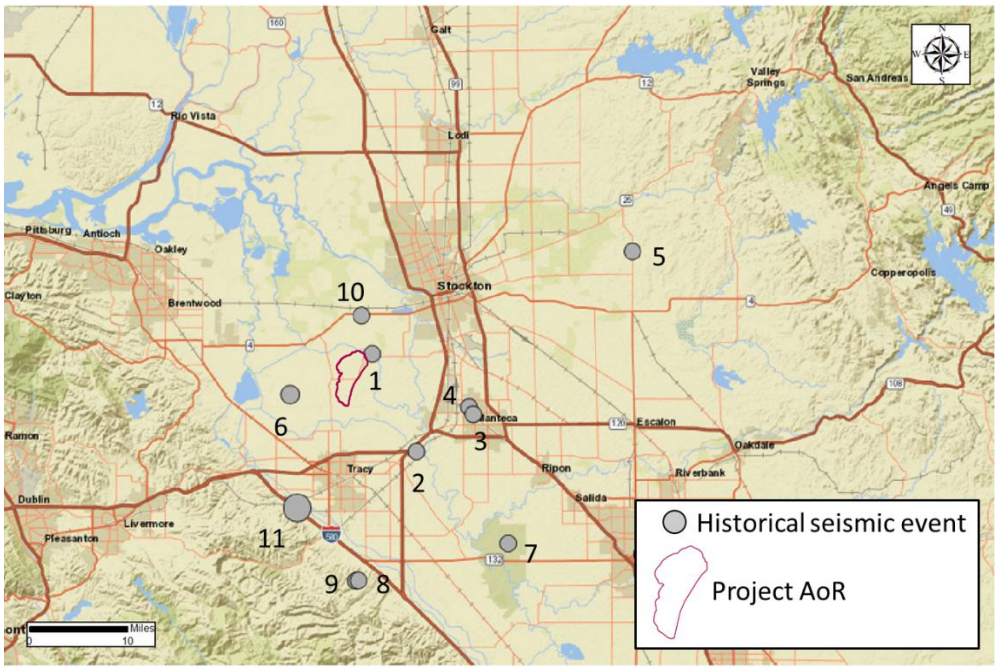

Figure 2.6-2. Image is modified from USGS search results. Data from these events are compiled in **Table 2.6-1** in chronological order associated with events 1 through 11 on the map.

The events in **Figure 2.6-2** that could be associated with the Stockton Arch Fault are events 1, 10, and 5. Event 1 is a deep event (14.6km) in 2010 which is likely related to basement movement, much deeper than the proposed injection zone or any of the sedimentary section in the basin. Event 10 is a shallower event (6.0km) which occurred in 1944, before the Union Island Field was discovered in 1972. Event 5 does sit along the trace of the Stockton Arch Fault but is further away from Union Island Field and is therefore unrelated to Union Island Field production or injection. The average depth of events from the USGS search results is 9.2km, substantially deeper than the proper Winters Formation and the entire sedimentary section within the AoR.

Table 2.6-1. Data from USGS earthquake catalog for faults in the region of CTV II.

Date	Latitude	Longitude	Depth (km)	Magnitude	Last Updated	Location
10/15/2010	37.88	-121.39	14.6	3.1	1/23/2017	9 km WSW of Taft Mosswood, California
2/10/1992	37.77	-121.32	14.6	3.1	2/9/2016	8km SSW of Lathrop, California
2/4/1991	37.81	-121.24	7.7	3.1	12/18/2016	2 km NW of Manteca, California
2/3/1991	37.82	-121.24	9.4	3.1	12/18/2016	2 km E of Lathrop, California
1/27/1980	38	-121	6	3.3	4/2/2016	8km ESE of Linden, CA
8/6/1979	37.83	-121.51	6	4.3	4/1/2016	6km NNE of Mountain House, CA
2/2/1979	37.66	-121.19	18	3.5	4/1/2016	10km WSW of Salida, CA
10/6/1976	37.61	-121.41	2.9	3.3	12/15/2016	13 km S of Tracy, California
9/5/1976	37.61	-121.41	6.5	3.5	12/15/2016	13 km S of Tracy, California
2/2/1944	37.93	-121.4	6	3.8	1/28/2016	7km SW of Country Club, CA
07/15/1866	37.7	-121.5		6	1/30/2021	Southwest of Stockton, California

While there is historical seismicity associated within the greater area, there is no clear link to the proposed injection site. There does not appear to be a causal relationship between natural gas and fluid production and any seismic event in cataloged history around the depths of the Winters Formation. By limiting the modeled reservoir pressure associated with the proposed injection to less than the original reservoir pressure, along with a 90% threshold, there is an effort to minimize any additional pressure on the fault beyond historical pressures. Additionally, due to the nature of the Stockton Arch Fault and Union Island Field being in the footwall of a thrust fault, the proposed Winters injection zone is offset against older strata with the same confining zones above. There would have to be significant re-activation of the fault as a normal fault to create offset that posed a risk for containment leaking across the fault. This would have to be in the order of thousands of feet. Pre-operational testing will include taking measured pressures from these shallower zones to confirm the Winters is an isolated reservoir with no vertical communication.

Lund-Snee and Zoback (2020) published updated maps for crustal stress estimates across North America. **Figure 2.6-3** shows a modified image from that work highlighting CTV II. This work is in agreement with previous estimates of maximum horizontal stress in the region of approximately N40°E in a strike-slip to reverse stress regime (Mount and Suppe 1992) and is consistent with World Stress map data for the area (Heidbach et al. 2016). During pre-operational testing and future injection, the fault will be monitored in both the hanging wall and footwall for pressure changes and any associated seismicity. Attachment C of this application discusses the seismicity monitoring plan for this injection site.

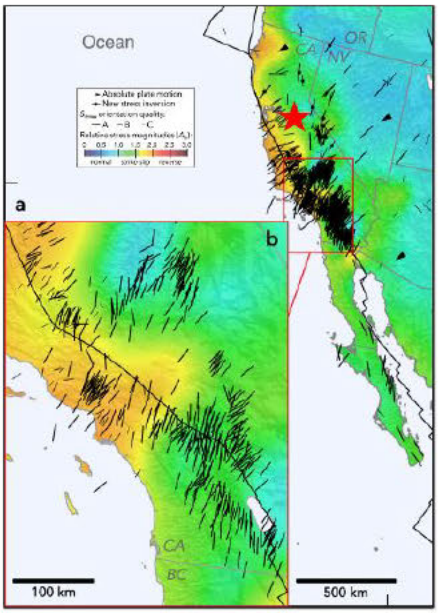

Figure 2.6-3. Image modified from Lund Snee and Zoback (2020) showing relative stress magnitudes across California. Red star indicates CTV II project site area.

2.6.2 Seismic Hazard Mitigation

The Union Island Gas Field is in an area of historical seismicity, but no events have impacted its reservoirs or oil and gas infrastructure. There are several confining zones, beginning with the Starkey-Sawtooth Shale, that separate the Winters injection interval from USDW.

The following is a summary of CTVs seismic hazard mitigation for CTV II:

The project has a geologic system capable of receiving and containing the volumes of CO_2 proposed to be injected

- Extensive historical operations in the Winters Formation at Union Island and other oil & gas fields that produce from the equivalent zone is valuable experience to understand operating conditions such as injection volumes and reservoir containment. The strategy to limit the injected CO_2 to beneath the initial reservoir pressure with a 90% threshold will mitigate the potential for induced seismic events and endangerment of the USDW
- There are no faults or fractures identified in the AoR that will impact the confinement of CO_2 injectate. The Stockton Arch Fault has proven to seal hydrocarbons at pressures above which CTV will operate.

Will be operated and monitored in a manner that will limit risk of endangerment to USDWs, including risks associated with induced seismic events

- The strategy to limit the injected CO_2 to at or beneath the initial reservoir pressure will mitigate the potential for induced seismic events and endangerment of the USDW

- Injection pressure will be lower than the fracture gradient of the sequestration reservoir with a safety factor (90% of the fracture gradient)
- Injection and monitoring well pressure monitoring will ensure that pressures are beneath the fracture pressure of the sequestration reservoir and confining zone. Injection pressure will be lower than the fracture gradients of the sequestration reservoir and confining zone with a safety factor (90% of the fracture gradients)
- A seismic monitoring program will be designed to detect events lower than seismic events that can be felt. This will ensure that operations can be modified with early warning events, before a felt seismic event

Will be operated and monitored in a way that in the unlikely event of an induced event, risks will be quickly addressed and mitigated

- Via monitoring and surveillance practices (pressure and seismic monitoring program) CTV personnel will be notified of events that are considered an early warning sign. Early warning signs will be addressed to ensure that more significant events do not occur
- CTV will establish a central control center to ensure that personnel have access to the continuous data being acquired during operations

Minimizing potential for induced seismicity and separating any events from natural to induced

- Pressure will be monitored in each injector and sequestration monitoring well to ensure that pressure does not exceed the fracture pressure of the reservoir or confining zone
- Seismic monitoring program will be installed pre-injection for a period to monitor for any baseline seismicity that is not being resolved by current monitoring programs
- Average depth of prior seismic hazard in the region based on reviewed historical seismicity has been approximately 9.2km. Significantly deeper than the proposed injection zone
- There is no evidence of causal seismicity associated with fluid production in the field

2.7 Hydrologic and Hydrogeologic Information [40 CFR 146.82(a)(3)(vi), 146.82(a)(5)]

The California Department of Water Resources has defined 515 groundwater basins and subbasins with the state. The AOR is within the Tracy Subbasin (Subbasin No. 5-22.15), which lies in the northwestern portion of the San Joaquin Valley Groundwater Basin. **Figure 2.7-1** shows the Tracy Subbasin and the surrounding areas. The Subbasin encompasses an area of about 238,429 acres (370 square miles) in San Joaquin and Alameda counties (DWR 2006).

2.7.1 Hydrologic Information

Major surface water bodies within the Tracy Subbasin consist of the San Joaquin, Old, and Middle rivers. **Figure 2.7-1** shows the location of these surface water bodies. The San Joaquin River makes up almost the entire eastern boundary of the Subbasin; It feeds water into the SWP Clifton Court Forebay, which is located just west of the Subbasin.

Two major pump stations pump water out of the Old River from the Clifton Court Forebay into two large canals: the California Aqueduct and the Delta-Mendota Canal. These large canals traverse the

southwestern portion of the Subbasin, and transport water from the Delta to other agricultural and urban water suppliers in the San Joaquin Valley and southern California. In addition to the major natural waterways there is a large network of irrigation canals, which convey surface water to agricultural properties.

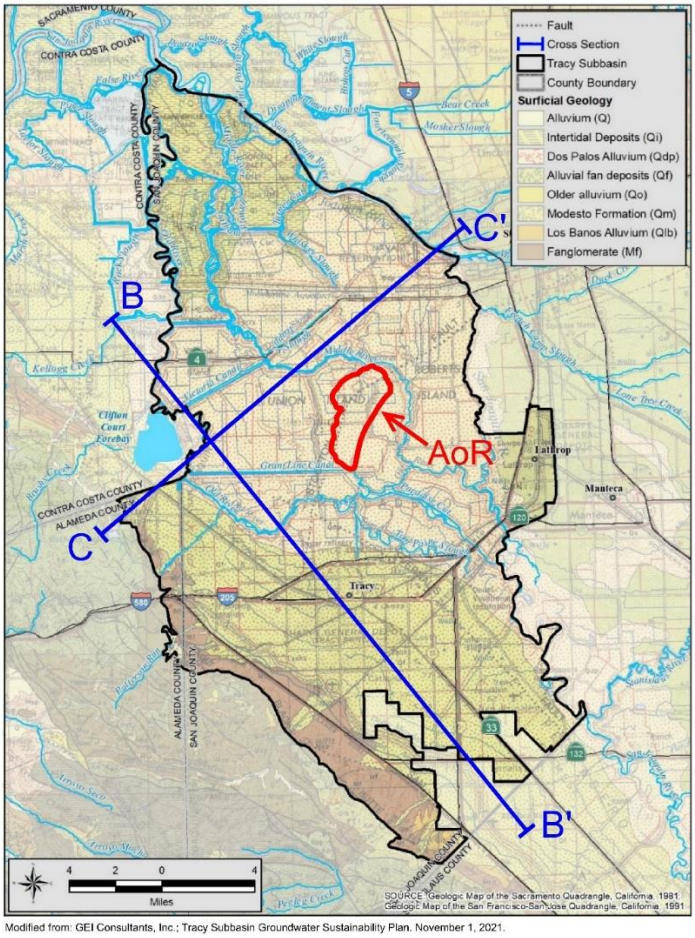

Modified from: GEI Consultants, Inc.; Tracy Subbasin Groundwater Sustainability Plan. November 1, 2021.

Figure 2.7-1. Tracy Subbasin, Surface Geology, and Cross Section Index Map

2.7.2 Base of Fresh Water and Base of USDWs

The owner or operator of a proposed Class VI injection well must define the general vertical and lateral limits of all USDWs and their positions relative to the injection zone and confining zones. The intent of this information is to demonstrate the relationship between the proposed injection formation and any USDWs, and it will support an understanding of the water resources near the proposed injection wells. A USDW is defined as an aquifer or its portion which supplies any public water system; or which contains a sufficient quantity of ground water to supply a public water system; and currently supplies drinking water for human consumption; or contains fewer than 10,000 mg/l total dissolved solids; and which is not an exempted aquifer.

2.7.2.1 Base of Fresh Water

The base of fresh water (BFW) helps define the aquifers that are used for public water supply. Local water agencies in the Tracy Subbasin have participated in various studies to comply with the 2014 Sustainable Groundwater Management Act (SGMA). Luhdorff & Scalmanini (2016) performed a study that focused on the geologic history of freshwater sediments from which groundwater is extracted for beneficial uses as defined and regulated under SGMA.

Few groundwater wells exist in the Tracy Subbasin because surface water is the source for irrigation use within delta islands. Groundwater usage is limited to eastern Contra Costa County and the Tracy area to the south. In most of western San Joaquin County in the Delta the fresh groundwater aquifers are limited to relatively shallow depths of 500 to 700 feet in the Contra Costa County area, and to 1,600 feet in the Tracy area (Luhdorff & Scalmanini, 2016).

Luhdorff & Scalmanini (1999) performed a study of over 500 well logs in eastern Contra Costa County groundwater for five water agencies. The focus of this study was the uppermost 500 feet, where most water wells were completed. Subsequently Luhdorff & Scalmanini (2016) used logs also examined for the nature of geologic units at greater depths to better define the BFW. The top of the geophysical logs tended to be at 800 feet or greater depths. These logs generally show fine-grained geologic units with few sand beds. The depth to base of fresh water was difficult to discern in available geophysical logs because of the lack of sand beds. The elevation of the base of freshwater aquifers determined from logs were plotted on a base map (see **Figure 2.7-2**). Contour lines of one hundred feet were drawn, but are variable based on well control.

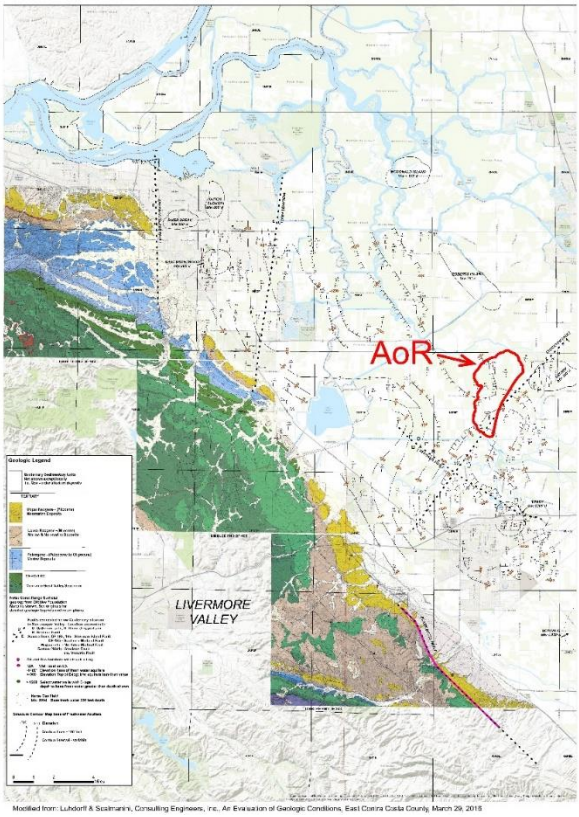

Modified from: Luhdorff & Scalmanini, Consulting Engineers, Inc. An Evaluation of Geologic Conditions, East Contra Costa County, March 29, 2016

Figure 2.7-2. Geologic Map and Base of Fresh Water

2.7.2.2 Base of USDWs

CTV has used geophysical logs to investigate the base of the USDW. The calculation of salinity from logs used by CTV is a four-step process:

(1) converting measured density or sonic to formation porosity

The equation to convert measured density to porosity is:

$$POR = \frac{(Rhom - RHOB)}{(Rhom - Rhof)} \quad (5)$$

Parameter definitions for the equation are:

POR is formation porosity

Rhom is formation matrix density grams per cubic centimeters (g/cc); 2.65 g/cc is used for sandstones

RHOB is calibrated bulk density taken from well log measurements (g/cc)

Rhof is fluid density (g/cc); 1.00 g/cc is used for water-filled porosity

The equation to convert measured sonic slowness to porosity is:

$$POR = -1\left(\frac{\Delta tma}{2\Delta tf} - 1\right) - \sqrt{\left(\frac{\Delta tma}{2\Delta tf} - 1\right)^2 + \frac{\Delta tma}{\Delta tlog} - 1} \quad (6)$$

Parameter definitions for the equation are:

POR is formation porosity

Δtma is formation matrix slowness (µs/ft); 55.5 µs/ft is used for sandstones

Δtf is fluid slowness (µs/ft); 189 µs/ft is used for water-filled porosity

Δtlog is formation compressional slowness from well log measurements (µs/ft)

(2) calculation of apparent water resistivity using the Archie equation,

The Archie equation calculates apparent water resistivity. The equation is:

$$Rwah = \frac{POR^m R_t}{a} \quad (7)$$

Parameter definitions for the equation are:

Rwah is apparent water resistivity (ohmm)

POR is formation porosity

m is the cementation factor; 2 is the standard value

R_t is deep reading resistivity taken from well log measurements (ohmm)

a is the archie constant; 1 is the standard value

(3) correcting apparent water resistivity to a standard temperature

Apparent water resistivity is corrected from formation temperature to a surface temperature standard of 75 degrees Fahrenheit:

$$Rwahc = Rwah\frac{TEMP + 6.77}{75 + 6.77} \quad (8)$$

Parameter definitions for the equation are:

Rwahc is apparent water resistivity (ohmm), corrected to surface temperature

TEMP is down hole temperature based on temperature gradient (DegF)

(4) converting temperature corrected apparent water resistivity to salinity.

The following formula was used (Davis 1988):

$$SAL\_a\_EPA = \frac{5500}{Rwahc} \quad (9)$$

Parameter definitions for the equation are:

SAL_a_EPA is salinity from corrected Rwahc (ppm)

The base of fresh water and the USDW are shown on the geologic Cross Section A-A' (**Figure 2.2-4**) The base of fresh water and based of the lowermost USDW are at a measure depths of approximately 600 ft bgs and 2,400 ft bgs, respectively.

2.7.3 Formations with USDWs

Formations with USDWs, from youngest to oldest, include Alluvium, Flood Basin and Intertidal deposits, Alluvial Fan Deposits, Older Alluvium, Modesto Formation, Los Banos Alluvium, Tulare Formation, and Fanglomerates. These formations, except for the Tulare Formation, are shown on **Figure 2.7-1**. The Tulare Formation is not exposed at ground surface. The cumulative thickness of these formations increases from about 330 feet near the Coast Range foothills to about 2,000 feet just north of Tracy. Information regarding the water-bearing units and groundwater conditions were taken from several sources (Hotchkiss and Balding 1971, Bertoldi et al. 1991, Davis G.H. et al. 1959) and sorted to agree with more recent geologic map compilation (Wagner et al. 1991).

2.7.3.1 Alluvium

The Alluvium (Q) includes sediments deposited in the channels of active streams as well as overbank deposits and terraces of those streams. They consist of unconsolidated silt, sand, and gravel. Sand and gravel zones in the younger alluvium are highly permeable and yield significant quantities of water to wells. The thickness of the younger alluvium in the Tracy Subbasin is less than 100 feet (DWR 2006).

2.7.3.2 Flood Basin and Intertidal Deposits

The Flood Basin Deposits (Dos Palos Alluvium [Qdp]) and Intertidal Deposits (Qi) are in the Delta portions of the Subbasin. These sediments consist of peaty mud, clay, silt, sand and organic materials. Stream-channel deposits of coarse sand and gravel are also included in this unit. The flood basin deposits have low permeability and generally yield low quantities of water to wells due to their fine-grained nature. Flood basin deposits generally contain poor quality groundwater with occasional zones of fresh water. The maximum thickness of the unit is about 1,400 feet (DWR 2006).

2.7.3.3 Alluvial Fan Deposits

Along the southern margin of the Subbasin, in the Non-Delta uplands areas of the Subbasin are fan deposits (Qf) from the Coast Ranges. These deposits consist of loosely to moderately compacted sand, silt, and gravel deposited in alluvial fans during the Pliocene and Pleistocene

ages. The fan deposits likely interfinger with the Flood Basin Deposits. The thickness of these fans is about 150 feet (DWR 2006).

2.7.3.4 Modesto Formation

The Modesto Formation (Qm) is located along the east side of the San Joaquin River and is slightly older that the Alluvial Fan Deposits. The formation consists of granitic sands over stratified silts and sands. Near the southern margin of the Tracy Subbasin, there are small occurrences of Los Banos Alluvium (Qlb) and Older Alluvium (Qo) that are of similar age as the Modesto Formation (GEI 2021).

2.7.3.5 Tulare Formation

The Tulare Formation is Pleistocene in age and consists of semi consolidated, poorly sorted, discontinuous deposits of clay, silt, sand and gravel. The Tulare Formation is not exposed at ground surface in the Tracy Subbasin. The Tulare Formation sand and gravel deposits are moderately permeable, and most of the larger agricultural, municipal, and industrial supply wells extract water from this formation. Wells completed in the Tulare Formation can produce up to 3,000 gallons per minute (gpm). The thickness of the Tulare Formation is about 1,400 feet (GEI 2021).

Within the Tulare Formation is the Corcoran Clay, one of the largest lakebed deposits in the San Joaquin Valley. The clay is about 60 to 100 feet thick**. Figure 2.7-3** shows the lateral extent and structure of the Corcoran Clay. Near the southern edge of the Subbasin the Corcoran Clay is apparently absent. The extent of the Corcoran Clay is not fully characterized to the west and north (Page 1986) due to the lack of deep wells. Geologic sections indicate that the clay likely continues to the west, into the East Contra Costa Subbasin (GEI 2007).

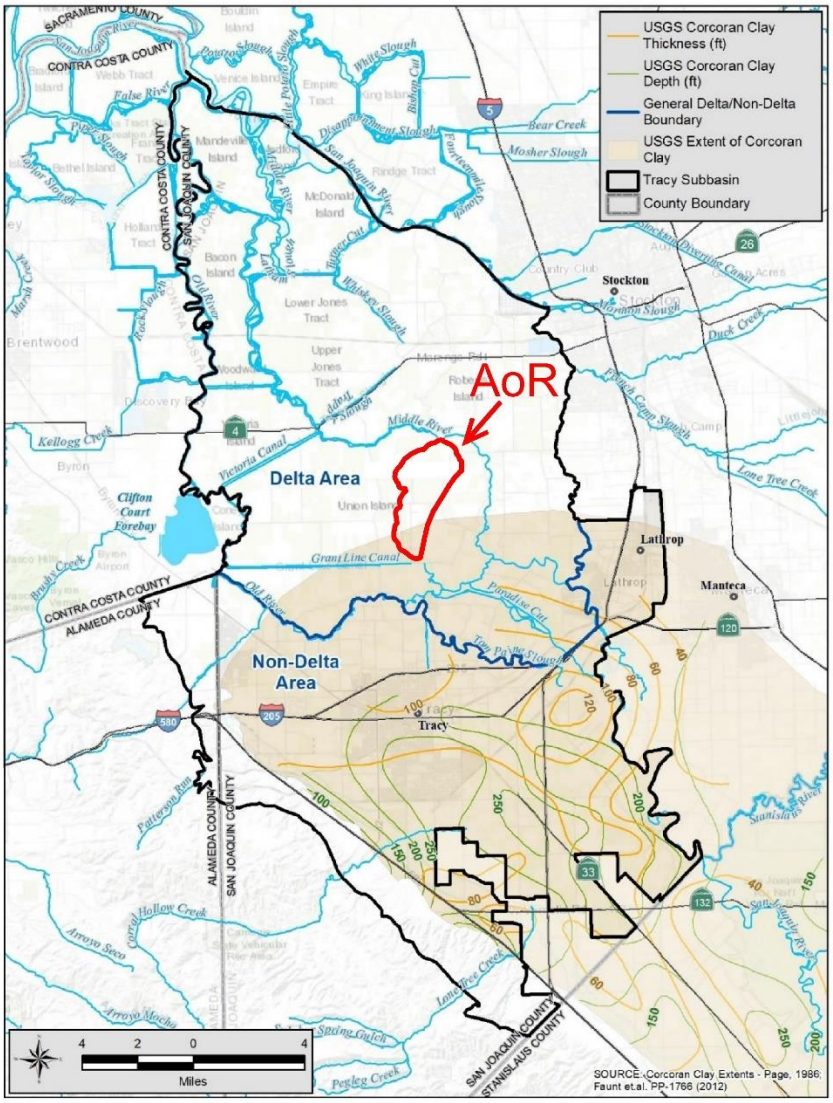

Modified from: GEI Consultants, Inc.; Tracy Subbasin Groundwater Sustainability Plan. November 1, 2021.

Figure 2.7-3. Estimated Corcoran Clay Thickness and Extent

2.7.3.6 Undifferentiated Non-marine Sediments

The upper Paleogene and Neogene sequence begin with the Valley Springs Formation which represents fluvial deposits that blanket the entire southern Sacramento Basin. The unconformity at the base of the Valley Springs marks a widespread Oligocene regression and separates the more deformed Mesozoic and lower Paleogene strata below from the less deformed uppermost Paleogene and Neogene strata above. These undifferentiated non-marine sediments contain approximately 3,000 - 10,000 milligrams per liter (mg/l) total dissolved solids (TDS) water and is the lowermost USDW in the A7oR (**Figure 2.2-4**).

2.7.4 Geologic Cross Sections Illustrating Formations with USDWs

Geologic sections (locations are shown on **Figures 2.7-1)**, cross the length of the Subbasin to illustrate the relationship of the geologic units. The geologic sections were originally prepared for the Tracy Subbasin Groundwater Management Plan (GEI 2007) and were modified for the Tracy Subbasin GSP ((GEI 2021)) to reflect additional information obtained since 2007. Lithologic information from well logs was normalized and digitized to generally conform with the Unified Soil Classification System. Lithology and well screens from groundwater monitoring wells constructed since the sections were created were also added to the geologic sections. The soil profiles show the subsurface relationships and location of the formations and coarse-grained sediments that comprise the principal aquifers. The cross sections show the sediment types, the approximate base of freshwater, and the estimated contact between the Tulare Formation sediments and younger formations. The cross sections also illustrate the location and extent of the Corcoran Clay (GEI 2021).

Geologic Cross Section B-B' (**Figure 2.7-4)** runs northwest-southeast through the non-Delta and Delta portions of the Tracy Subbasin. The Subbasin generally has low permeability clays and silts (shown in brown color) near surface and permeable sediments (sands and gravels shown in light blue) scattered throughout the profile. Continuous layers of sand and gravels, other than one at the top of the Corcoran Clay have not been identified. The lack of continuous layers of sand and gravels is likely due to the nature of the river channels, and flood deposits associated with these types of sediments. The Corcoran Clay (or its equivalent) seems to extend to the west and into the East Contra Costa Subbasin. In the southern non-Delta portion of the Subbasin, fine-grained sediments are more prevalent. Based upon groundwater levels and water quality information, the shallow aquifer is likely unconfined and separated from the deeper confined aquifer (GEI 2021).

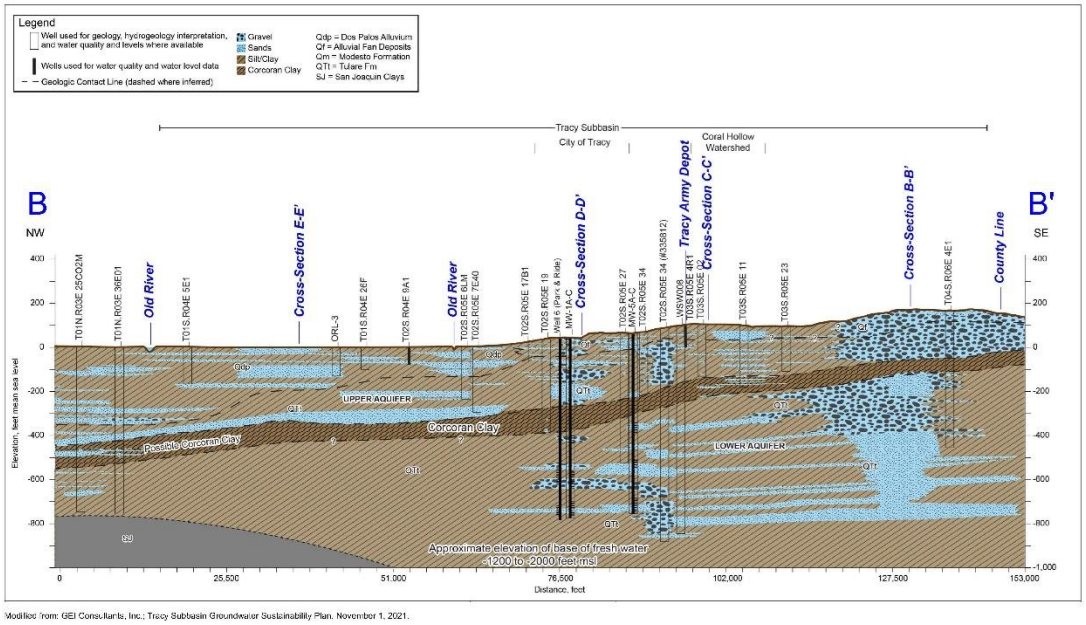

Modified from: GEI Consultants, Inc.; Tracy Subbasin Groundwater Sustainability Plan. November 1, 2021.

Figure 2.7-4. Geologic Cross Section B-B'

Geologic Cross Section C-C' (**Figure 2.7-5**) runs a northeast-southwest orientation across the Delta area. This geologic section illustrates the types of sediments, the estimated base of freshwater, the possible location of the Corcoran Clay (or its equivalent). Where the clay location is uncertain, no wells were present that penetrated deep enough to confirm its presence or absence. The base of fresh water varies throughout the Subbasin and is shown on the sections. It is as shallow as -400 feet msl to as much as -2,000 feet msl (GEI 2021).

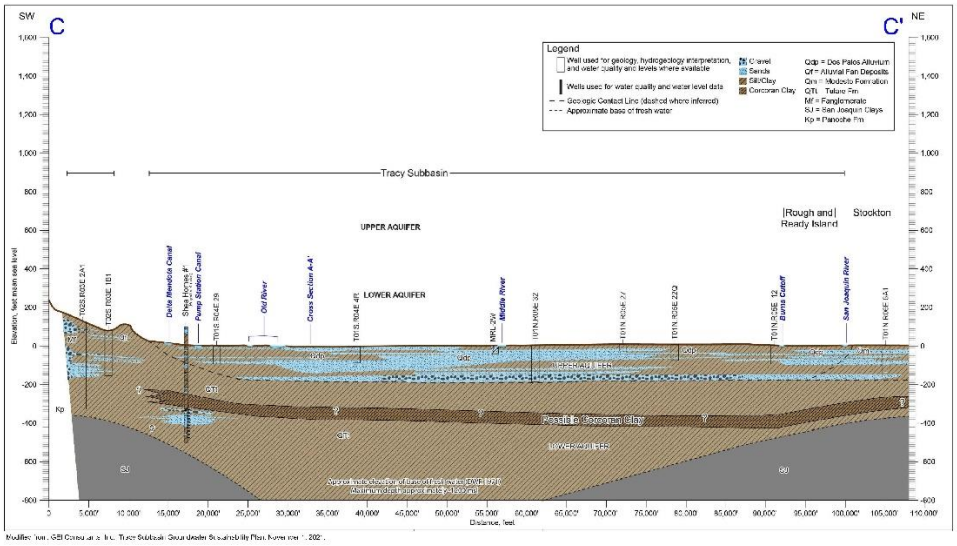

Figure 2.7-5. Geologic Cross Section C-C'

2.7.5 Principal Aquifers

The Tracy Subbasin has two principal aquifers that are separated by the Corcoran Clay. Where the clay is absent, which is the condition within most of the Delta area, only the Upper Aquifer is present. The Upper and Lower Aquifers combine where the Corcoran Clay is absent, near the southwestern portion of the subbasin adjacent to the foothills. In this area, the aquifers would be unconfined and are the Upper Aquifer. The Upper and Lower Aquifers also merge north of the Old River in the northern part of the Subbasin (GEI 2021).

2.7.5.1 Upper Aquifer

The Upper Aquifer is used by domestic, community water systems, and for agriculture. The Upper aquifer also supports native vegetation where groundwater levels are less than 30 feet bgs (GEI 2021).

The Upper Aquifer is an unconfined to semi-confined aquifer. It is present above the Corcoran Clay and where the clay is absent. The Upper aquifer exists in the Alluvial Fan Deposits, Intertidal Deposits, Modesto Formation, Flood Basin Deposits, the upper portions of the Tulare Formation.

There are multiple coarse-grained sediment layers that make up the unconfined aquifer, however the water levels are generally similar. Generally, the aquifer confinement tends increase with depth becoming semi-confined conditions. There is also typically a downward gradient in the aquifers (Hotchkiss and Balding 1971) in the non-Delta areas; the gradient ranges from a few feet bgs to as much as 70 feet bgs. The groundwater levels in the Upper Aquifer are usually 10 to 30 feet higher than in the Lower Aquifer. The groundwater levels In the Delta are typically at sea level and artesian flowing wells are common in the center of the islands (Hydrofocus 2015).

The hydraulic characteristics of the unconfined aquifer are highly variable. The USGS estimated horizontal hydraulic conductivity values for organic sediments ranging from 0.0098 ft/d to 133.86 ft/d (Hydrofocus 2015). Wells in the unconfined aquifer produce 6 to 5,300 gpm. The transmissivity of the unconfined aquifers, ranges between 600 to greater than 2,300 gallons per day per foot (gpd/ft). The storativity is about 0.05 (GEI 2021).

Water quality in the Upper Aquifer is mostly transitional, with no single predominate anion. Most water are characterized as sulfate bicarbonate and chloride bicarbonate type (Hotchkiss and Balding 1971). The TDS of these transitional water ranges between 400 to 4,200 mg/L. Nitrate is generally high in the Upper aquifer in the non-Delta portions of the Subbasin. Nitrate is generally low in the Delta portions of the Subbasin (GEI 2021).

2.7.5.2 Lower Aquifer

The Lower Aquifer is typically used by community water systems (City of Tracy) and agriculture. The Lower Aquifer is mainly comprised of the lower portions of the Tulare Formation below the Corcoran Clay and extends to the base of fresh water. The clay is present in the southern third of

the Subbasin; the clay's extent to the west and north is uncertain and has been estimated to have a vertical permeability ranging from 0.01 to 0.007 feet per day (Burow et al. 2004).

The groundwater levels are generally deeper than water levels in the Upper Aquifer (Hotchkiss and Balding 1971). Groundwater levels in the confined aquifer are about -25 to -75 feet msl. The groundwater levels are normally 60 to 200 feet above the top of the Corcoran Clay.

Wells in the Lower Aquifer produce about 700 to 2,500 gpm. The transmissivity typically ranges from 12,000 to 37,000 gpd/ft, but can be 120,000 gpd/ft. The storage coefficient or storativity has been measured to be 0.0001 (Padre 2004).

Water quality in the Lower Aquifer in the western portions are chloride type water but mostly transitional type of sulfate chloride near the valley margins and sulfate bicarbonate and bicarbonate sulfate near the San Joaquin River (Hotchkiss and Balding 1971). In general, the TDS ranges between 400 and 1,600 mg/L. Nitrate is typically low in the Lower Aquifer. Wells completed below the Corcoran Clay sometimes have elevated levels of sulfate and total dissolved solids above the drinking water MCLs. Only at one deep location, east of Tracy, are chloride levels elevated (GEI 2021).

2.7.6 Potentiometric Maps

The Tracy Subbasin GSP (GEI 2021) used groundwater level measurements in over 226 wells, which have been reported to DWR's CASGEM or Water Data Library systems. To evaluate groundwater levels, the GSP only used wells with known total depths and construction details so that the wells were assigned to a principal aquifer. To supplement data from these wells, additional monitoring wells were located that were being used for other regulatory programs.

2.7.6.1 Upper Aquifer

Groundwater elevations in the Delta area are typically below sea level because the ground surface in the islands have subsided to below sea level; the drains within the island keep groundwater levels bgs to allow for farming. **Figure 2.7-6** shows a schematic profile for groundwater surfaces that are expected at the islands. Although each island has distinct groundwater elevations, there are similar hydraulics on all islands. Groundwater elevations are higher near the island edges (adjacent to waterways) and deepen equivalent with the deepest land surface and drain. Groundwater elevations in the islands are managed by the elevations of the drains and canals. There is very little, if any, pumping of wells for agriculture. Since drains and canals control the groundwater elevations, groundwater contours are not developed/monitored for the Delta islands (GEI 2021).

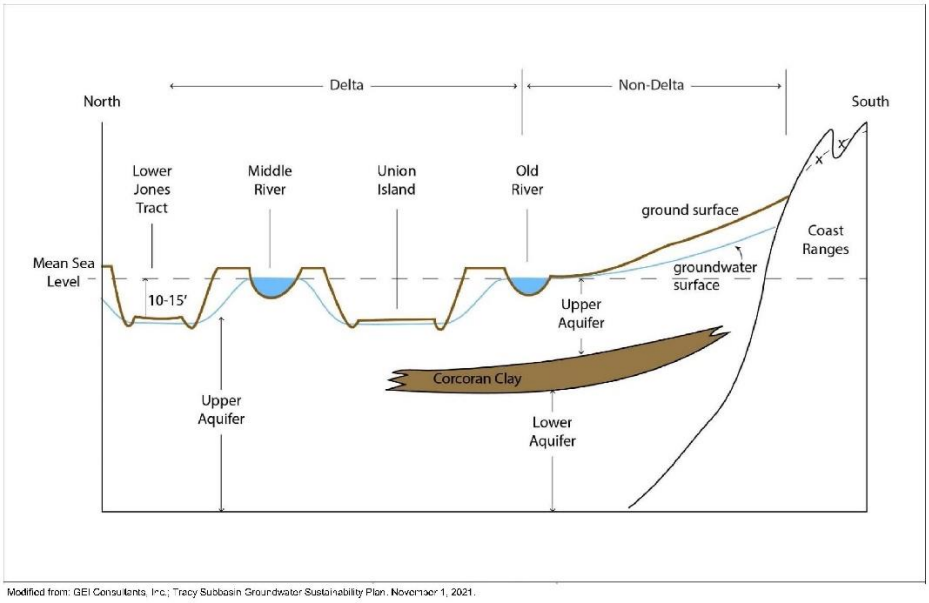

Figure 2.7-6. Principal Aquifer Schematic Profile

In the non-Delta areas west of the San Joaquin River, groundwater contours for the Upper Aquifer indicate groundwater elevations are highest near the Coast Ranges and decrease toward the Delta. Flow directions indicate that recharge areas are present along the foothills and that groundwater discharges into the Old River and/or Tom Paine Slough (**Figure 2.7-7**). Groundwater gradients in the non-Delta portions of the Subbasin are the steepest, at approximately 0.008 foot/foot. East of the San Joaquin River, near Lathrop, the river recharges the Upper Aquifer; flows towards a pumping depression near Stockton. Groundwater contours at the southeastern edge of the Subbasin are perpendicular to the Stanislaus-San Joaquin County line, suggesting that there is no flow in the Upper Aquifer between the subbasins, other than the areas of the Delta Mendota Subbasin north of the County line, where water apparently flows into and out of both subbasins.

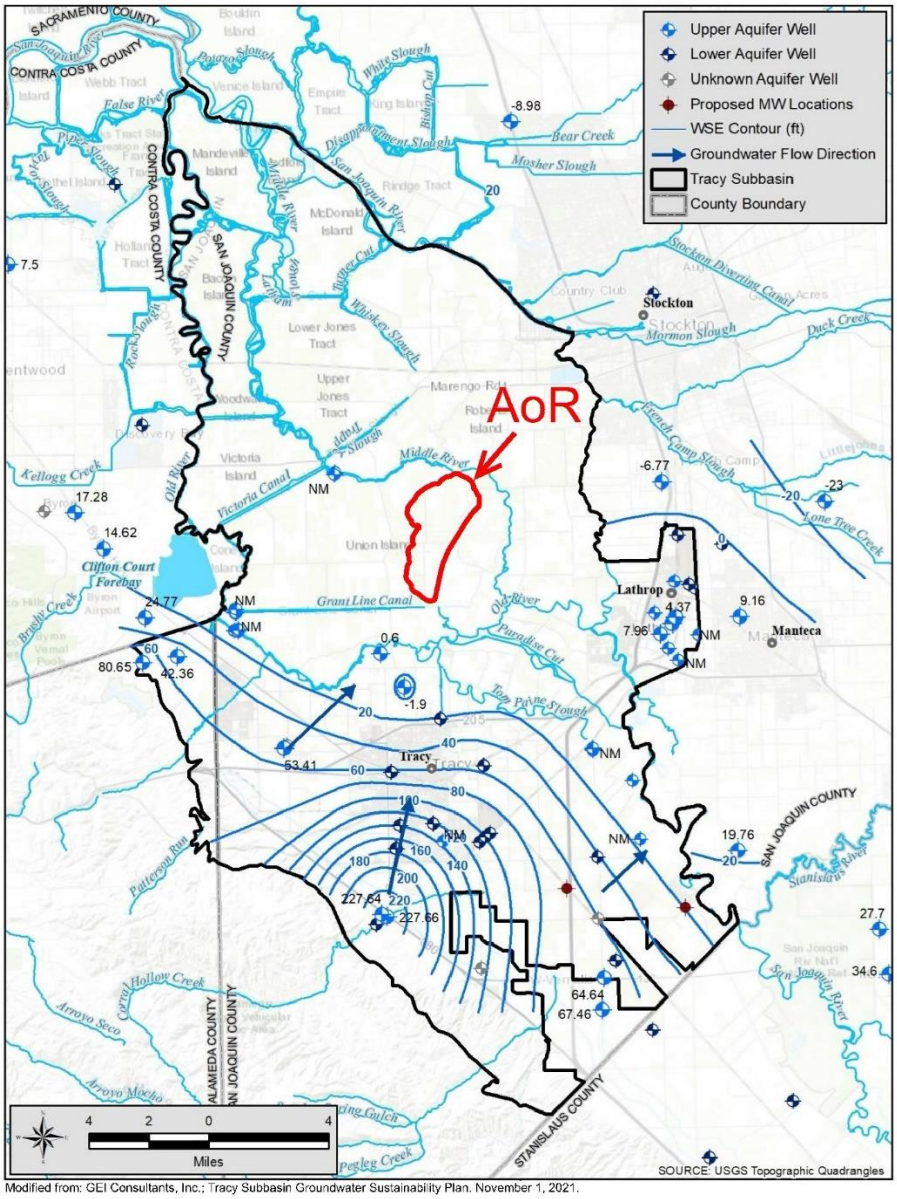

Modified from: GEI Consultants, Inc.; Tracy Subbasin Groundwater Sustainability Plan. November 1, 2021.

Figure 2.7-7. Upper Aquifer Groundwater Elevations Fall 2019

2.7.6.2 Lower Aquifer

The Corcoran Clay extends throughout the non-Delta areas and only slightly into the Delta area, at Union Island. Groundwater contours for the Lower Aquifer were developed using data from the CASGEM monitoring wells that are constructed below the Corcoran Clay and supplemented by data from municipal wells (**Figure 2.7-8**). Groundwater monitoring well data were used from the adjacent Delta Mendota Subbasin (GEI 2021).

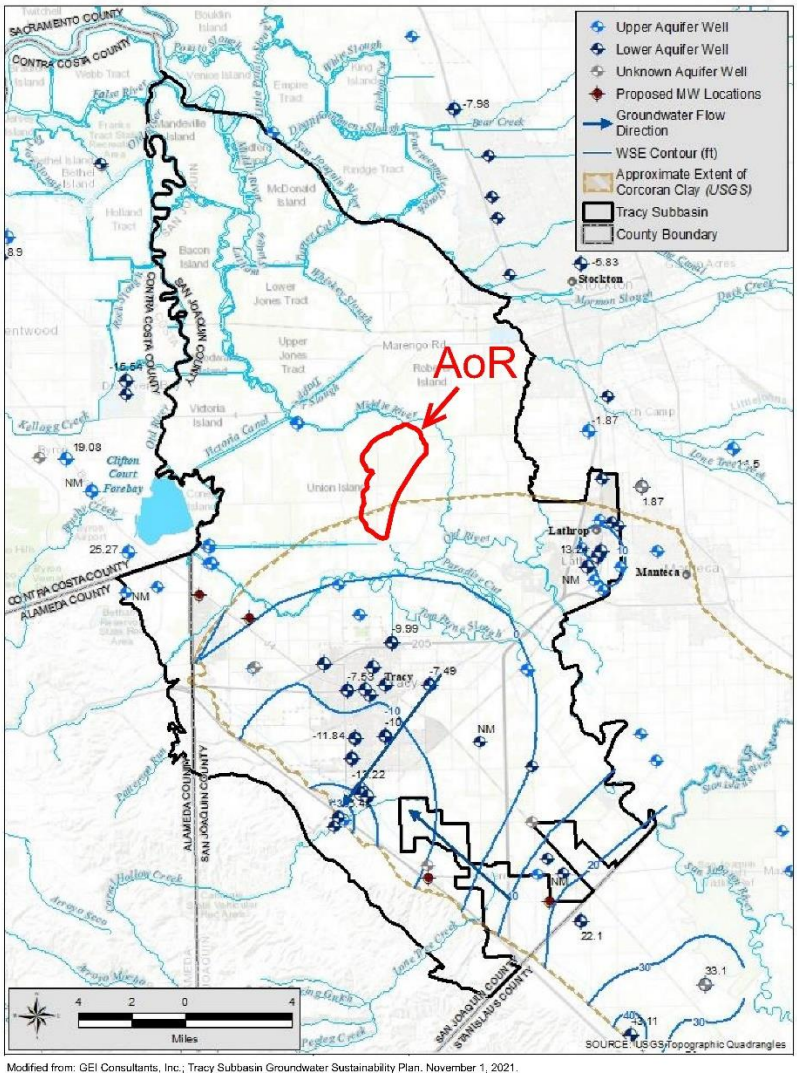

Modified from: GEI Consultants, Inc.; Tracy Subbasin Groundwater Sustainability Plan. November 1, 2021.

Figure 2.7-8. Lower Aquifer Groundwater Elevations Spring 2019

Groundwater elevation contours in the Lower Aquifer imply groundwater is entering the subbasin from the south (Delta Mendota Subbasin) and from the east (Eastern San Joaquin Subbasin). Pumping in the vicinity of the City of Tracy has apparently modified this overall regional flow, resulting in a pumping depression towards the City of Tracy. The groundwater levels are expected to be at sea level near the northern edge of the Corcoran Clay extent (GEI 2021).

The groundwater gradient in Fall 2019 from the Delta Mendota and the Eastern San Joaquin subbasins is estimated to be 0.0009 foot/foot into the Tracy Subbasin. Due to the pumping depression, the gradient increases around the City of Tracy. The gradient near the western edge

of the subbasin cannot be determined to the lack of monitoring wells constructed below the Corcoran Clay (GEI 2021).

2.7.7 Water Supply and Groundwater Monitoring Wells

The California State Water Resources Control Board Groundwater Ambient Monitoring Assessment Program (GAMA), the Department of Water Resources (DWR), CASGEM, and other public databases were searched to identify any water supply and groundwater monitoring wells within a one-mile radius of the AOR. 35 water supply wells were identified within one mile of the AoR. Data provided from public databases indicate that the wells identified are completed much shallower than the proposed injection zone. A map of well locations and table of information are found in **Figure 2.7-9** Water Well Map and **Table 2.7-1** Water Well Information, respectively.

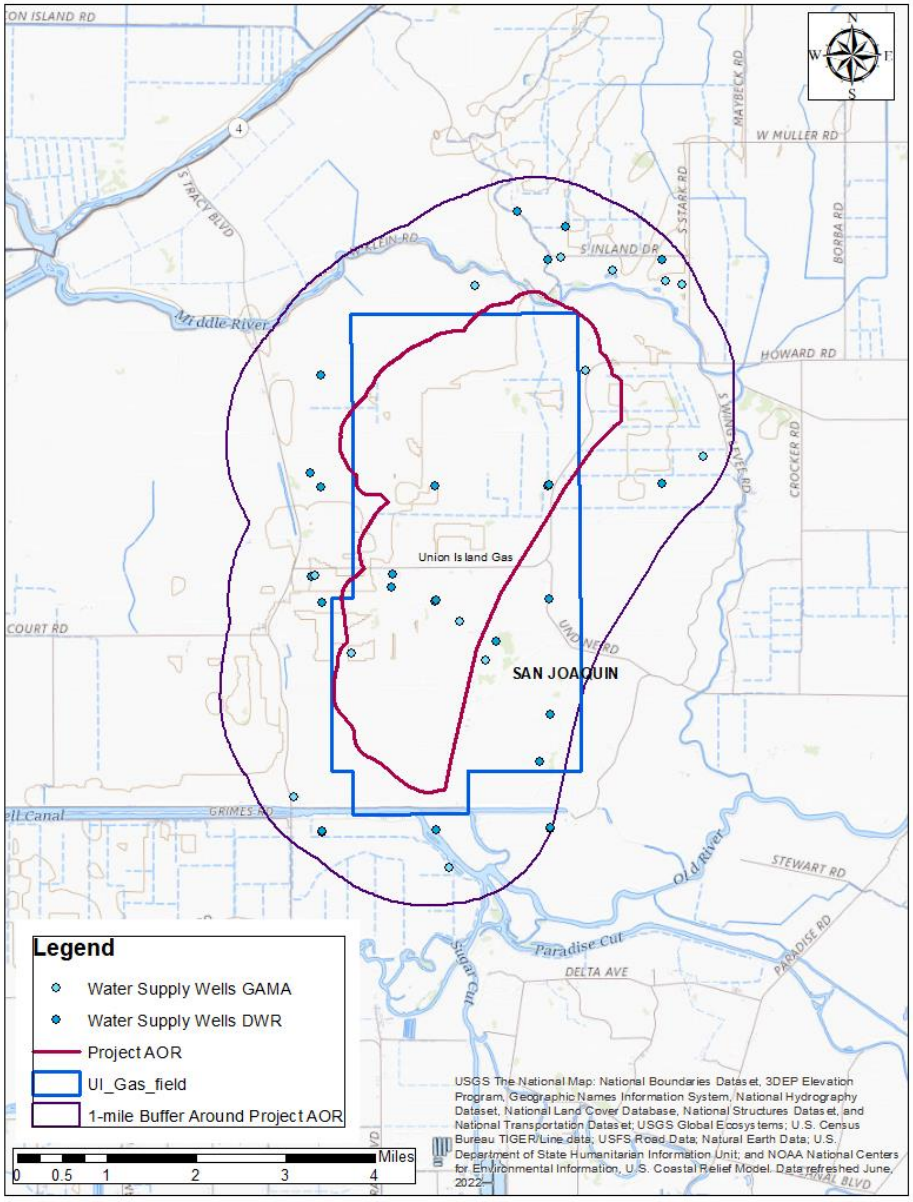

Figure 2.7-9. Water Well Location Map

Groundwater in the Subbasin is used for municipal, industrial, irrigation, domestic, stock watering, frost protection, and other purposes. The number of water wells is based on well logs filed and contained within public records may not reflect the actual number of active wells because many of the wells contained in files may have been destroyed and others may not have been recorded.

There are many more wells in the non-Delta areas, south of the Old River, than in the Delta area of the Subbasin. The depths of wells are generally deeper in the non-Delta portion of the Subbasin as compared to the Delta portion of the Subbasin. Typically, the domestic wells are constructed to shallower depths than the production wells. The municipal wells are generally constructed deeper than either the domestic or production wells (GEI 2021).

2.8 Geochemistry [40 CFR 146.82(a)(6)]

2.8.1 Formation Geochemistry

2.8.1.1 Winters Formation

As noted in the mineralogy section (section 2.4.1).

2.8.1.2 Upper Confining Zone (Starkey-Sawtooth Shale)

As noted in the mineralogy section (section 2.4.1).

2.8.1.3 Delta Shale

As noted in the mineralogy section (section 2.4.1).

2.8.2 Fluid Geochemistry

The Winters Formation contains both saline water and gaseous hydrocarbon within the AoR. The well Sonol_Securities_4 was sampled for water in 2015. The measurement of total dissolved solids (TDS) for the sample is 15595 mg/L. The complete water chemistry is shown in **Figure 2.8-1**.

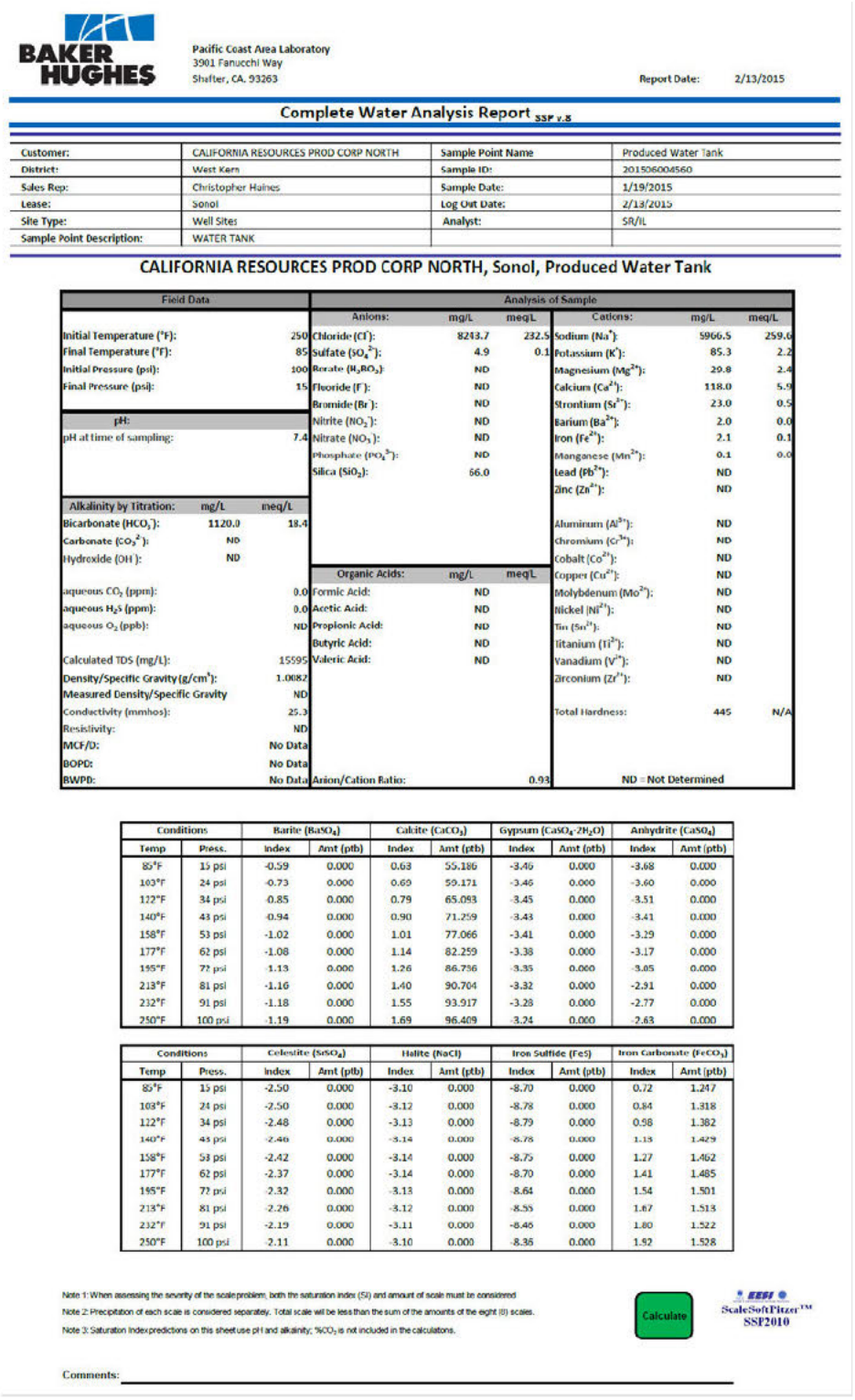

BAKER HUGHES

Pacific Coast Area Laboratory
3901 Fanucchi Way
Shafter, CA. 93263

Report Date: 2/13/2015

Complete Water Analysis Report SSP v.8

Customer:	CALIFORNIA RESOURCES PROD CORP NORTH	Sample Point Name	Produced Water Tank
District:	West Kern	Sample ID:	201506004560
Sales Rep:	Christopher Haines	Sample Date:	1/19/2015
Lease:	Sonol	Log Out Date:	2/18/2015
Site Type:	Well Sites	Analyst:	SR/IL
Sample Point Description:	WATER TANK		

CALIFORNIA RESOURCES PROD CORP NORTH, Sonol, Produced Water Tank

Field Data

Initial Temperature (°F):	250
Final Temperature (°F):	85
Initial Pressure (psi):	100
Final Pressure (psi):	15

pH:

pH at time of sampling:	7.4

Alkalinity by Titration:	mg/L	meq/L
Bicarbonate (HCO_3^-):	1120.0	18.4
Carbonate (CO_3^{2-}):	ND	
Hydroxide (OH^-):	ND	

aqueous CO_2 (ppm):	0.0
aqueous H_2S (ppm):	0.0
aqueous O_2 (ppb):	ND
Calculated TDS (mg/L):	15595
Density/Specific Gravity (g/cm³):	1.0082
Measured Density/Specific Gravity	ND
Conductivity (mmhos):	25.3
Resistivity:	ND
MCF/D:	No Data
BOPD:	No Data
BWPD:	No Data

Analysis of Sample

Anions:	mg/L	meq/L
Chloride (Cl^-):	8243.7	232.5
Sulfate (SO_4^{2-}):	4.9	0.1
Borate ($H_2BO_3^-$):	ND	
Fluoride (F^-):	ND	
Bromide (Br^-):	ND	
Nitrite (NO_2^-):	ND	
Nitrate (NO_3^-):	ND	
Phosphate (PO_4^{3-}):	ND	
Silica (SiO_2):	66.0	

Organic Acids:	mg/L	meq/L
Formic Acid:	ND	
Acetic Acid:	ND	
Propionic Acid:	ND	
Butyric Acid:	ND	
Valeric Acid:	ND	

Cations:	mg/L	meq/L
Sodium (Na^+):	5966.5	259.6
Potassium (K^+):	85.3	2.2
Magnesium (Mg^{2+}):	29.8	2.4
Calcium (Ca^{2+}):	118.0	5.9
Strontium (Sr^{2+}):	23.0	0.5
Barium (Ba^{2+}):	2.0	0.0
Iron (Fe^{2+}):	2.1	0.1
Manganese (Mn^{2+}):	0.1	0.0
Lead (Pb^{2+}):	ND	
Zinc (Zn^{2+}):	ND	
Aluminum (Al^{3+}):	ND	
Chromium (Cr^{3+}):	ND	
Cobalt (Co^{2+}):	ND	
Copper (Cu^{2+}):	ND	
Molybdenum (Mo^{2+}):	ND	
Nickel (Ni^{2+}):	ND	
Tin (Sn^{2+}):	ND	
Titanium (Ti^{3+}):	ND	
Vanadium (V^{2+}):	ND	
Zirconium (Zr^{4+}):	ND	
Total Hardness:	445	N/A

Anion/Cation Ratio:	0.93

ND = Not Determined

Conditions		Barite ($BaSO_4$)		Calcite ($CaCO_3$)		Gypsum ($CaSO_4 \cdot 2H_2O$)		Anhydrite ($CaSO_4$)	
Temp	Press.	Index	Amt (ptb)	Index	Amt (ptb)	Index	Amt (ptb)	Index	Amt (ptb)
85°F	15 psi	-0.59	0.000	0.63	55.186	-3.46	0.000	-3.68	0.000
103°F	24 psi	-0.73	0.000	0.69	59.171	-3.46	0.000	-3.60	0.000
122°F	34 psi	-0.85	0.000	0.79	65.093	-3.45	0.000	-3.51	0.000
140°F	43 psi	-0.94	0.000	0.90	71.259	-3.43	0.000	-3.41	0.000
158°F	53 psi	-1.02	0.000	1.01	77.066	-3.41	0.000	-3.29	0.000
177°F	62 psi	-1.08	0.000	1.14	82.259	-3.38	0.000	-3.17	0.000
195°F	72 psi	-1.13	0.000	1.26	86.736	-3.35	0.000	-3.05	0.000
213°F	81 psi	-1.16	0.000	1.40	90.704	-3.32	0.000	-2.91	0.000
232°F	91 psi	-1.18	0.000	1.55	93.917	-3.28	0.000	-2.77	0.000
250°F	100 psi	-1.19	0.000	1.69	96.409	-3.24	0.000	-2.63	0.000

Conditions		Celestite ($SrSO_4$)		Halite (NaCl)		Iron Sulfide (FeS)		Iron Carbonate ($FeCO_3$)	
Temp	Press.	Index	Amt (ptb)	Index	Amt (ptb)	Index	Amt (ptb)	Index	Amt (ptb)
85°F	15 psi	-2.50	0.000	-3.10	0.000	-8.70	0.000	0.72	1.247
103°F	24 psi	-2.50	0.000	-3.12	0.000	-8.78	0.000	0.84	1.318
122°F	34 psi	-2.48	0.000	-3.13	0.000	-8.79	0.000	0.98	1.382
140°F	43 psi	-2.46	0.000	-3.14	0.000	-8.78	0.000	1.13	1.429
158°F	53 psi	-2.42	0.000	-3.14	0.000	-8.75	0.000	1.27	1.462
177°F	62 psi	-2.37	0.000	-3.14	0.000	-8.70	0.000	1.41	1.485
195°F	72 psi	-2.32	0.000	-3.13	0.000	-8.64	0.000	1.54	1.501
213°F	81 psi	-2.26	0.000	-3.12	0.000	-8.55	0.000	1.67	1.513
232°F	91 psi	-2.19	0.000	-3.11	0.000	-8.46	0.000	1.80	1.522
250°F	100 psi	-2.11	0.000	-3.10	0.000	-8.36	0.000	1.92	1.528

Note 1: When assessing the severity of the scale problem, both the saturation index (SI) and amount of scale must be considered
Note 2: Precipitation of each scale is considered separately. Total scale will be less than the sum of the amounts of the eight (8) scales.
Note 3: Saturation Index predictions on this sheet use pH and alkalinity; $\%CO_2$ is not included in the calculations.

Calculate

EESI ScaleSoftPitzer™ SSP2010

Comments: _____

Figure 2.8-1. Water geochemistry for the Sonol_Securities_4 well.

Gas analysis for the Sonol_Securities_5 was performed in 2022. The gas is primarily methane and nitrogen, with very minor ethane and carbon dioxide. The full gas chromatography is included in **Figure 2.8-2.**

Dick Brown's Technical Service

Gas & Oilfield Measurement and Control Specialist
Design - Installation - Service

Company: CRC
Location: Sonol #5
Meter ID:
Analysis Time: 03/01/2022 15:14 Sample Type: Spot
Flowing Temp.: 80 Deg. F Flowing Pressure: 15 psig

Comp	UnNorm %	Normal %	Liquids (USgal/MCF)	Ideal (Btu/SCF)	Rel. Density
Propane	0.07668	0.07727	0.02131	1.94427	0.00118
Hydrogen Sulfide	0.00000	0.00000	0.00000	0.00000	0.00000
IsoButane	0.01738	0.01751	0.00574	0.56938	0.00035
Butane	0.02022	0.02038	0.00644	0.66485	0.00041
NeoPentane	0.00000	0.00000	0.00000	0.00000	0.00000
IsoPentane	0.01515	0.01526	0.00559	0.61062	0.00038
Pentane	0.01556	0.01568	0.00569	0.62846	0.00039
Hexane+	0.06383	0.06432	0.00000	0.00000	0.00000
Nitrogen	13.19429	**13.29594**	0.00000	0.00000	0.12861
Methane	84.99076	**85.64405**	0.00000	865.00488	0.47444
CarbonDioxide	0.20376	**0.20533**	0.00000	0.00000	0.00312
Ethane	0.63934	0.64426	0.17262	11.40145	0.00669
Hexane	0.00000	0.06432	0.02649	3.05896	0.00191
Heptane+	0.00000	0.00000	0.00000	0.00000	0.00000
Heptane	0.00000	0.00000	0.00000	0.00000	0.00000
Octane	0.00000	0.00000	0.00000	0.00000	0.00000
Nonane+	0.00000	0.00000	0.00000	0.00000	0.00000
Nonane	0.00000	0.00000	0.00000	0.00000	0.00000
Decane	0.00000	0.00000	0.00000	0.00000	0.00000
Undecane	0.00000	0.00000	0.00000	0.00000	0.00000
Dodecane	0.00000	0.00000	0.00000	0.00000	0.00000
Ethane-	0.00000	0.00000	0.00000	0.00000	0.00000
Propane +	0.00000	0.00000	0.00000	0.00000	0.00000
Total	99.23697	100.00000	0.24387	883.88293	0.61831

Inferior Wobbe 1109.2899 (Btu/SCF) Superior Wobbe 1128.8501 (Btu/SCF)
Compressibility 0.9983 Density 0.0473 (lbm/ft3)
Real Rel. Density 0.6183 Ideal CV 883.8829 (Btu/SCF)
Wet CV 872.2740 (Btu/SCF) Dry CV 887.4617 (Btu/SCF)
Contract Temp. 60.0000 (deg F) Contract Press. 14.7300 (psia)
Number of Cycles 2 Connected Stream 1
Atmospheric Pressure 14.73

Figure 2.8-2. Gas chromatography for the Sonol_Securities_5 well.

The location of the Sonol_Securities_4 and the Sonol_Securities_5 is shown in Figure 2.8-3.

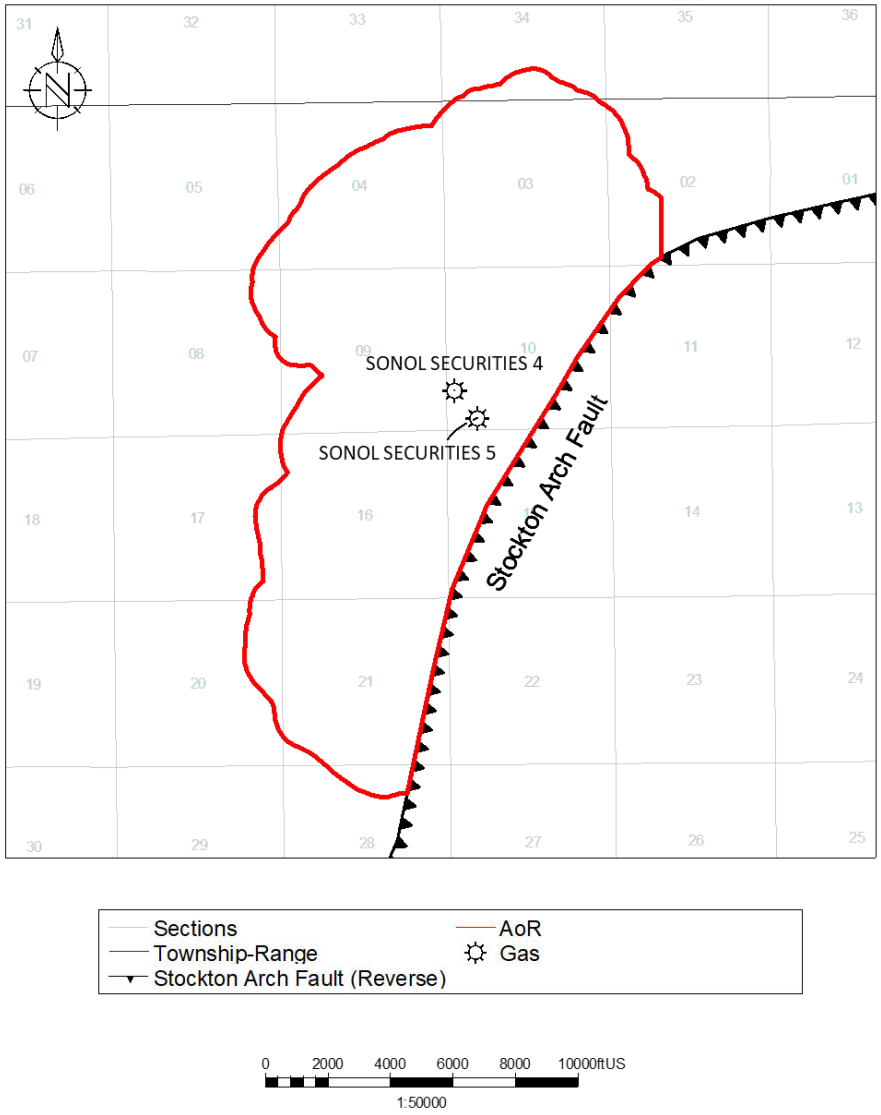

Figure 2.8-3. Location of wells with geochemistry data.

The properties of the formation fluids is summarized in Table 2.8-1.

Table 2.8-1: Formation fluid properties

Formation Fluid Property	Formation Water	Formation Gas
Density, g/cm^3	1.0082	0.00076
Viscosity, cp	1.26	0.029
TDS, ppm	~15,000	NA

2.8.3 Fluid-Rock Reactions

2.8.3.1 Winters Formation

Mineralogy and formation fluid interactions have been assessed for the Winters Formation. The following applies to potential reactions associated with the CO_2 injectate:

1. The Winters Formation has a negligible quantity of carbonate minerals and is instead dominated by quartz and feldspar. These minerals are stable in the presence of CO_2 and carbonic acid and any dissolution or changes that occur will be on grain surfaces.

2. The water within the Winters Formation contains minimal calcium and magnesium cations, which would be expected to react with CO_2 to form calcium bearing minerals in the pore space. Also, the relatively low salinity will reduce the "salting out" effect seen in higher salinity brine under the presence of CO_2.

2.8.3.2 Upper Confining Zone (Starkey-Sawtooth Shale)

There is no fluid geochemistry analysis for the upper confining zone. The shale will only provide fluid for analysis if stimulated. However, given the low permeability of the rock and the low carbonate content, the upper confining zone is not expected to be impacted by the CO_2 injectate.

2.8.3.2 Delta Shale

There is no fluid geochemistry analysis for the Delta Shale. The shale will only provide fluid for analysis if stimulated. However, given the low permeability of the rock and the low carbonate content, the Delta Shale is not expected to be impacted by the CO_2 injectate.

2.8.3.3 Geochemical Modeling

Using fluid geochemistry data for the Injection zone, and the available mineralogy data for the Injection Zone and the Upper Confining zone, geochemical modeling was conducted using PHREEQC (ph-REdox-Equilibrium), the USGS geochemical modeling software, to evaluate the compatibility of the Injectates being considered for the Project with formation rocks and fluid.

The PHREEQC software was used to evaluate the behavior of minerals and changes in aqueous chemistry and mineralogy over the life of the project, and to identify major potential reactions that may affect injection or containment.

Based on the geochemical modeling, the injection of CO_2 at the CTV II site does not cause significant reactions that will affect injection or containment. Detailed methodology and results can be found in "Appendix 3: CTV II Geochemical Modeling" submitted with this application.

2.9 Other Information (Including Surface Air and/or Soil Gas Data, if Applicable)

No additional information necessary.

2.10 Site Suitability [40 CFR 146.83]

Sufficient data from both wells and seismic demonstrate the lateral continuity of the Starkey-Sawtooth Shale confining zone and the Winters Formation Injection zone. Regional mapping completed by West

Coast Regional Carbon Sequestration Partnership (WESTCARB), California Geological Surgery (CGS), and the National Energy and Technology Lab (NETL) support our local stratigraphy, both indicating lateral continuity and regional thickness across the AoR (Downey 2010). This study covers formations with sequestration and seal potential from southern Sutter County down to the Stockton Arch Fault San Joaquin County, encompassing an area far beyond the AoR presented in Attachment B.

The vertically confined and laterally continuous reservoir, described in Attachment A, will compensate for the CO_2 as the plume migrates further to the northwest away from the barrier and Stockton Arch Fault. The Starkey-Sawtooth is a continuous shale, described in section Attachment A, and will guide the lateral dispersion of CO_2 across the AoR (**Figure 2.10-1**). Surrounding oil and gas fields in the area demonstrate adequate seal capacity in the upper confining zone and surrounding faults.

Thickness maps and petrophysics demonstrate confinement based on the upper confining intervals laterally continuity, low-permeability, and thickness. Faulting does exist on the east edge of the CO_2 plume however thickness maps support an adequate seal across this offset as discussed in section 2.6. Pressures along bounding faults will be estimated using computational modeling and in-zone monitoring wells, to mitigate the possibility of fault re-activation.

Due to the regional continuity and low permeability of the upper confining zone (Starkey-Sawtooth), no secondary confinement is necessary, however other shale barriers do exist above the Mokelumne River Formation monitoring sand. These act as additional impermeable zone of confinement separating the injection zone from the USDW.

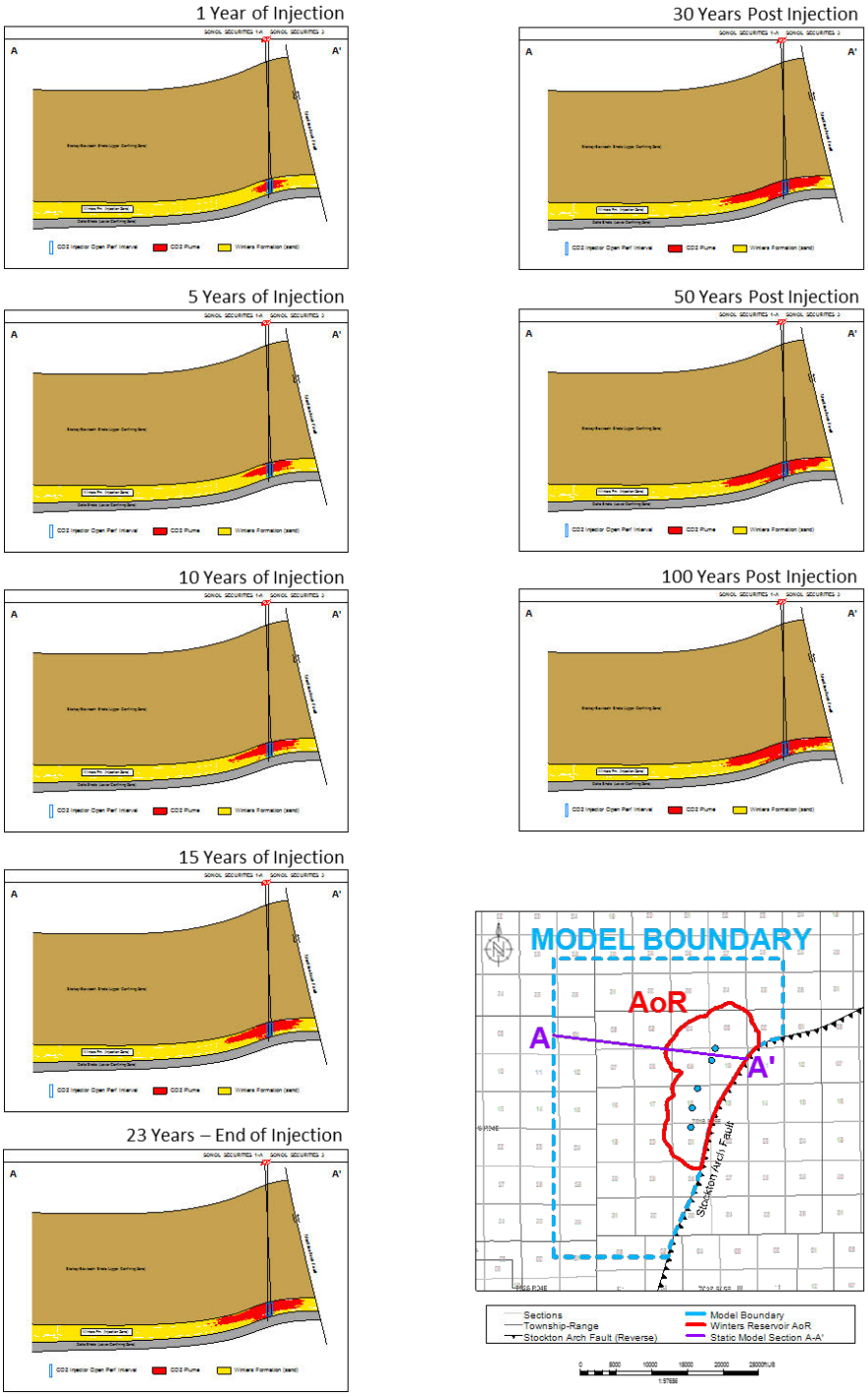

Figure 2.10-1A. Section showing proximity of CO2 (Injectate 1) to the Stockton Arch Fault and lateral dispersion of CO2 throughout time and confinement under the overlying Starkey-Sawtooth through time for the five injector modeled Base scenario. As the sections show, plume growth over time is driven by the reservoir anticlinal structure, and is thus representative of the plume growth at all injector locations.

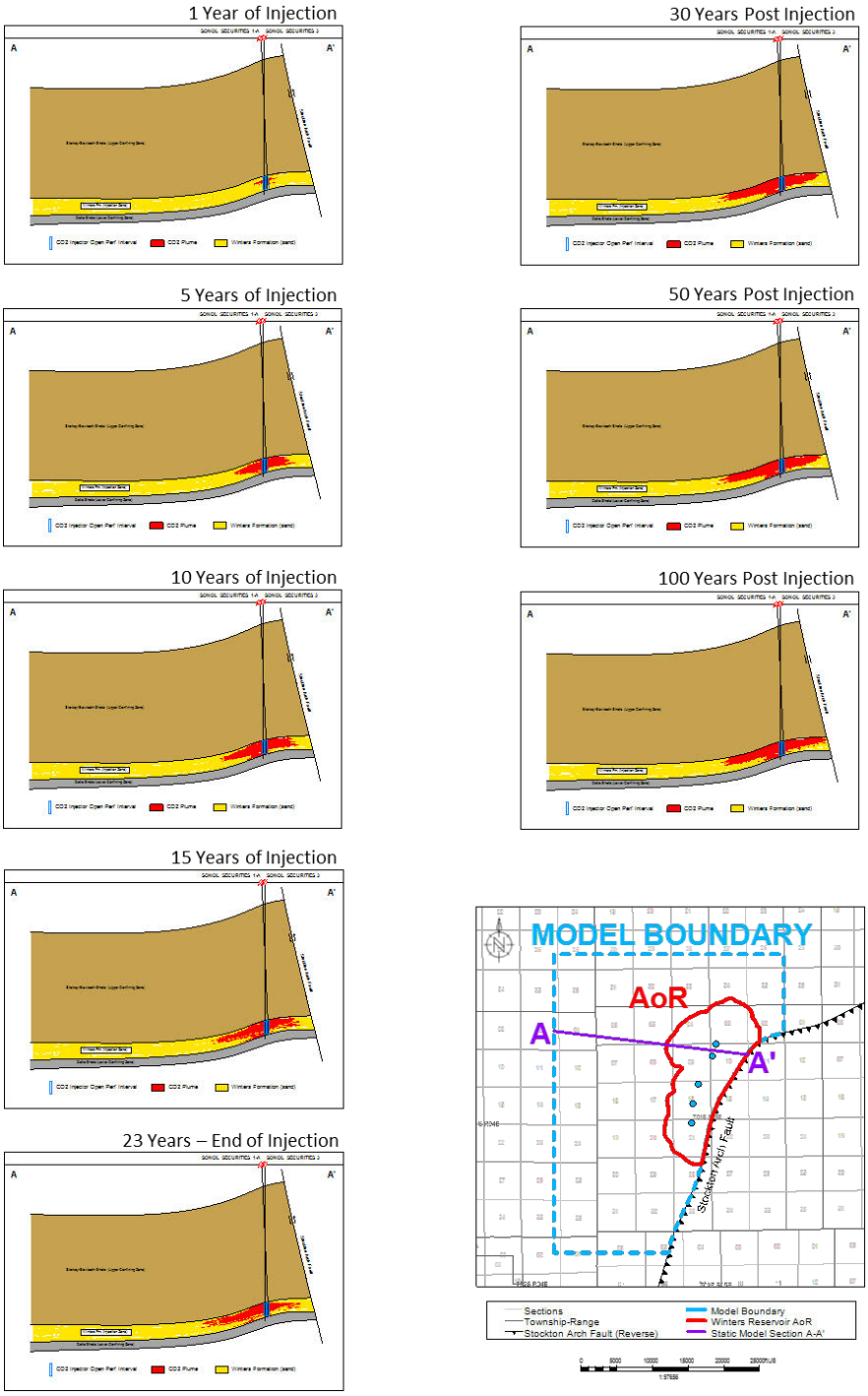

Figure 2.10-1B. Section showing proximity of CO2 (Injectate 2) to the Stockton Arch Fault and lateral dispersion of CO2 throughout time and confinement under the overlying Starkey-Sawtooth through time for the five injector modeled Base scenario. As the sections show, plume growth over time is driven by the reservoir anticlinal structure, and is thus representative of the plume growth at all injector locations.

CTV estimates maximum storage for the proposed project is 23 MMT of CO_2. This was derived from computational modeling.

3.0 AoR and Corrective Action

CTV's AoR and Corrective Action plan pursuant to 40 CFR 146.82(a)(4), 40 CFR 146.82(a)(13) and 146.84(b), and 40 CFR 146.84(c) describes the process, software, and results to establish the AoR, and the wells that require corrective action.

AoR and Corrective Action GSDT Submissions

GSDT Module: AoR and Corrective Action
Tab(s): All applicable tabs

Please use the checkbox(es) to verify the following information was submitted to the GSDT:
☒ Tabulation of all wells within AoR that penetrate confining zone ***[40 CFR 146.82(a)(4)]***
☒ AoR and Corrective Action Plan ***[40 CFR 146.82(a)(13) and 146.84(b)]***
☒ Computational modeling details ***[40 CFR 146.84(c)]***

4.0 Financial Responsibility

CTV's Financial Responsibility demonstration pursuant to 140 CFR 146.82(a)(14) and 40 CFR 146.85 is met with a line of credit for Injection Well Plugging and Post-Injection Site Care and Site Closure and insurance to cover Emergency and Remedial Responses.

Financial Responsibility GSDT Submissions

GSDT Module: Financial Responsibility Demonstration
Tab(s): Cost Estimate tab and all applicable financial instrument tabs

Please use the checkbox(es) to verify the following information was submitted to the GSDT:
☐ Demonstration of financial responsibility ***[40 CFR 146.82(a)(14) and 146.85]***

5.0 Injection and Monitoring Well Construction

CTV requires 14 wells for injection and monitoring associated with CTV II including five injectors, four injection zone monitoring wells, two above zone monitoring well, and three USDW monitoring well. CTV plans to repurpose eight existing wells by converting three to injectors and five to monitoring wells. One injection zone monitoring well and three USDW monitoring well will be designed and constructed specifically for CTV II. During pre-operational testing, the existing wells will undergo diagnostic testing to ensure suitability for conversion and re-use with CTV II. Based on results, CTV will either demonstrate

applicability pursuant to 40 CFR 146.81(c) or will propose to construct a new well in the same location. Figure 5.1 shows the wells proposed for the project.

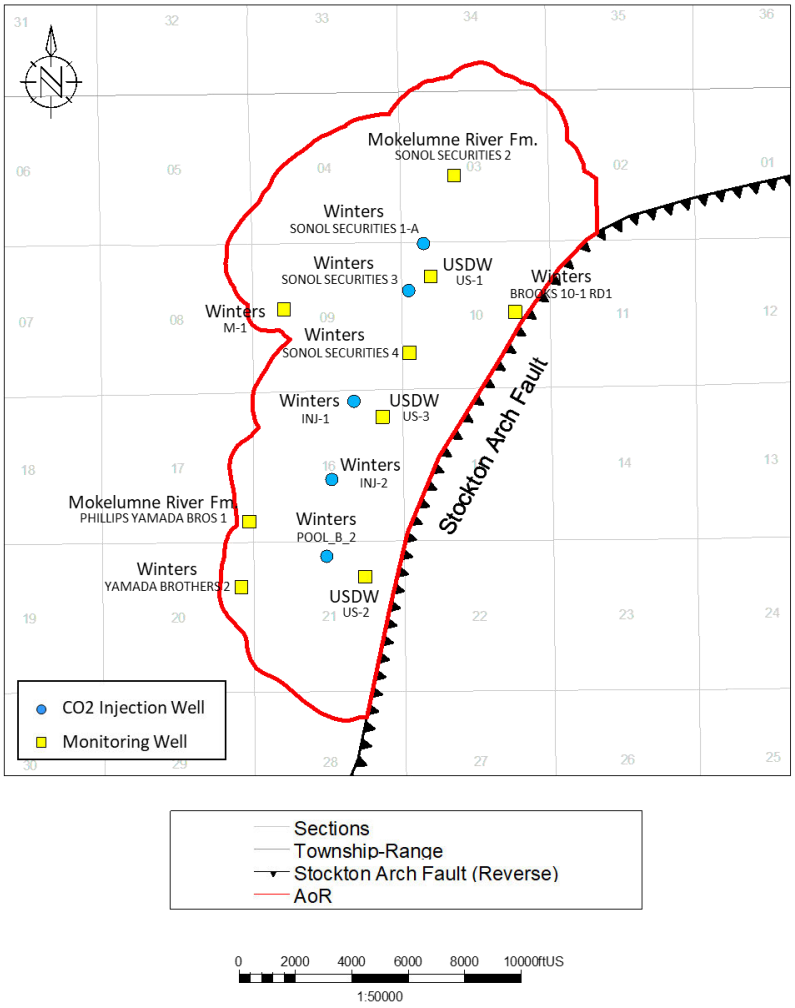

Figure 5.1. Map showing the location of injection wells and monitoring wells.

All planned new wells will be constructed with components that are compatible with the injectate and formation fluids encountered such that corrosion rates and cumulative corrosion over the duration of the project are acceptable. The proposed well materials will be confirmed based on actual CO_2 composition such that material strength is sufficient to withstand all loads encountered throughout the life of the well with an acceptable safety factor incorporated into the design. Casing points will be verified by trained geologists using real-time drilling data such as LWD and mud logs to ensure non-endangerment of USDW. Due to the depth of the base of USDW, an intermediate casing string will be utilized to isolate the USDW. Cementing design, additives, and placement procedures will be sufficient to ensure isolation of the injection zone and protection of USDW using cementing materials that are compatible with injectate, formation fluids, and subsurface pressure and temperature conditions.

The pressure within the injection zone has been depleted to ~1200 psi, and the temperature is approximately 218 degrees Fahrenheit. These conditions are not extreme, and CTV has extensive experience successfully constructing, operating, working over, and plugging wells in depleted reservoirs.

Appendix 5: Injection and Monitoring Well Schematics provides casing diagram figures for all injection and monitoring wells with construction specifications and anticipated completion details in graphical and/or tabular format.

5.1 Proposed Stimulation Program [40 CFR 146.82(a)(9)]

There are currently no proposed stimulation programs.

5.2 Well Construction Procedures [40 CFR 146.82(a)(12)]

CTV has created Construction and Plugging documents for each project well throughout the application documentation pursuant to 40 CFR 146.82(a)(8). Each attachment G: Well Construction and Plugging Plan document includes well construction information based on requirements defined within 40 CFR 146.82. The relevant attachments are:

- Attachment G1: Sonol Securities 1-A Construction and Plugging Plan
- Attachment G2: Sonol Securities 3 Construction and Plugging Plan
- Attachment G3: Pool B-2 Construction and Plugging Plan
- Attachment G4: UI_INJ-1 Construction and Plugging Plan
- Attachment G5: UI_INJ-2 Construction and Plugging Plan

6.0 Pre-Operational Logging and Testing

CTV has indicated a proposed pre-operational logging and testing plan throughout the application documentation pursuant to 40 CFR 146.82(a)(8). Each Attachment G: Well Construction and Plugging Plan document (listed in Section 5.2) includes logging and testing plans for each individual project well based on requirements defined within 40 CFR 146.87.

Pre-Operational Logging and Testing GSDT Submissions

GSDT Module: Pre-Operational Testing
Tab(s): Welcome tab

Please use the checkbox(es) to verify the following information was submitted to the GSDT:
☐ Proposed pre-operational testing program ***[40 CFR 146.82(a)(8) and 146.87]***

7.0 Well Operation

7.1 Operational Procedures [40 CFR 146.82(a)(10)]

The Operational Procedures for all injectors associated with the project are detailed in the "Appendix 4: Operational Procedures" document attached with this application.

7.2 Proposed Carbon Dioxide Stream [40 CFR 146.82(a)(7)(iii) and (iv)]

CTV is planning to construct a carbon capture and sequestration "hub" project (*i.e.*, a project that collects carbon dioxide (CO_2) from multiple sources over time and injects the CO_2 stream(s) via a Class VI UIC permitted injection well(s)). Therefore, CTV is currently considering multiple sources of anthropogenic CO_2 for the project. The potential sources include capture from existing and potential future industrial sources, as well as Direct Air Capture (DAC). CTV would expect the CO_2 stream to be sampled at the transfer point from the source and between the final compression stage and the wellhead. Samples will be analyzed according to the analytical methods described in the "Appendix 11: QASP" (Table 4) document and the Attachment C (Table 1) document.

For the purposes of Geochemical modeling, CO2 Plume modeling, AoR determination, and Well design, two major types of Injectate compositions were considered based on the source.

- Injectate 1: is a potential injectate stream composition from Direct Air Capture or a Pre-Combustion source (such as a Blue Hydrogen facility that produces Hydrogen using Steam Methane Reforming process) or a Post-Combustion source (such as a Natural Gas fired power plant or Steam Generator). The primary impurity in the injectate is Nitrogen.
- Injectate 2: is a potential injectate stream composition from a Biofuel Capture source (such as a Biodiesel plant that produces Biodiesel from a biologic source feedstock) or from an Oil & Gas refinery. The primary impurity in the injectate is light end Hydrocarbons (Methane and Ethane).

The compositions for these two injectates are shown in Table 7.1, and are based on engineering design studies and literature.

Table 7.1. Injectate compositions

Component	Injectate 1	Injectate 2
	Mass%	**Mass%**
CO2	99.213%	99.884%
H2	0.051%	0.006%
N2	0.643%	0.001%
H2O	0.021%	0.000%
CO	0.029%	0.001%
Ar	0.031%	0.000%
O2	0.004%	0.000%
SO2+SO3	0.003%	0.000%
H2S	0.001%	0.014%
CH4	0.004%	0.039%
NOx	0.002%	0.000%
NH3	0.000%	0.000%
C2H6	0.000%	0.053%
Ethylene	0.000%	0.002%
Total	**100.00%**	**100.00%**

For Geochemical and Plume modeling scenarios, these injectate compositions were simplified to a 4-component system, shown in Table 7.2 and then normalized for use in the modeling. The 4 component simplified compositions cover 99.9% by mass of Injectate 1 & 2 and cover particular impurities of concern (H2S and SO2). The estimated properties of the injectates at downhole conditions are specified in Table 7.3

Table 7.2. Simplified 4 component composition for Injectate 1

Injectate 1	
Component	**mass%**
CO2	99.213%
N2	0.643%
SO2+SO3	0.003%
H2S	0.001%

Injectate 2	
Component	**mass%**
CO2	99.884%
CH4	0.039%
C2H6	0.053%
H2S	0.014%

Table 7.3. Injectate properties range over project life at downhole conditions for Injectate 1 and Injectate 2

Injectate property at downhole conditions	Injectate 1	Injectate 2
Viscosity, cp	0.022 – 0.054	0.022 – 0.056
Density, lb/ft^3	9.1 - 40.6	9.1 – 41.5
Compressibility factor, Z	0.81 - 0.67	0.80 – 0.66

The anticipated injection temperature at the wellhead is 90 – 130° F.

No corrosion is expected in the absence of free phase water provided that the entrained water is kept in solution with the CO_2. This is ensured by maintaining a <25 lb/mmscf injectate specification limit, and this specification will be a condition of custody transfer at the capture facility. For transport through pipelines, which typically use standard alloy pipeline materials, this specification is critical to the mechanical integrity of the pipeline network, and out of specification product will be immediately rejected. Therefore, all product transported through pipeline to the injection wellhead is expected to be dry phase CO_2 with no free phase water present.

Injectate water solubility will vary with depth and time as temperature and pressures change. The water specification is conservative to ensure water solubility across super-critical operating ranges. CRA tubing will be used in the injection wells to mitigate any potential corrosion impact should free-phase water from the reservoir become present in the wellbore, such as during shut-in events when formation liquids, if present, could backflow into the wellbore. CTV may further optimize the maximum water content specification prior to injection based on technical analysis.

8.0 Testing and Monitoring

CTV's Testing and Monitoring plan pursuant to 40 CFR 146.82 (a) (15) and 40 CFR 146.90 describes the strategies for testing and monitoring to ensure protection of the USDW, injection well mechanical integrity, and plume monitoring.

Testing and Monitoring GSDT Submissions
GSDT Module: Project Plan Submissions ***Tab(s):*** Testing and Monitoring tab Please use the checkbox(es) to verify the following information was submitted to the GSDT: ☐ Testing and Monitoring Plan ***[40 CFR 146.82(a)(15) and 146.90]***

9.0 Injection Well Plugging

CTV's Injection Well Plugging Plan pursuant to 40 CFR 146.92 describes the process, materials and methodology for injection well plugging.

Injection Well Plugging GSDT Submissions
GSDT Module: Project Plan Submissions ***Tab(s):*** Injection Well Plugging tab Please use the checkbox(es) to verify the following information was submitted to the GSDT: ☐ Injection Well Plugging Plan ***[40 CFR 146.82(a)(16) and 146.92(b)]***

10.0 Post-Injection Site Care (PISC) and Site Closure

CTV has developed a Post-Injection Site Care and Site Closure plan pursuant to 40 CFR 146.93 (a) to define post-injection testing and monitoring.

At this time CTV is not proposing an alternative PISC timeframe.

PISC and Site Closure GSDT Submissions
GSDT Module: Project Plan Submissions ***Tab(s):*** PISC and Site Closure tab Please use the checkbox(es) to verify the following information was submitted to the GSDT: ☐ PISC and Site Closure Plan ***[40 CFR 146.82(a)(17) and 146.93(a)]***

PISC and Site Closure GSDT Submissions
GSDT Module: Alternative PISC Timeframe Demonstration ***Tab(s):*** All tabs (only if an alternative PISC timeframe is requested) Please use the checkbox(es) to verify the following information was submitted to the GSDT: ☐ Alternative PISC timeframe demonstration ***[40 CFR 146.82(a)(18) and 146.93(c)]***

11.0 Emergency and Remedial Response

CTV's Emergency and Remedial Response plan pursuant to 40 CFR 164.94 describes the process and response to emergencies to ensure USDW protection.

Emergency and Remedial Response GSDT Submissions
GSDT Module: Project Plan Submissions ***Tab(s):*** Emergency and Remedial Response tab Please use the checkbox(es) to verify the following information was submitted to the GSDT: ☐ Emergency and Remedial Response Plan ***[40 CFR 146.82(a)(19) and 146.94(a)]***

12.0 Injection Depth Waiver and Aquifer Exemption Expansion

No depth waiver or Aquifer Exemption expansion is being requested as part of this application.

Injection Depth Waiver and Aquifer Exemption Expansion GSDT Submissions
GSDT Module: Injection Depth Waivers and Aquifer Exemption Expansions ***Tab(s):*** All applicable tabs Please use the checkbox(es) to verify the following information was submitted to the GSDT: ☐ Injection Depth Waiver supplemental report ***[40 CFR 146.82(d) and 146.95(a)]*** ☐ Aquifer exemption expansion request and data ***[40 CFR 146.4(d) and 144.7(d)]***

13.0 References

Bartow. 1985. Maps showing Tertiary stratigraphy and structure of the Northern San Joaquin Valley, California. United States Geological Survey (USGS).

Berkstresser, C.F. Jr. 1973. Base of Fresh Ground-Water -- Approximately 3,000 micromhos -- in the Sacramento Valley and Sacramento-San Joaquin Delta, California. U.S. Geological Survey Water-Resource Inv. 40-73. 1973 Bertoldi, G., Johnston, R., & Evenson, K. 1991. Groundwater in the Central Valley, California - A Summary Report. USGS Professional Paper 1401-A. https://doi.org/10.3133/pp1401A.

Beyer, L.A. Summary of Geology and Petroleum Plays Used to Assess Undiscovered Recoverable Petroleum Resources of Sacramento Basin Province, California. United States Department of the Interior Geological Survey, 1988.

Burow, Karen R., Jennifer L. Shelton, Joseph A. Hevesi, and Gary S. Weissmann. 2004. Hydrologic Characterization of the Modesto Area, San Joaquin Valley, California. Preliminary Draft. U.S. Geological Survey. Water-Resources Investigation Report. Prepared in cooperation with Modesto Irrigation District. Sacramento, California.

California Department of Water Resources (DWR). 1995. Sacramento Delta San Joaquin Atlas.

California Department of Water Resources (DWR). 2006. California's Groundwater, Bulletin 118. San Joaquin Valley Groundwater Basin Tracy Subbasin. Last updated November 2021.

Davis G.H., J.H. Green, S.H. Olmstead, and D.W. Brown 1959. Davis, G. H., J.H. Green, S.H. Olmstead, and D.W. Brown. 1959. Ground water conditions and storage capacity in the San Joaquin Valley, California. U.S. Geological Survey Water Supply Paper No. 1469, 287 p.

Downey, C., and Clinkenbeard, J. 2010. Preliminary Geologic Assessment of the Carbon Sequestration Potential of the Upper Cretaceous Mokelumne River, Starkey, and Winters Formations – Southern Sacramento Basin, California. California Geological Survey.

Downey, C., and Clinkenbeard, J. 2006. An overview of geologic carbon sequestration potential in California, California Energy Comission, PIER Energy-Related Environmental Research Program.

GEI Consultants, Inc. (GEI) 2007. Tracy Regional Groundwater Management Plan.

GEI Consultants, Inc. (GEI) 2021. Tracy Subbasin Groundwater Sustainability Plan. November 1, 2021.

Graham, S.A., McCloy, C., Hitzman, M., Ward, R., Turner, R. 1984. Basin Evolution During Chance from Convergent to Transform Continental Margin in Central California. The American Association of Petroleum Geologists Bulletin V.68 No. 3.

Hotchkiss, W. R., and G.O. Balding. 1971. Geology, hydrology, and water quality of the Tracy-Dos Palos area, San Joaquin Valley, California. U.S. Geological Survey. Open-File Report. Hotchkiss and Balding. 1971.

Heidbach, O., M. Rajabi, X. Cui, K. Fuchs, B. Müller, J. Reinecker, K. Reiter, M. Tingay, F. Wenzel, F. Xie, M. O. Ziegler, M.-L. Zoback, and M. D. Zoback (2018): The World Stress Map database release 2016: Crustal stress pattern across scales. Tectonophysics, 744, 484-498, doi:10.1016/j.tecto.2018.07.007

Heidbach, Oliver; Rajabi, Mojtaba; Reiter, Karsten; Ziegler, Moritz; WSM Team (2016): World Stress Map Database Release 2016. GFZ Data Services, doi:10.5880/WSM.2016.001
Hydrofocus, 2015. San Joaquin County and Delta Quality Coalition Groundwater Quality Assessment Report, April 27, 2015.

Ingram G. M., Urai J. L., Naylor M. A. 1997. in Hydrocarbon Seals: Importance for Exploration and Production, Sealing processes and top seal assessment, Norwegian Petroleum Society (NPF) Special Publication, eds Moller-Pedersen P., Koestler A. G. 7, pp 165–175.

Ingram, Gary and Urai, Janos. 1999. Top-seal leakage through faults and fractures: the role of mudrock properties. Geological Society, London, Special Publications. 158. 125-135. 10.1144/GSL.SP.1999.158.01.10.

Johnson, D.S. 1990. Depositional environment of the Upper Cretaceous Mokelumne River Formation, Sacramento Basin. California. American Assoc. of Petroleum Geologists Bulletin 74: 5 1990: 686 p.

Leong, J.K., and J.R. Tenzer. 1994. Production Optimization of a Mature Gas Field. Paper presented at the SPE Western Regional Meeting, Long Beach, California.

Lund Snee, J-E, and Zoback, M. 2020. Multiscale variations of the crustal stress field throughout North America", Nature Communications 11, 1951.

Magoon, L.B., and Valin, Z.C. 1995. Sacramento Basin Province (009). United States Department of the Interior Geological Survey, National assessment of United States oil and gas resources-results, methodology, and supporting data.

Mount, Van and Suppe, John. 1992. Present-day stress orientations adjacent to active strike-slip faults - California and Sumatra. Journal of Geophysical Research. 971. 11995-12013. 10.1029/92JB00130.

Nilsen, T. H., and Clarke, Jr. S.H. 1975. Sedimentation and Tectonics in the Early Tertiary Continental Borderland of Central California. Geological Survey Professional Paper 925,.

O'Geen A, Saal M, Dahlke H, Doll D, Elkins R, Fulton A, Fogg G, Harter T, Hopmans J, Ingels C, Niederholzer F, Sandoval Solis S, Verdegaal P, Walkinshaw M. 2015. Soil suitability index identifies potential areas for groundwater banking on agricultural lands.

Padre and Associates, Inc. 2004. personnel communication with Mike Burke regarding aquifer testing at City of Tracy Well 8.

Page, R.W. 1986. Geology of the Fresh Ground-Water Basin of the Central Valley, California, with Texture Maps and Sections. USGS Professional Paper 1401-C.

Sullivan, Ray and Sullivan, Morgan. 2012. Sequence Stratigraphy and Incised Valley Architecture of the Domengine Formation, Black Diamond Mines Regional Preserve and the Southern Sacramento Basin, California, U.S.A. Journal of Sedimentary Research.

Towell, T. 1992. Public Health and Safety- Seismic and Geological Hazards July

U.S. Environmental Protection Agency Underground Injection Control Program. 1988. Survey of Methods to Determine Total Dissolved Solids Concentrations. Prepared by Ken E. Davis Associates under subcontract to

Engineering Enterprises, INC. EPA LOE Contract No. 68-03-3416, Work Assignment No. 1-0-13, Keda Project No. 30-956.

Williamson, C.R., and Hill, D.R. 1981. Submarine-Fan Deposition of the Upper Cretaceous Winters Sandstone, Union Island Gas Field, Sacramento Valley, California.: The Society of Evonomic Paleontologists and Mineralogists (SEPM) Deep-Water Clastic Sediments (CW2).

Wagner, D.L., Bortugno, E.J., and Mc Junkin, R.D. 1991. Geologic Map of the San Francisco – San Jose Quadrangle. California Geological Survey, Regional Geologic Map No. 5A, 1:250,000 scale.

IEAGHG, 2011. Effects of impurities on geological storage of CO2. International Energy Agency Greenhouse Gas programme

B. Wetenhall et al. / International Journal of Greenhouse Gas Control 30 (2014) 197–211

NARRATIVE - FIGURES

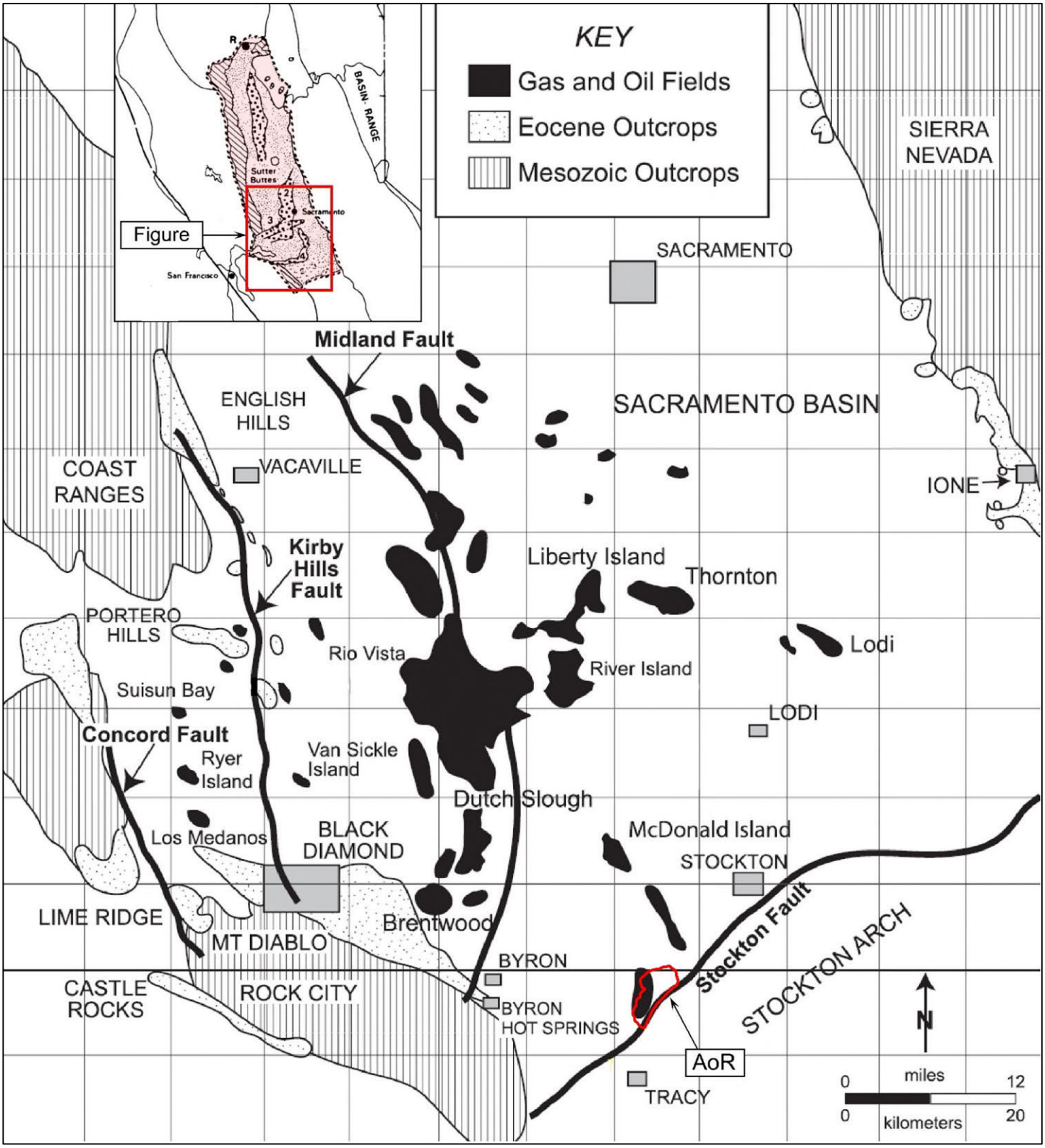

Figure 2.1-1. Location map of the Union Island field with the proposed injection AoR in relation to the Sacramento Basin.

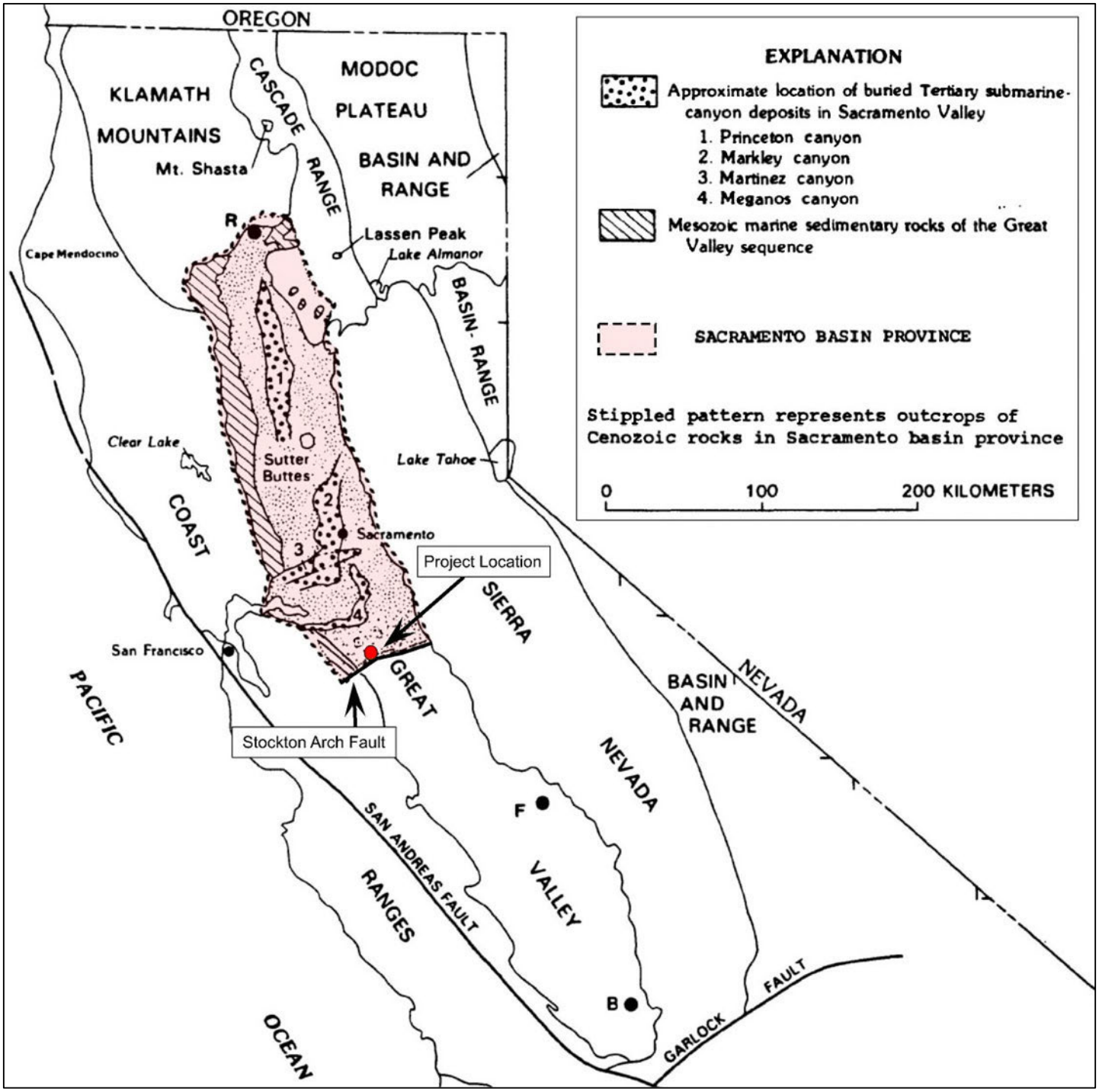

Figure 2.1-2. Location map of California modified from (Beyer, 1988) & (Sullivan, 2012). The Sacramento Basin regional study area is outlined by a dashed black line. B – Bakersfield; F – Fresno; R – Redding.

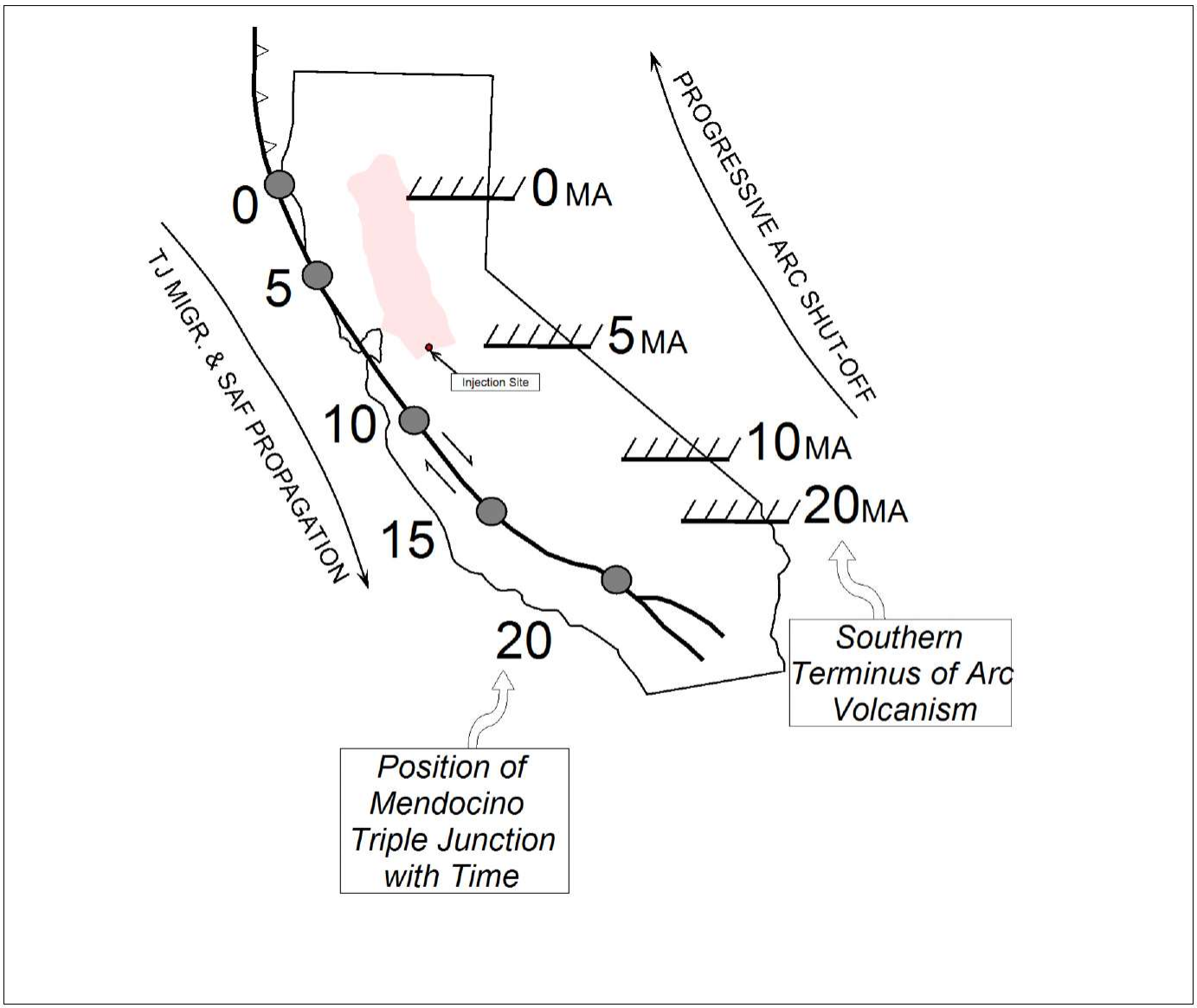

2.1-3. Migrational position of the Mendocino triple junction (Connection point of the Gorda, North American and Pacific plates) on the west and migrational position of Sierran arc volcanism in the east (Graham, 1984). Figure indicates space-time relations of major continental-margin tectonic events in California during Miocene.

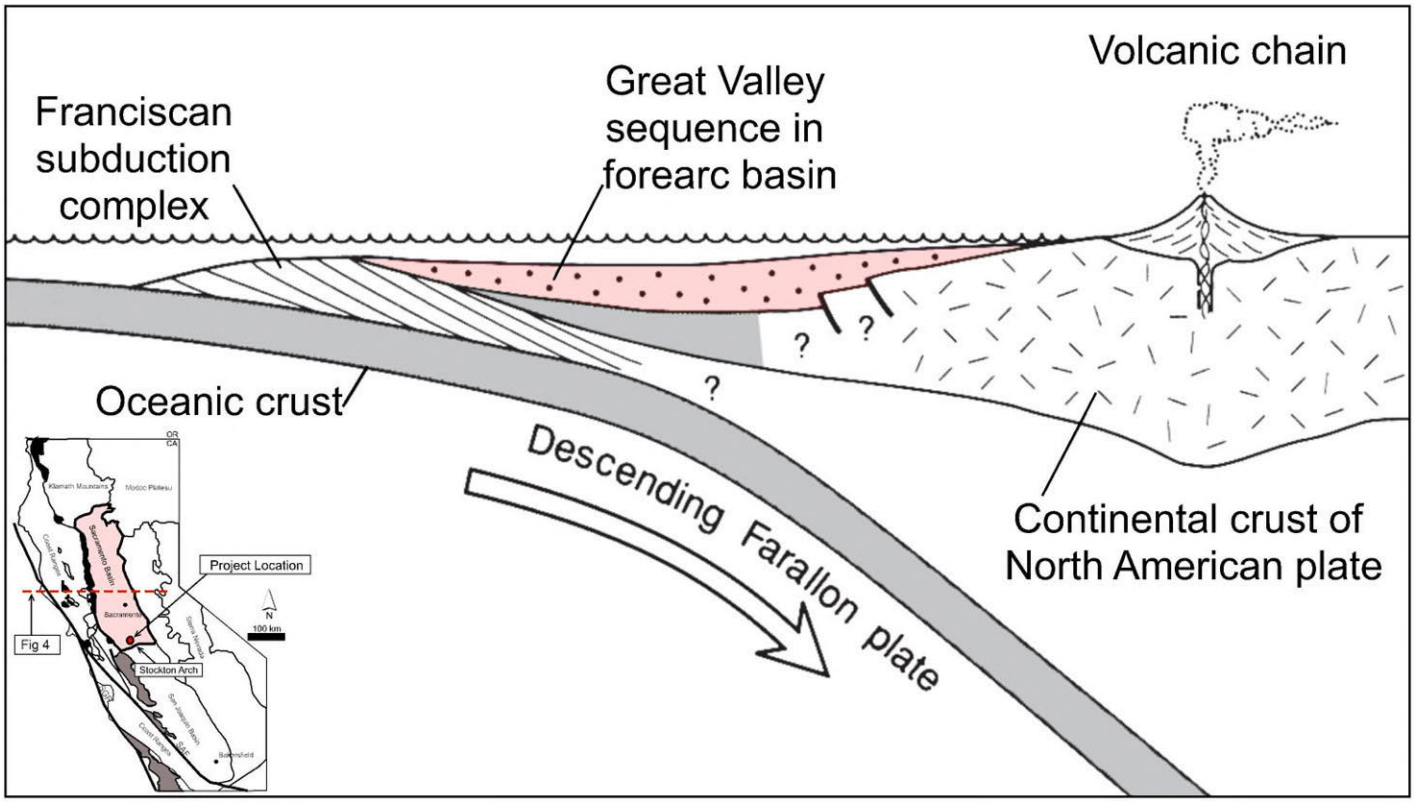

Figure 2.1-4. Schematic W-E cross-section of California, highlighting the Sacramento Basin, as a continental margin during late Mesozoic. The oceanic Farallon plate was forced below the west coast of the North American continental plate.

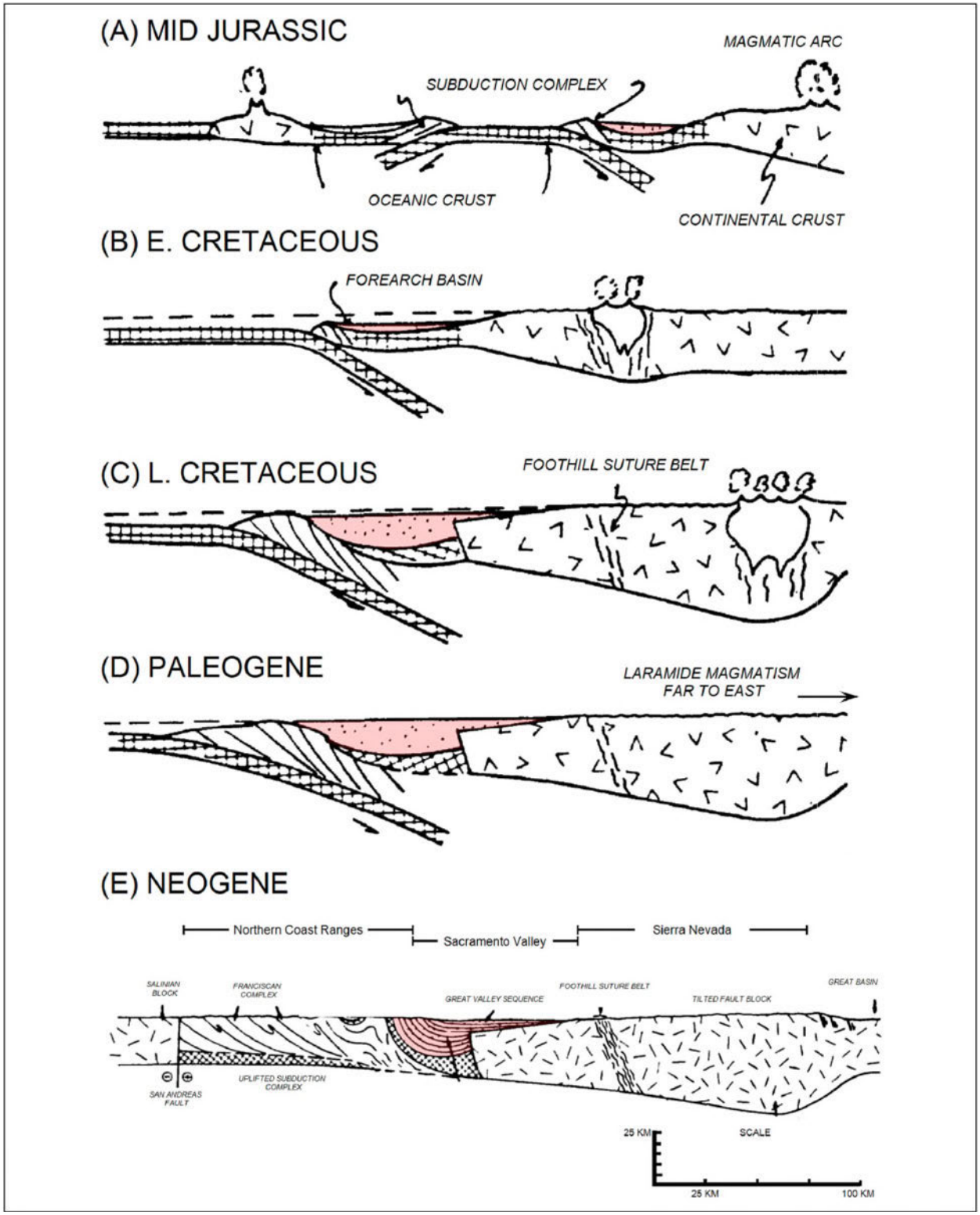

Figure 2.1-5. Evolutionary stages showing the history of the arc-trench system of California from Jurassic (A) to Neogene (E) (modified from Beyer, 1988).

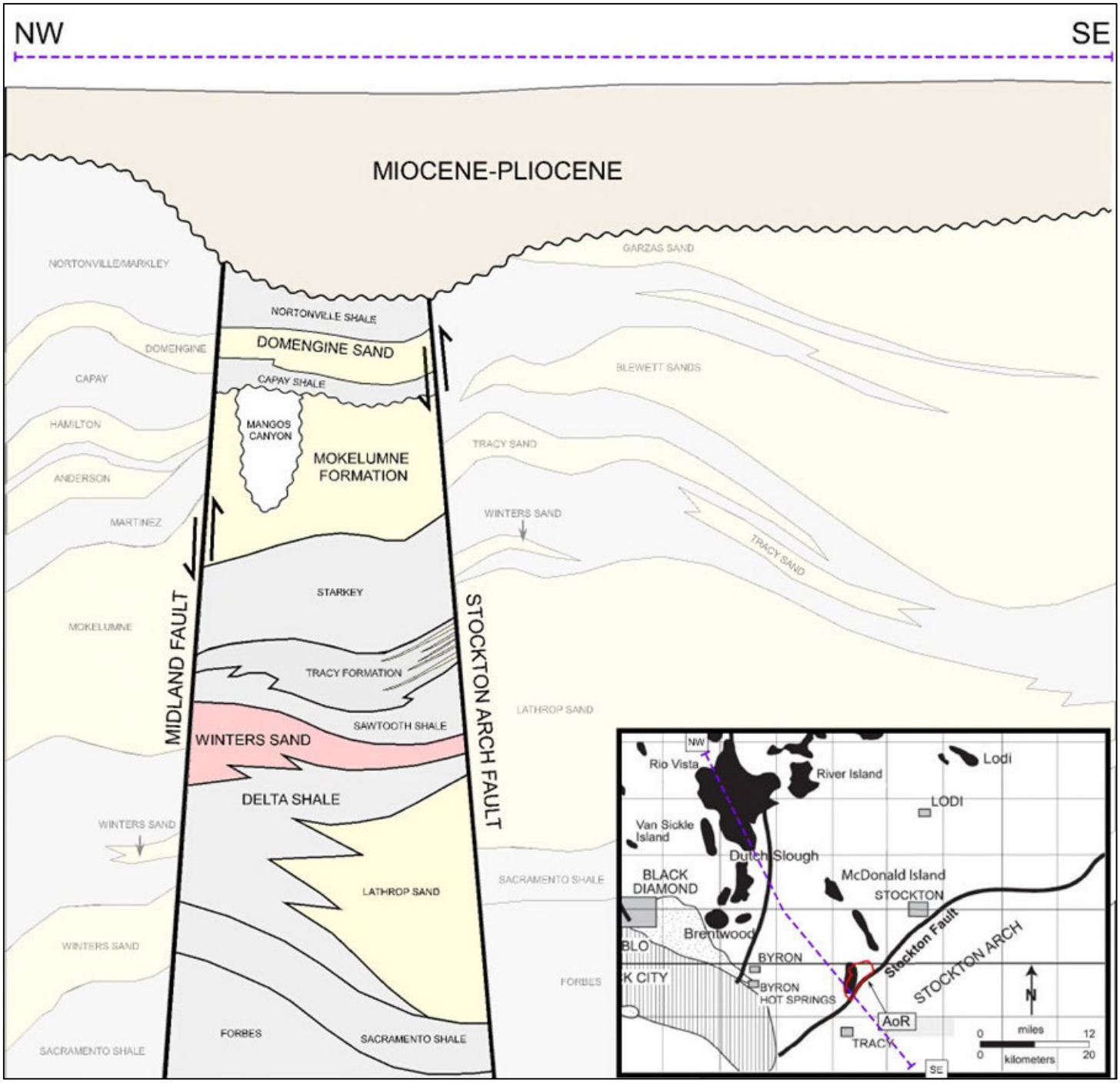

Figure 2.1-6. Schematic northwest to southeast cross section in the Sacramento basin, intersecting the project AoR.

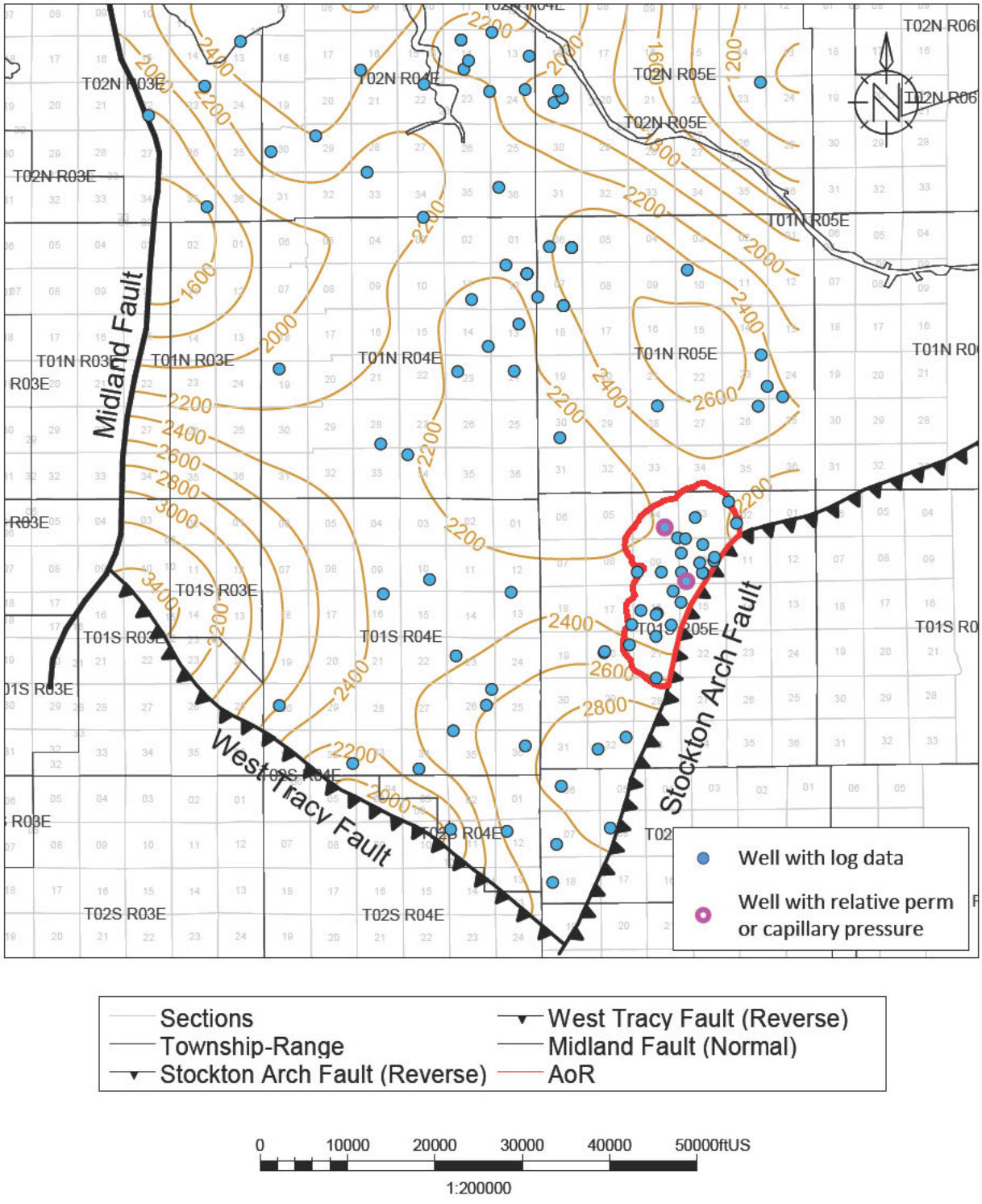

FIGURE 2.1-7. Starkey-Sawtooth Shale isopach map for the greater storage project area. Wells shown as blue dots on the map penetrate the Starkey-Sawtooth Shale and have open-hole logs. Wells with relative permeability or capillary pressure data are shown as magenta circles.

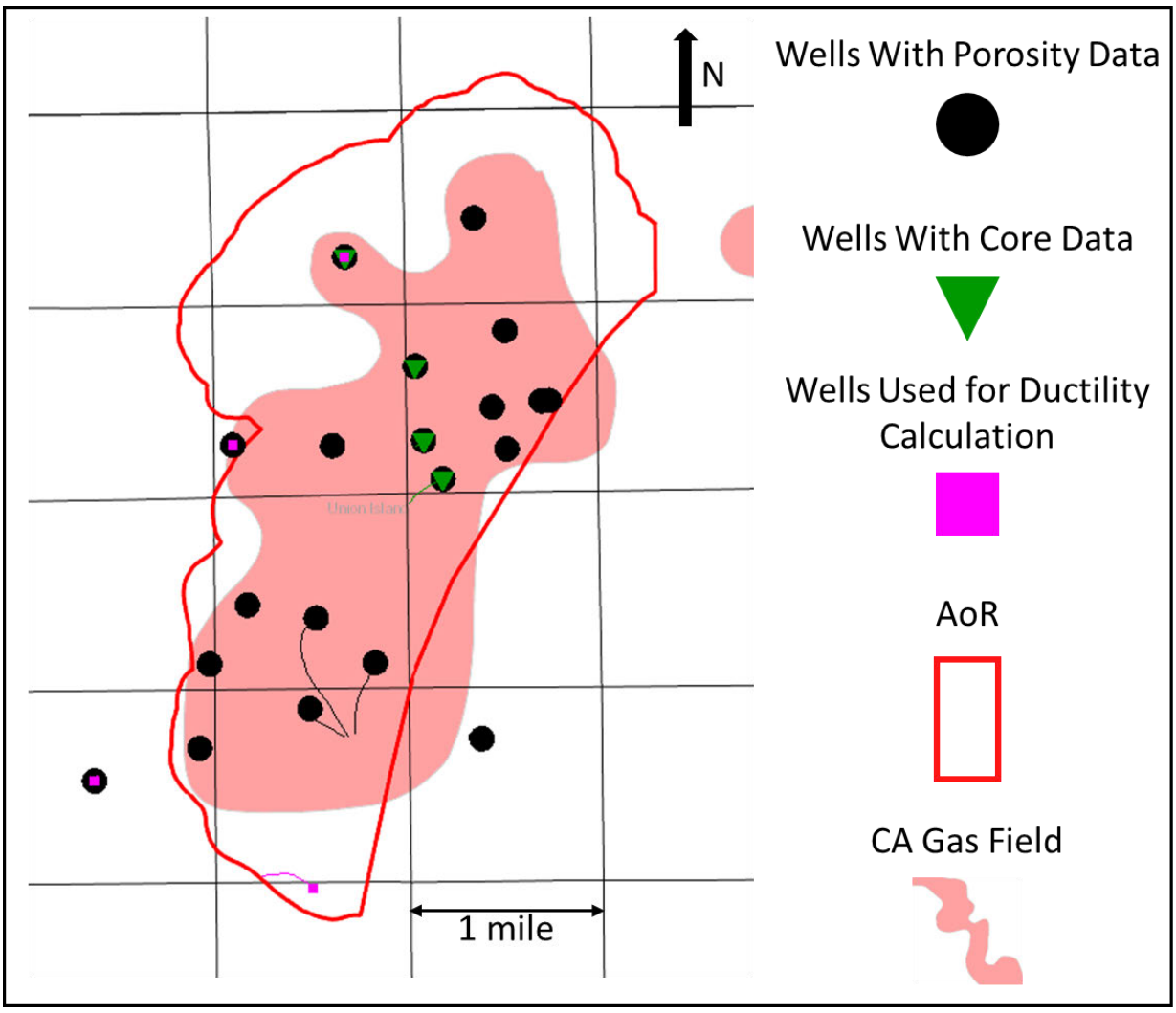

Figure 2.2-1. Wells drilled in the Union Island Field with porosity data are shown in black, wells with core are shown in green and wells used for ductility calculation are shown in pink.

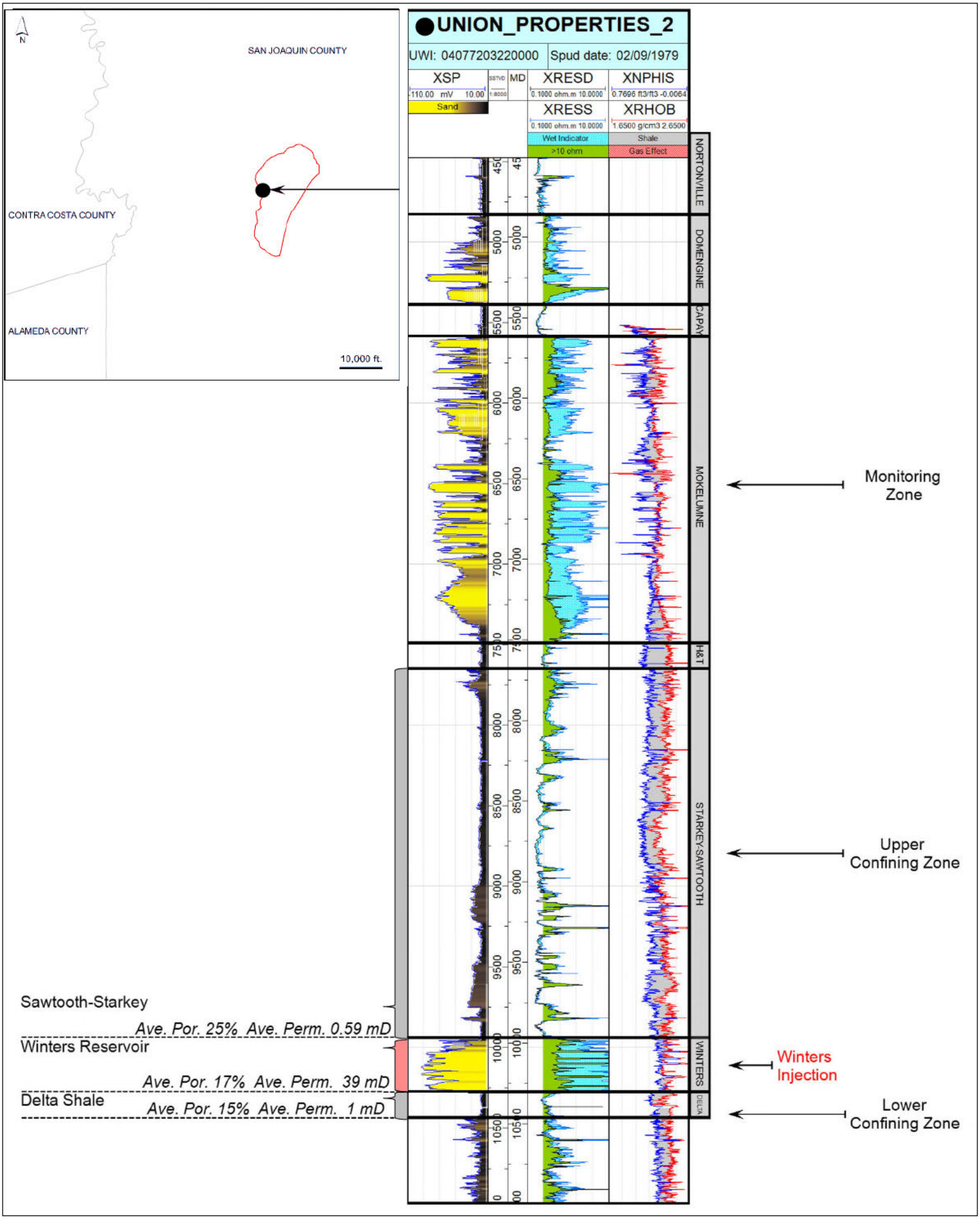

Figure 2.2-2. Type well taken from south of the AoR showing average rock properties used in the model for confining and injection zones.

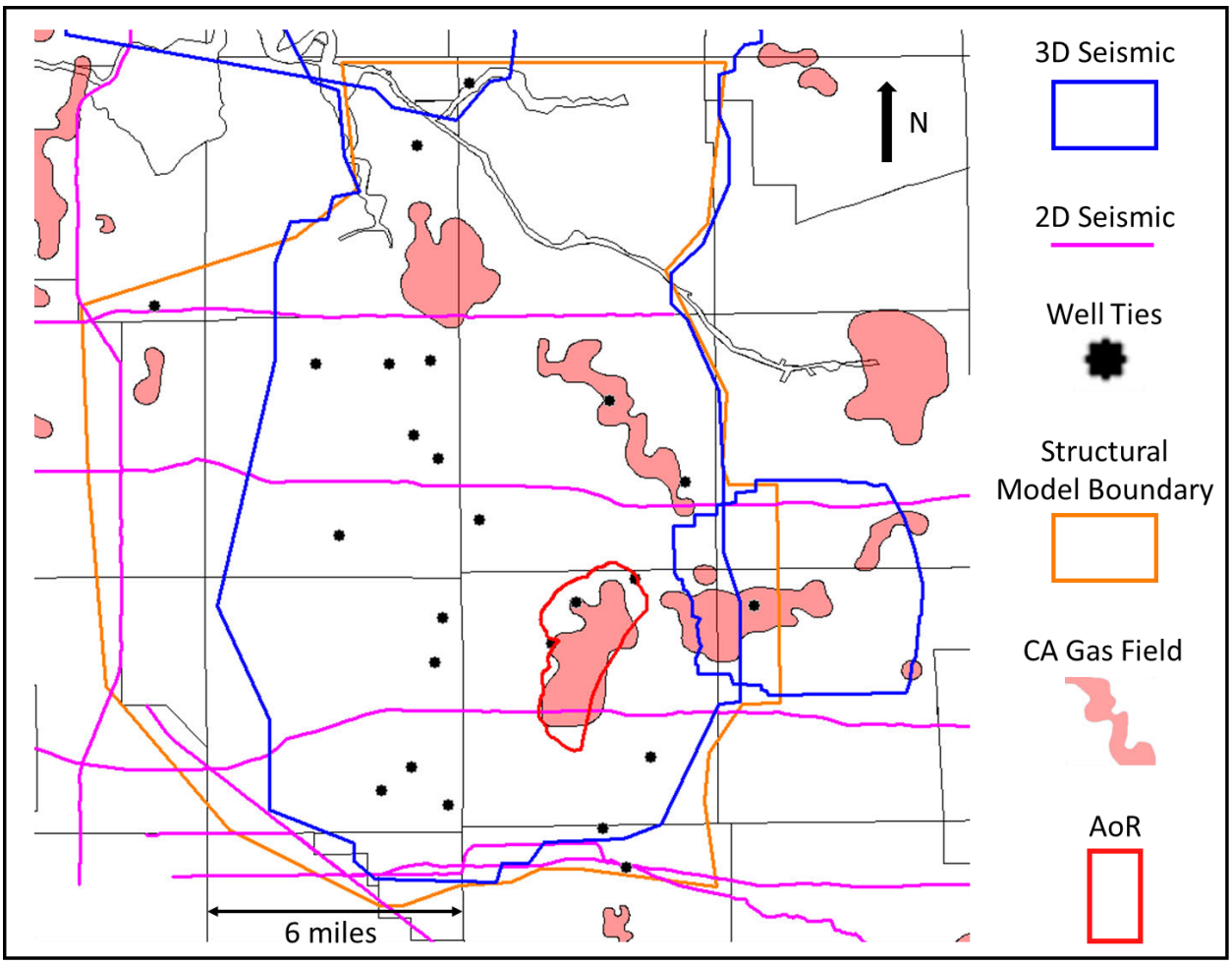

Figure 2.2-3. Summary map and area of seismic data used to build structural model. Both of the 3D surveys were acquired in 1998 and reprocessed in 2013. The 2D seismic were acquired between 1980 and 1985. California gas fields are shown for reference.

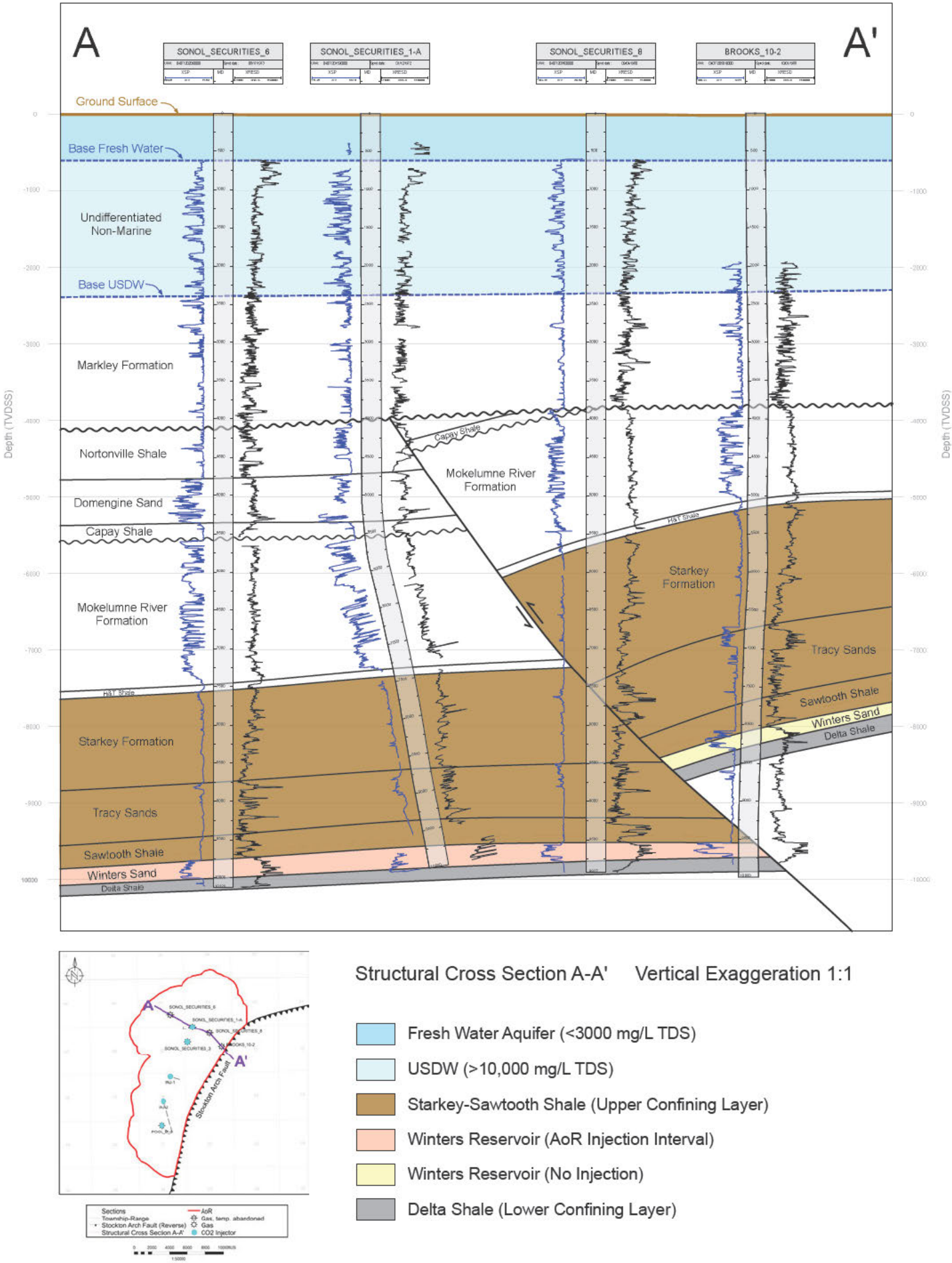

Figure 2.2-4. Dip cross section showing stratigraphy and lateral continuity of major formations across the project area. Section is representative of formations and sand continuity at all five CO2 injector locations.

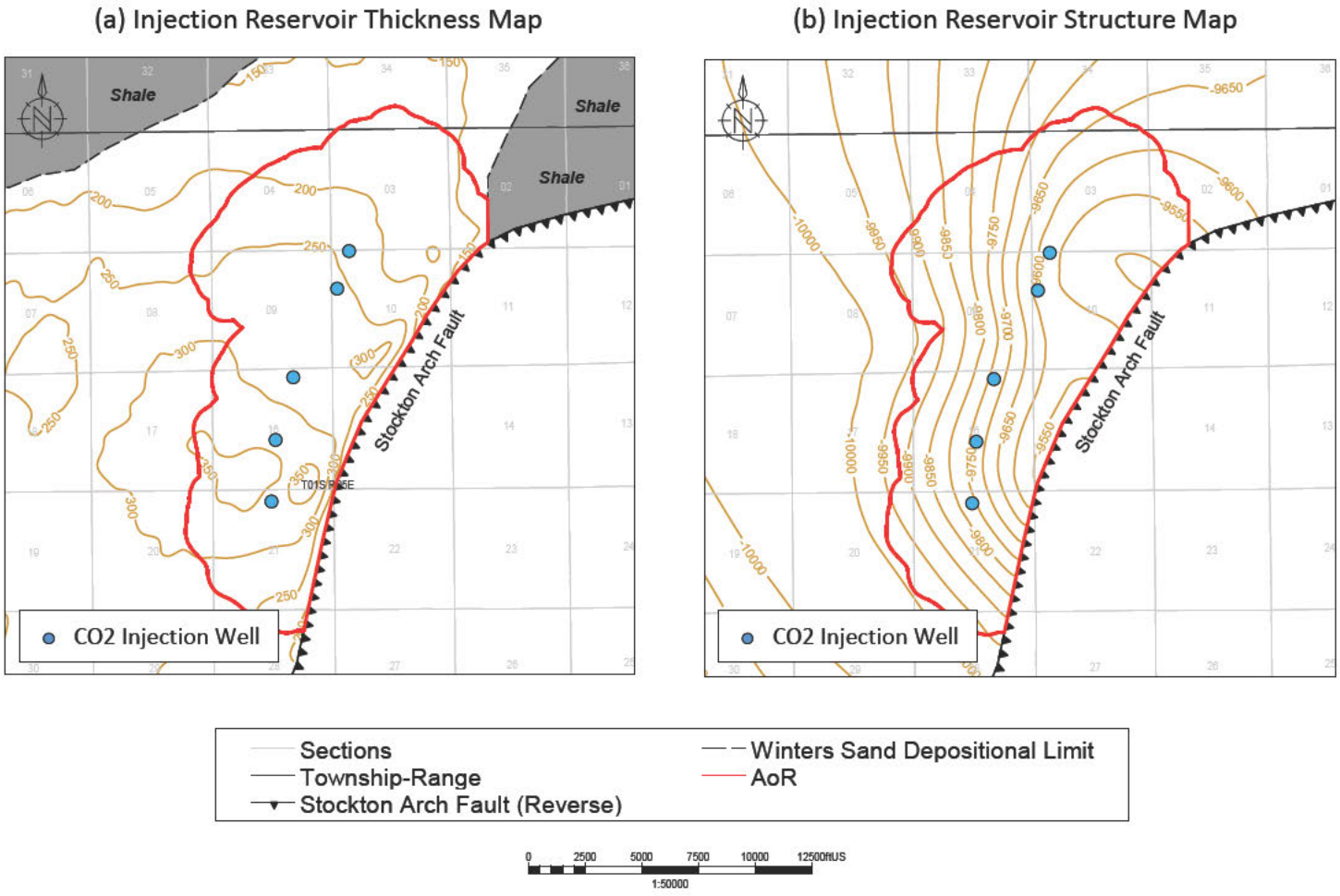

Figure 2.2-5. (a) Injection reservoir thickness map. (b) Injection reservoir structure map.

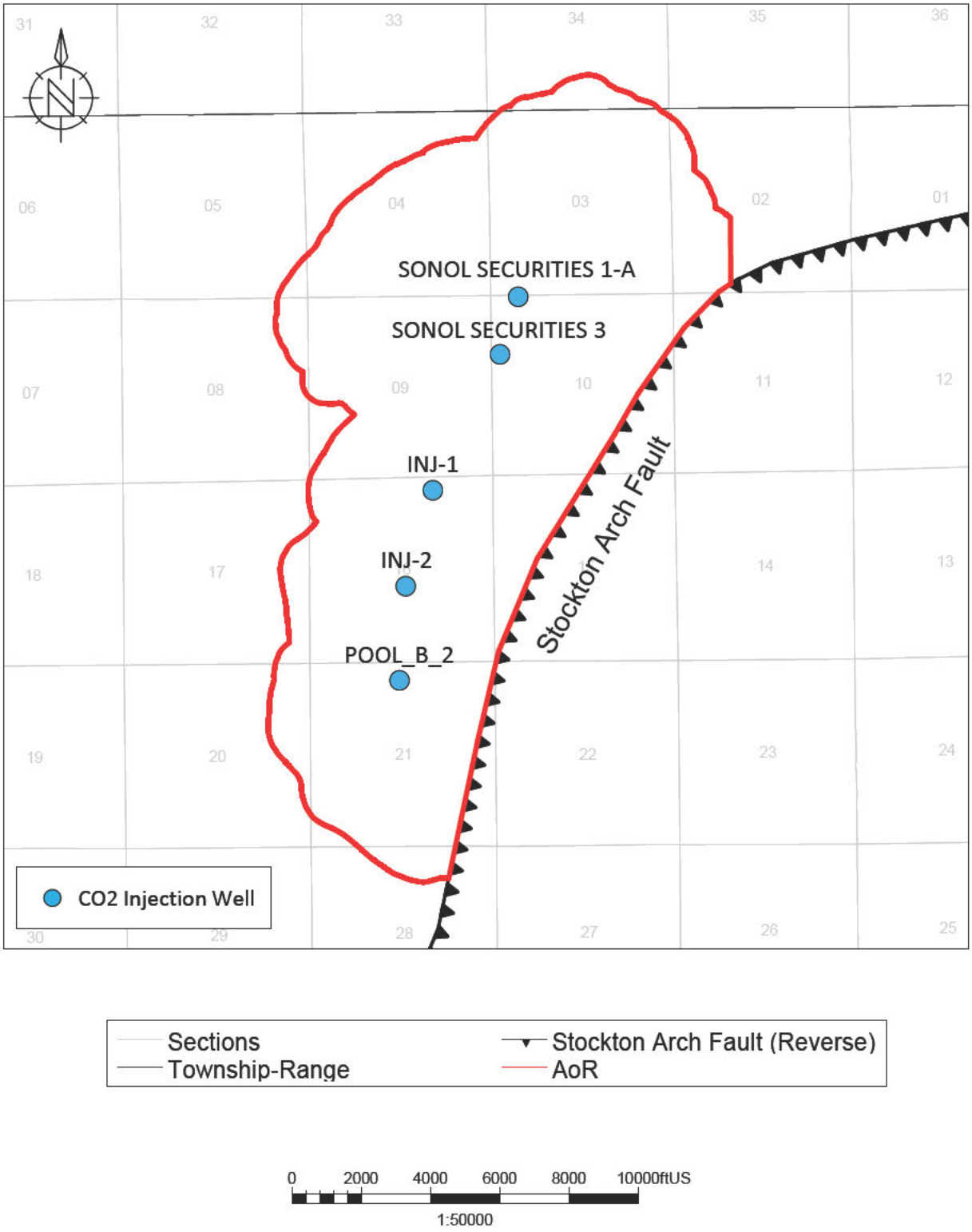

Figure 2.2-6. Injection well location map for the project area. Minimum distance between injection wells is 1,735 ft. and maximum distance is 4,390 ft.

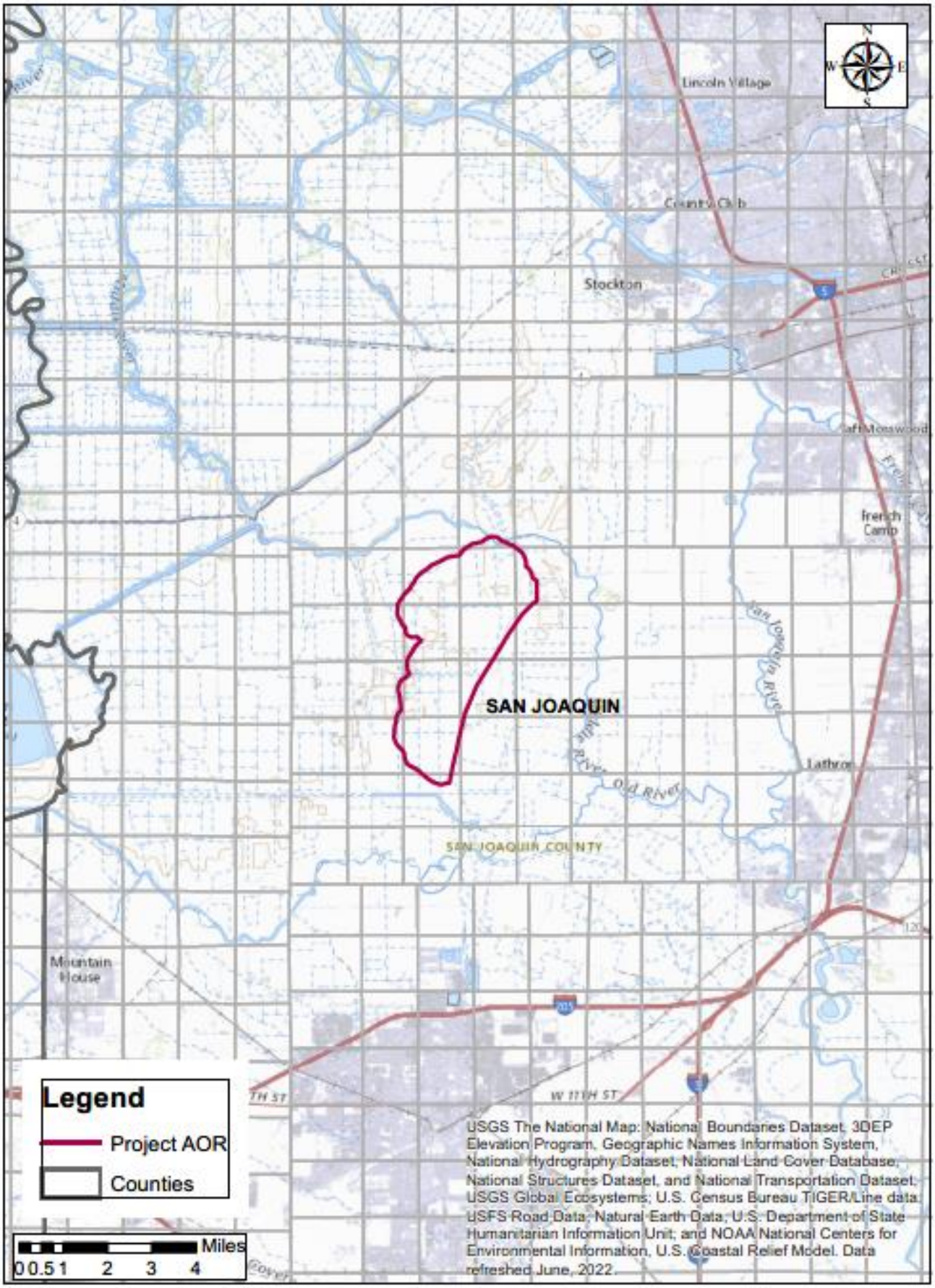

Figure 2.2-7. Surface Features and the AoR

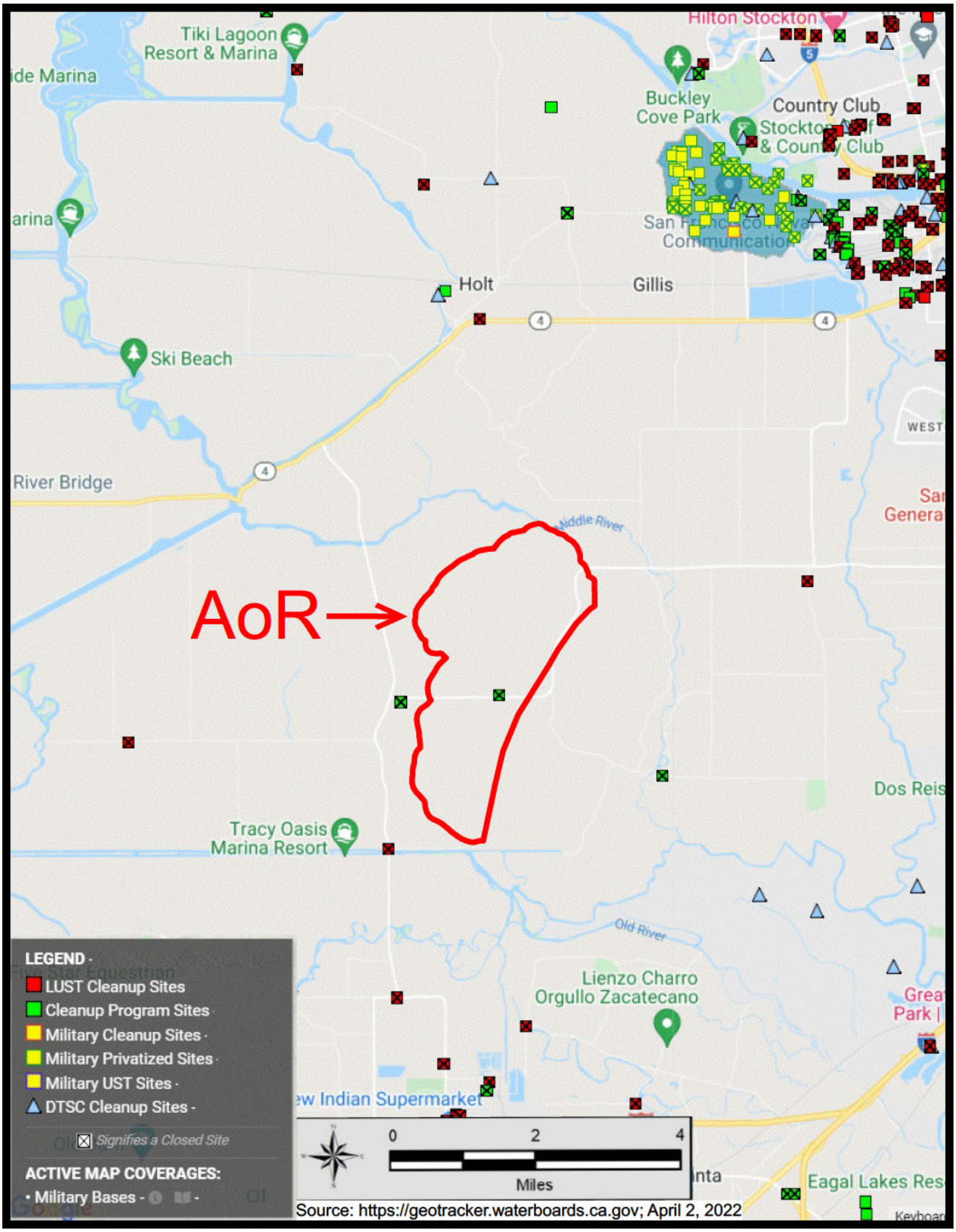

Figure 2.2-8 State and EPA approved Cleanup Sites

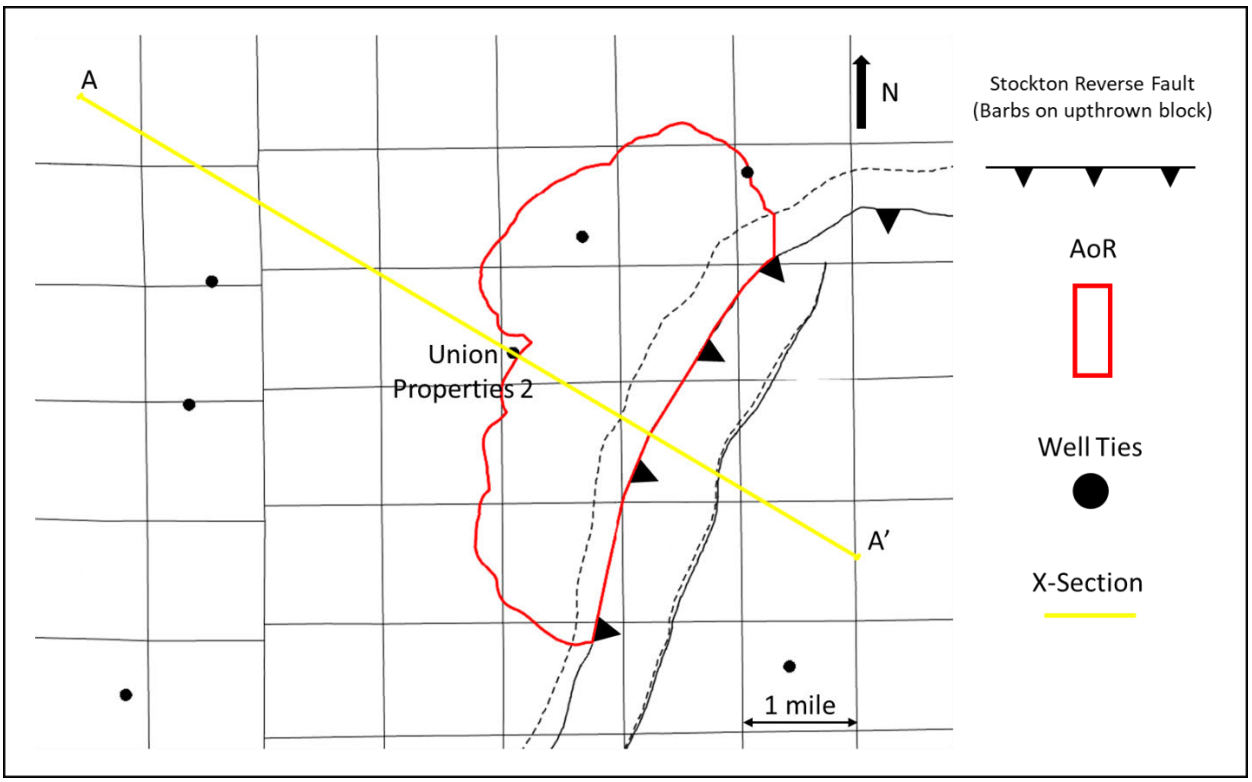

Figure 2.3-1. The two faults within the model are shown at the Winters level. The fault to the east is believed to be antithetic to the main Stockton Arch fault and is dashed into it in cross-section. Yellow line highlights the cross-section shown in **Figure 2.3-2**.

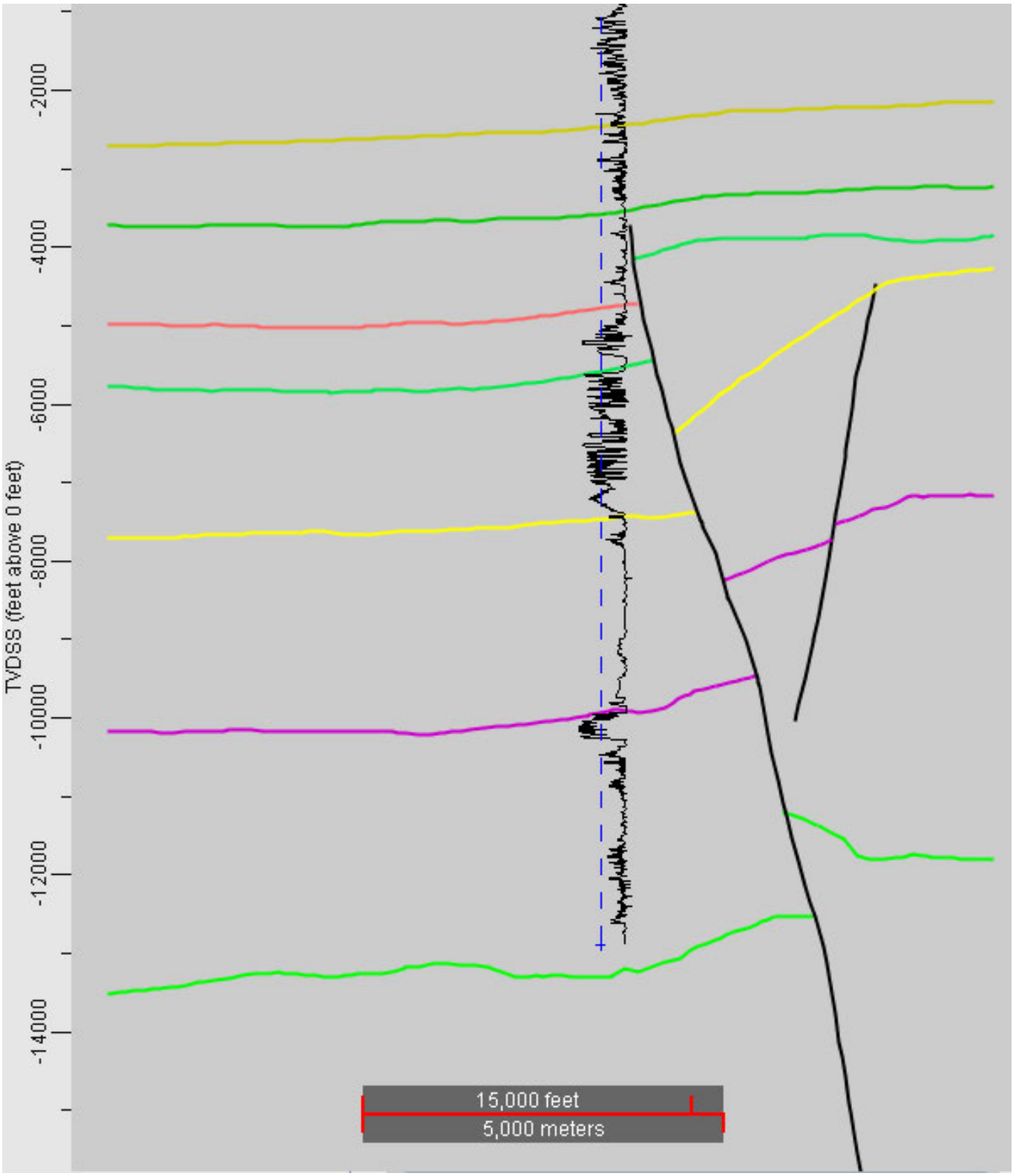

Figure 2.3-2. Structural cross section across the geologic model. Well Union Properties 2 (04077203220000) is shown with SP log (negative values to left) for correlation and geologic packages. Geologic surfaces developed from seismic interpretation. The Stockton Arch Fault is cut-off by the Base Valley Springs. The interpreted antithetic fault to the east is dashed into the Stockton Arch Fault

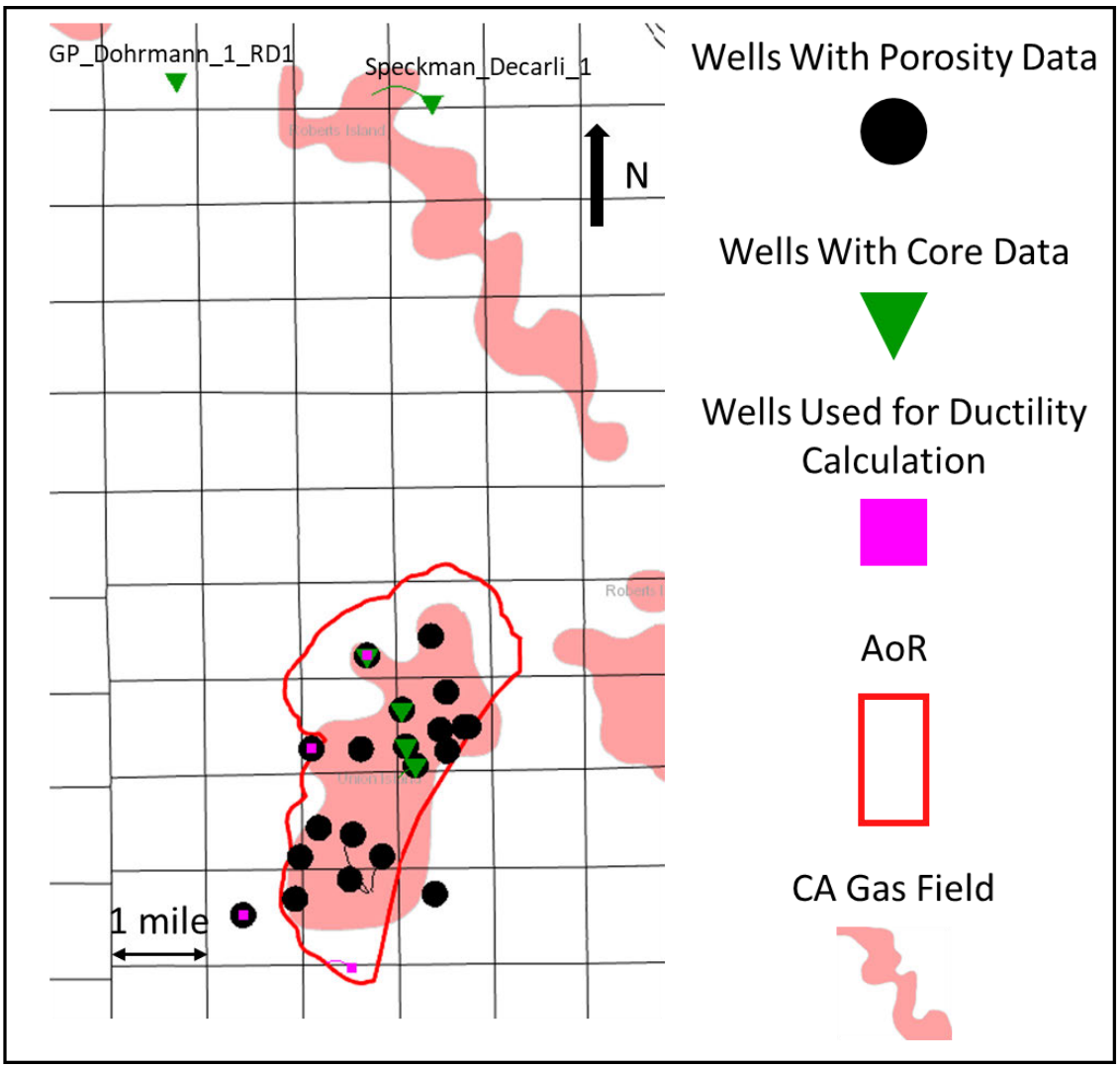

Figure 2.4-1. Map showing location of wells with mineralogy data relative to the AoR.

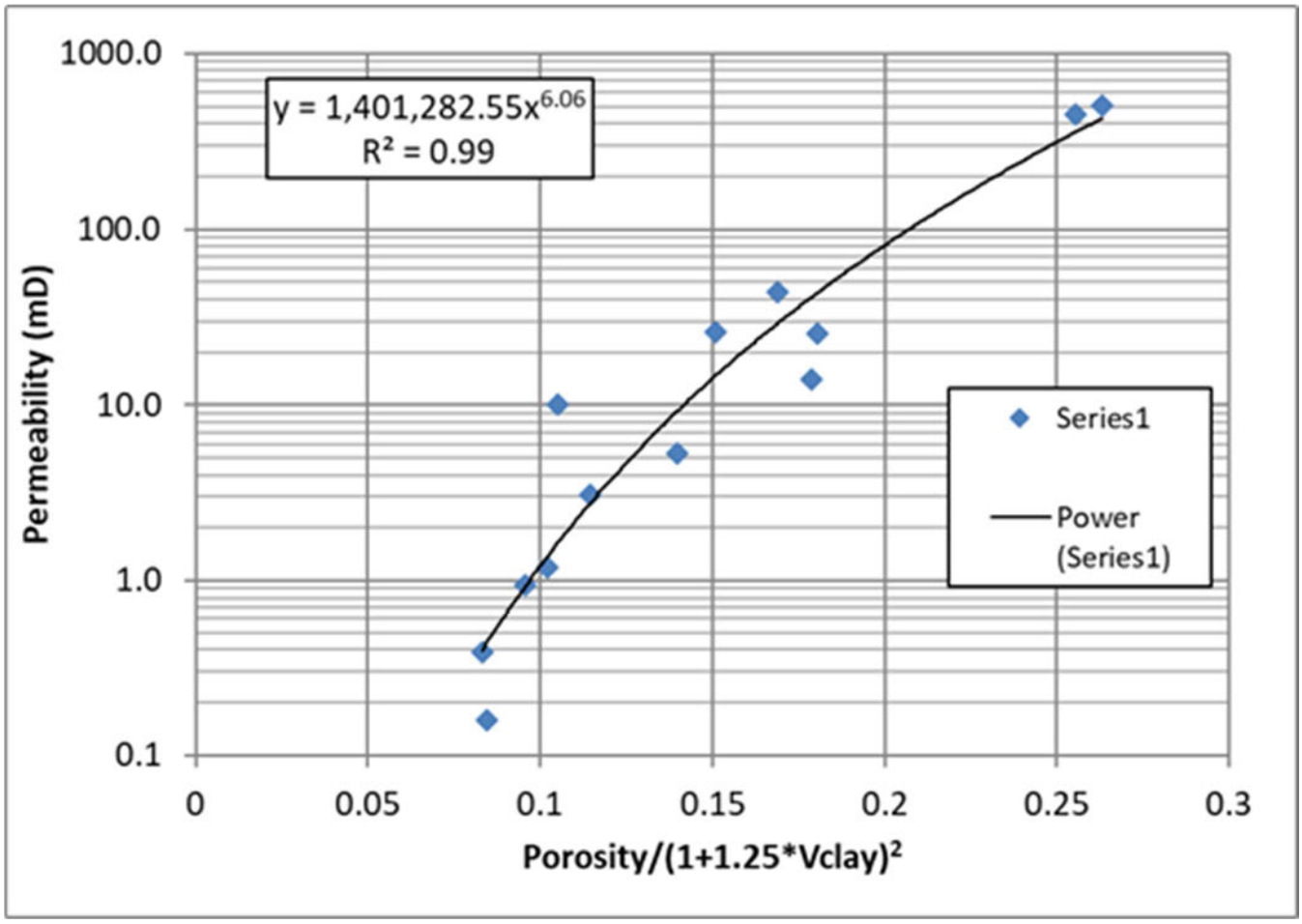

Figure 2.4-2. Permeability transform for Sacramento basin zones.

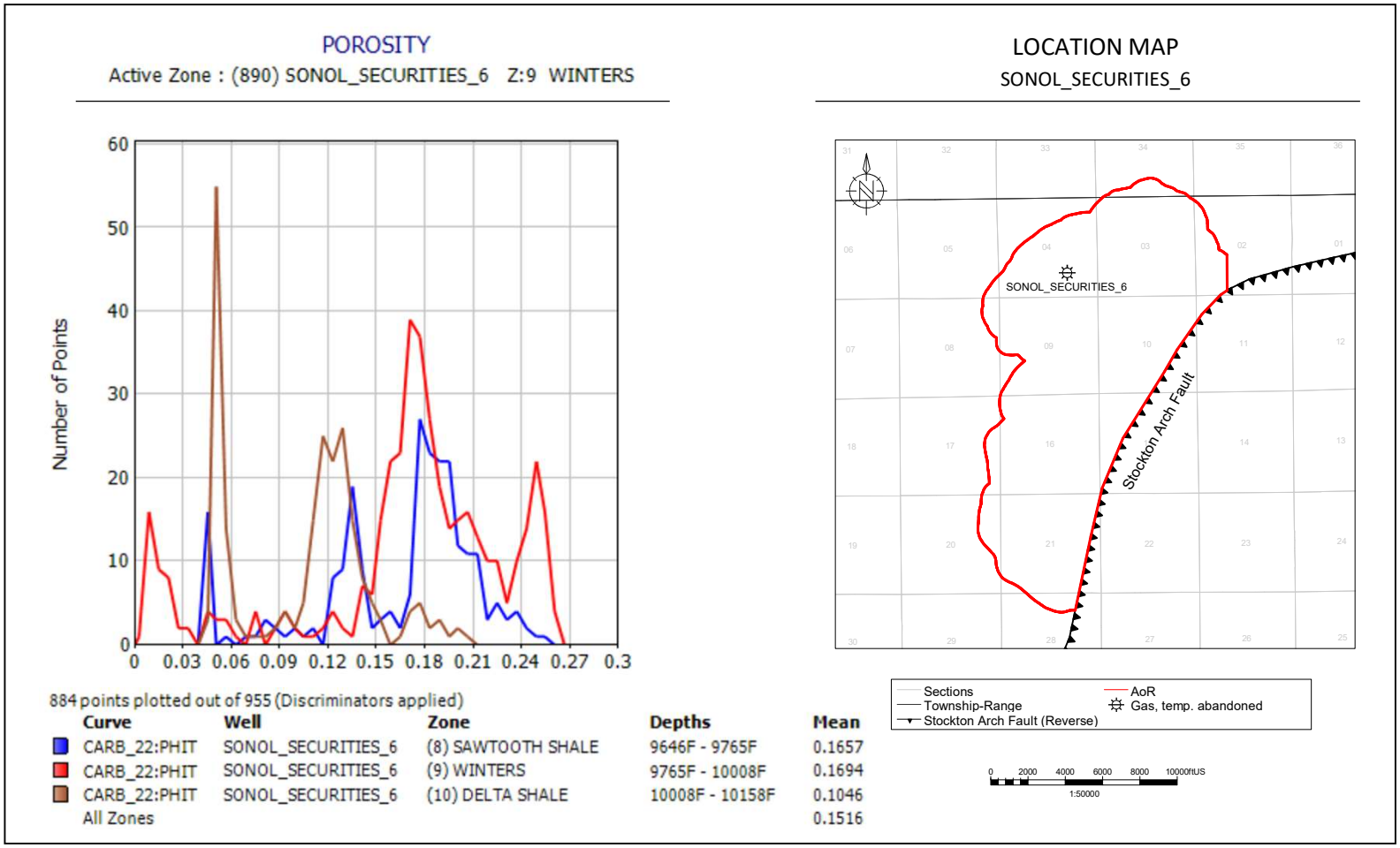

Figure 2.4-3. Porosity histogram for well Sonol_Securities_6. In the histogram, blue represents the Sawtooth Shale, red the Winters Formation, and brown the Delta Shale. For the two shale intervals, only data with VCL>0.25 is shown, and for the Winters only data with VCL<=0.25 is shown.

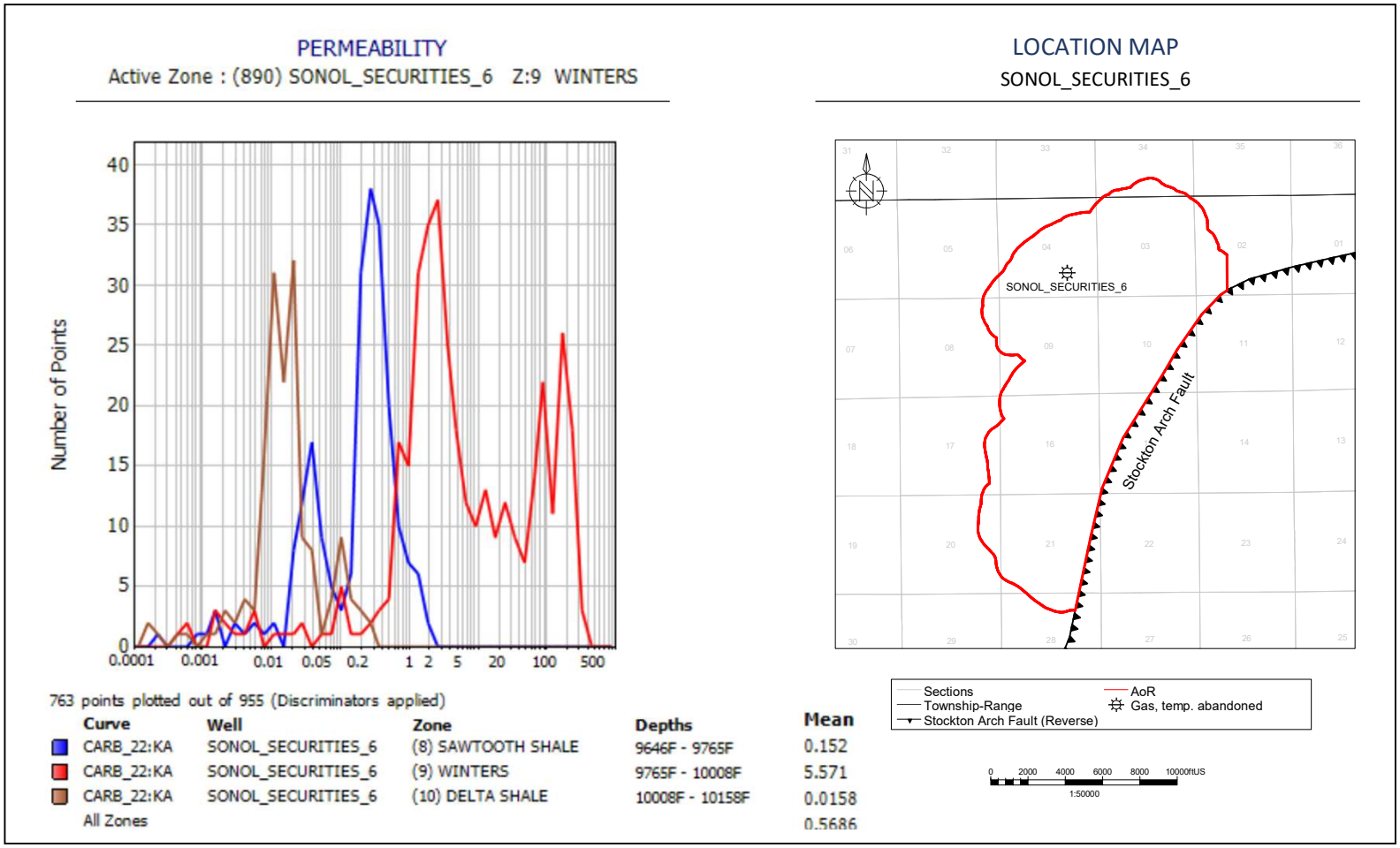

Figure 2.4-4. Permeability histogram for well Sonol_Securities_6. In the histogram, blue represents the Sawtooth Shale, red the Winters Formation, and brown the Delta Shale. For the two shale intervals, only data with VCL>0.25 is shown, and for the Winters only data with VCL<=0.25 is shown.

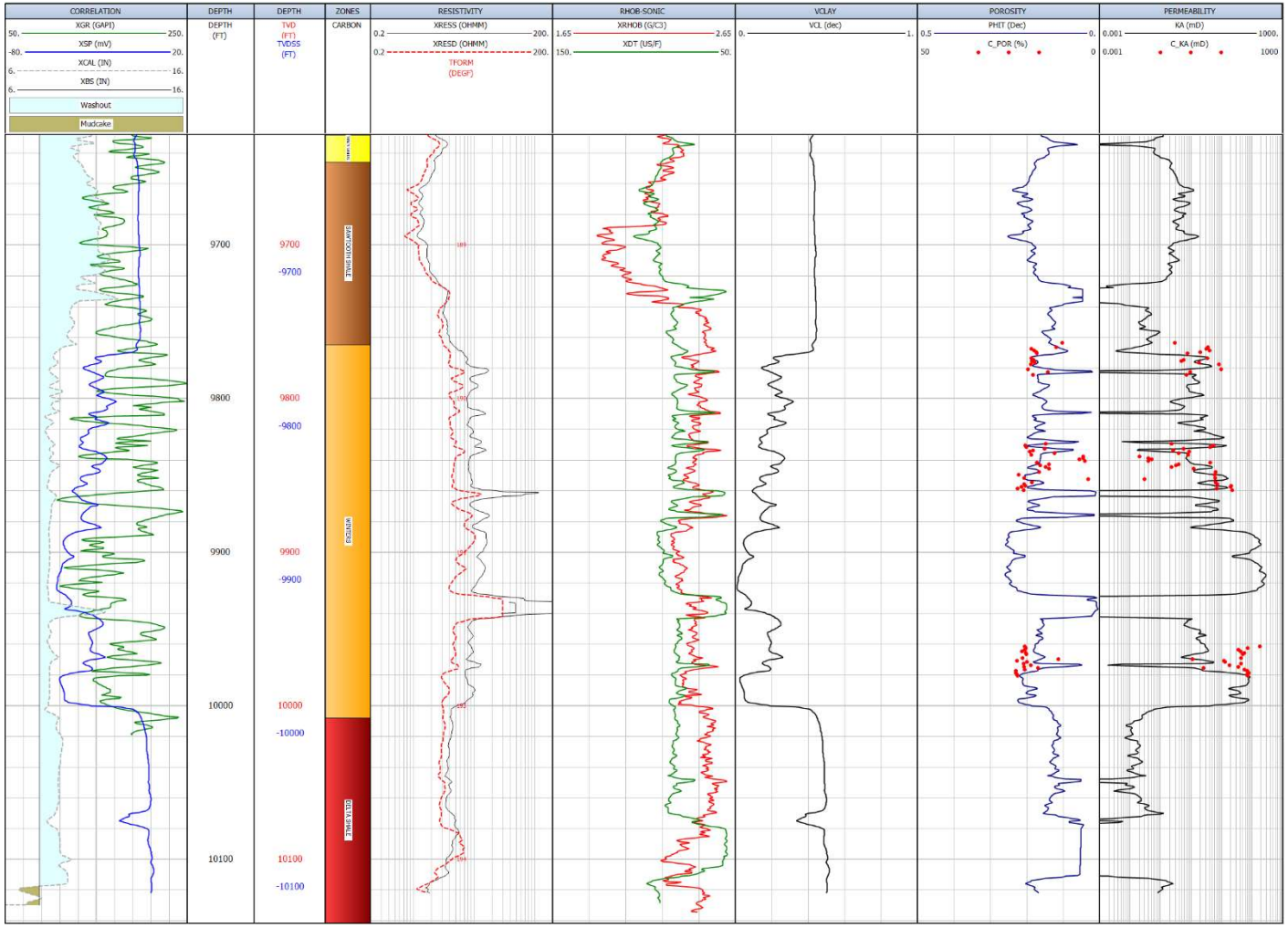

Figure 2.4-5. Log plot for well Sonol_Securities_6, showing the log curves used as inputs into calculations of clay volume, porosity and permeability, and their outputs. Core data for porosity and permeability is shown for comparison to the log model. Track 1: Correlation and caliper logs. Track 2: Measured depth. Track 3: Vertical depth and vertical subsea depth. Track 4: Zones. Track 5: Resistivity. Track 6: Compressional sonic and density logs. Track 7: Volume of clay. Track 8: Porosity calculated from log curves and core porosity. Track 9: Permeability calculated using transform and core permeability.

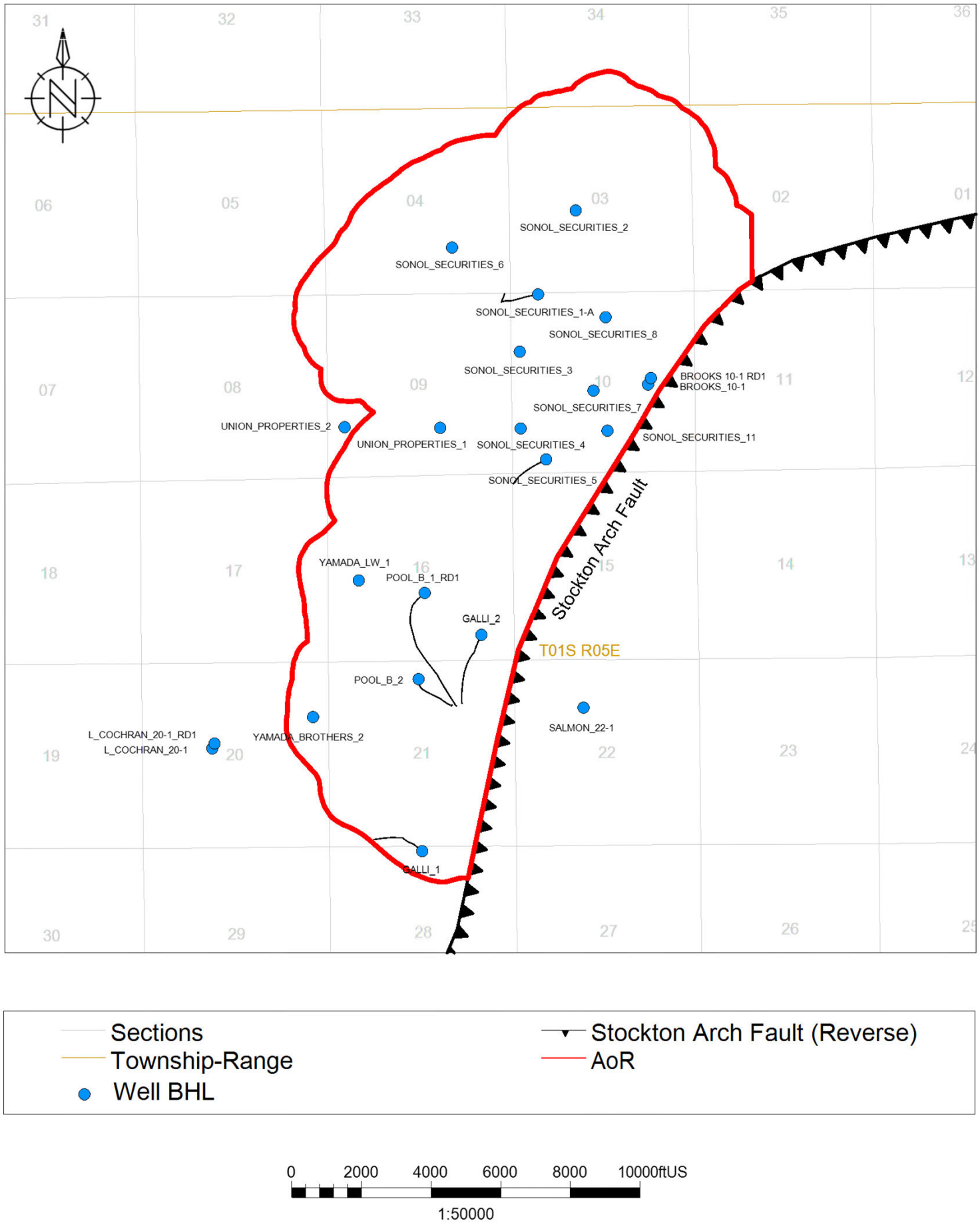

Figure 2.4-6. Map of wells with porosity and permeability data.

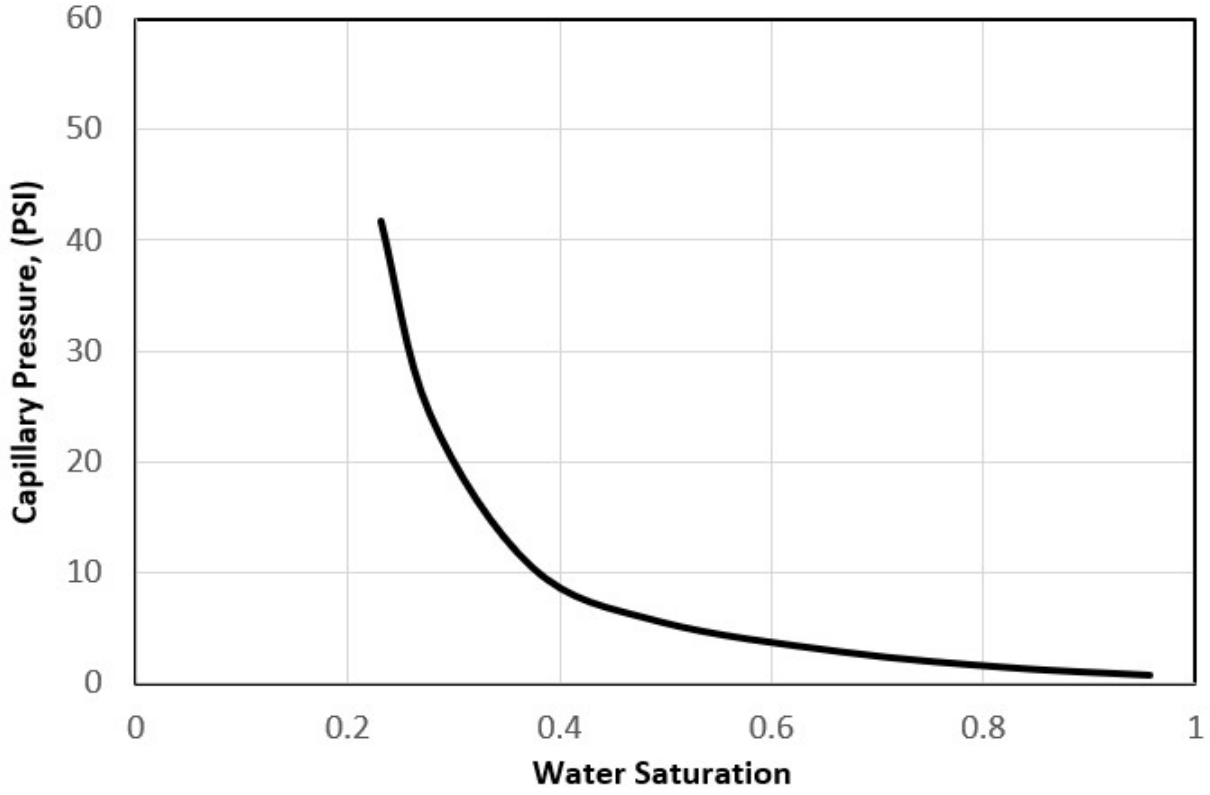

Figure 2.4-7. Injection zone Cappillary pressure curve used in Computational modeling. Obtained from core sample from Sonol Securities 5 in the Union Gas Field

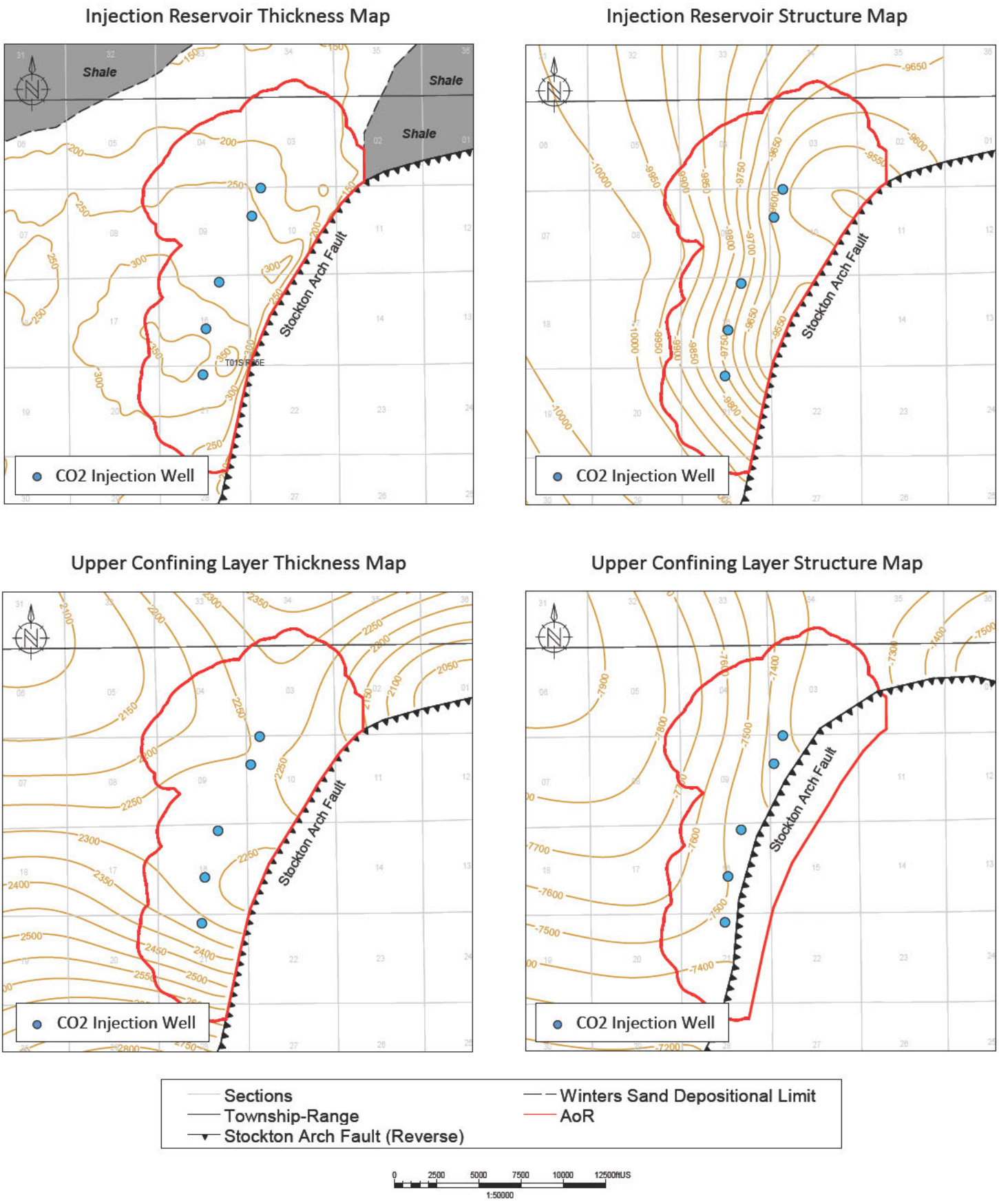

Figure 2.4-8. Thickness and depth maps within the AoR for the injection reservoir and the upper confining layer.

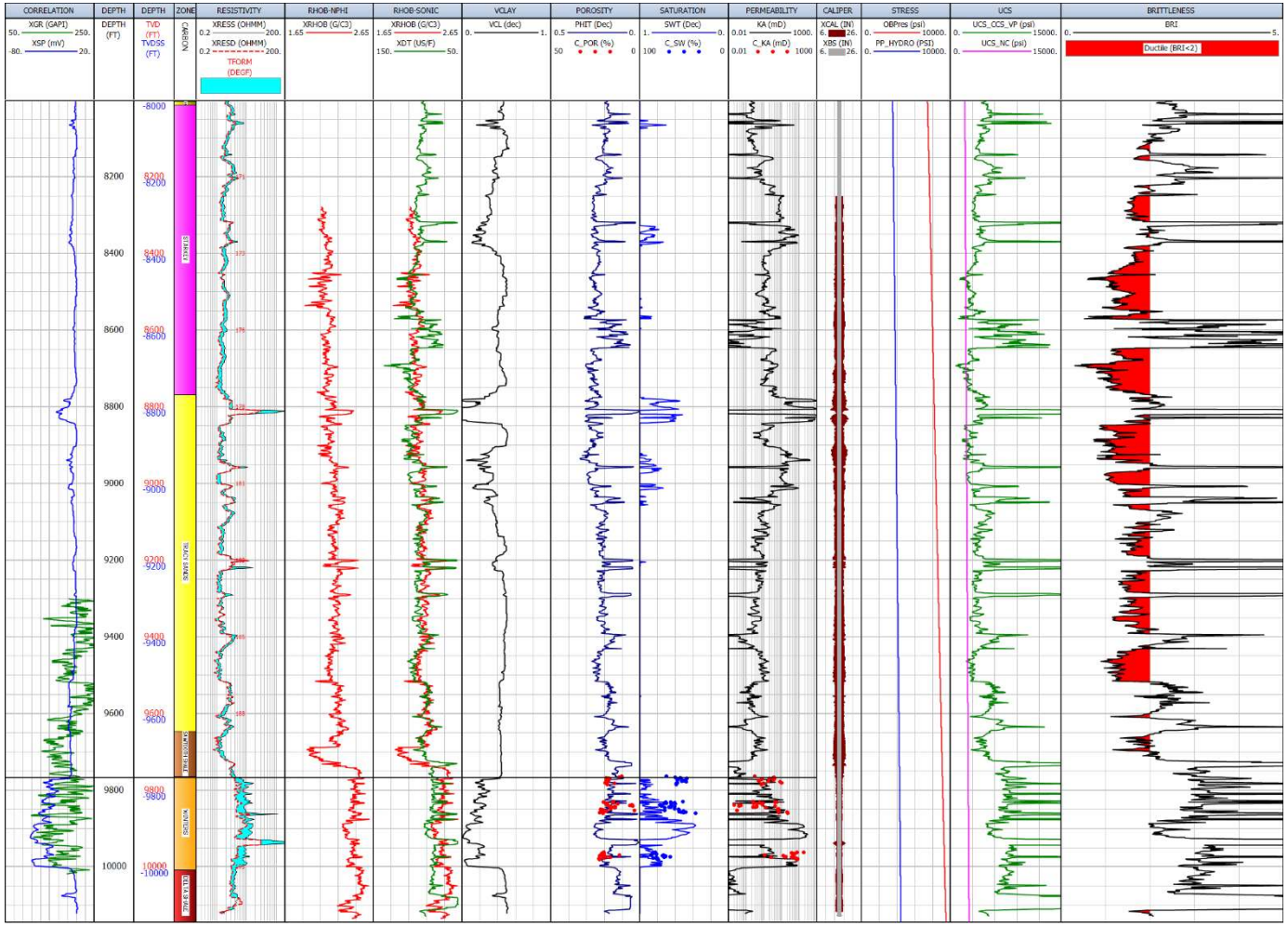

Figure 2.5-1. Unconfined compressive strength and ductility calculations for well Sonol_Securities_6. The upper confining zone ductility is less than two. Track 1: Correlation logs. Track 2: Measured depth. Track 3: Vertical depth and vertical subsea depth. Track 4: Zones. Track 5: Resistivity. Track 6: Density log. Track 7: Density and compressional sonic logs. Track 8: Volume of clay. Track 9: Porosity calculated from sonic and density. Track 10: Water saturation. Track 11: Permeability. Track 12: Caliper. Track 13: Overburden pressure and hydrostatic pore pressure. Track 14: UCS and UCS_NC. Track 15: Brittleness

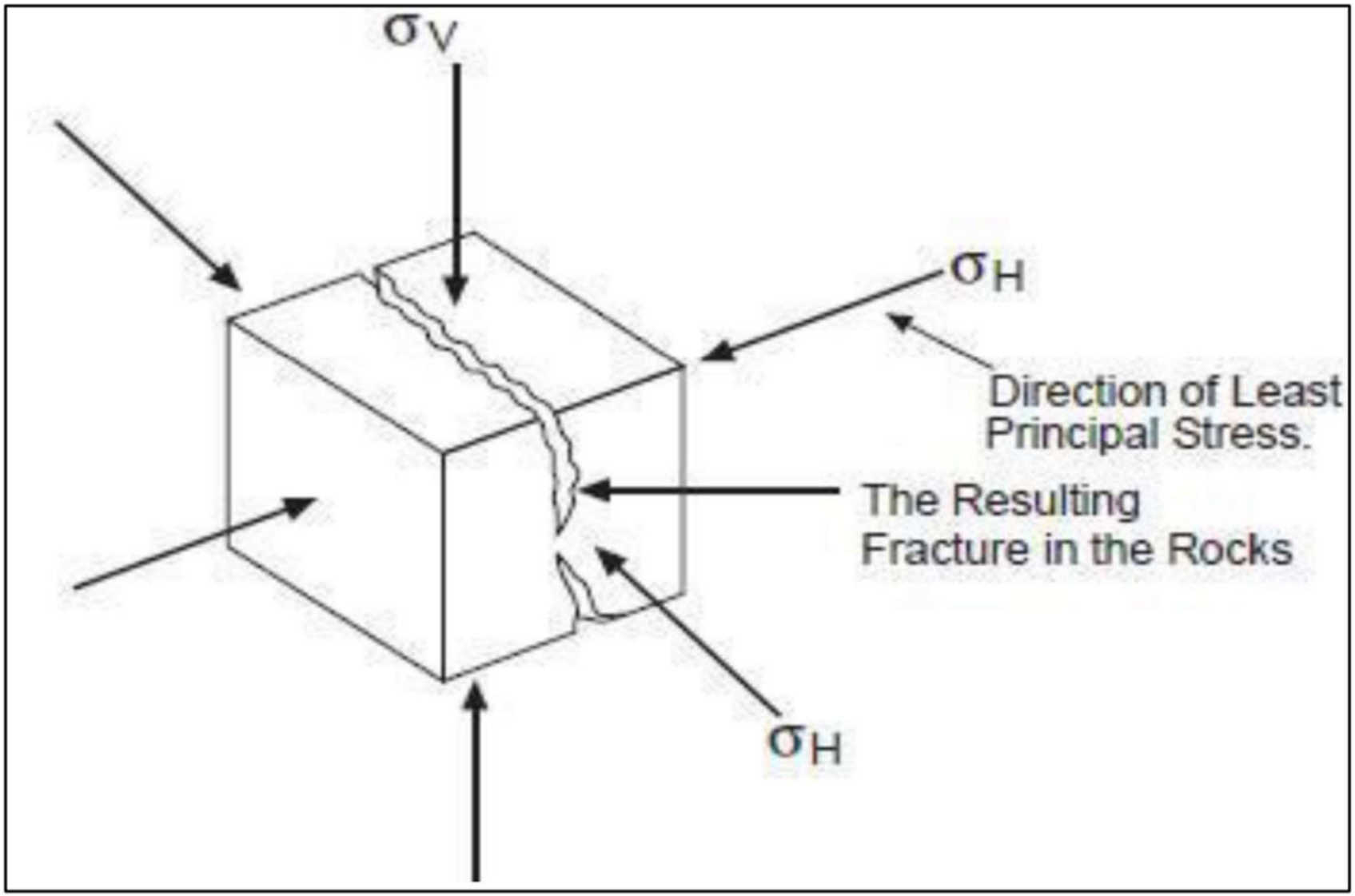

Figure 2.5-2. Stress diagram showing the three principal stresses and the fracturing that will occur perpendicular to the minimum principal stress

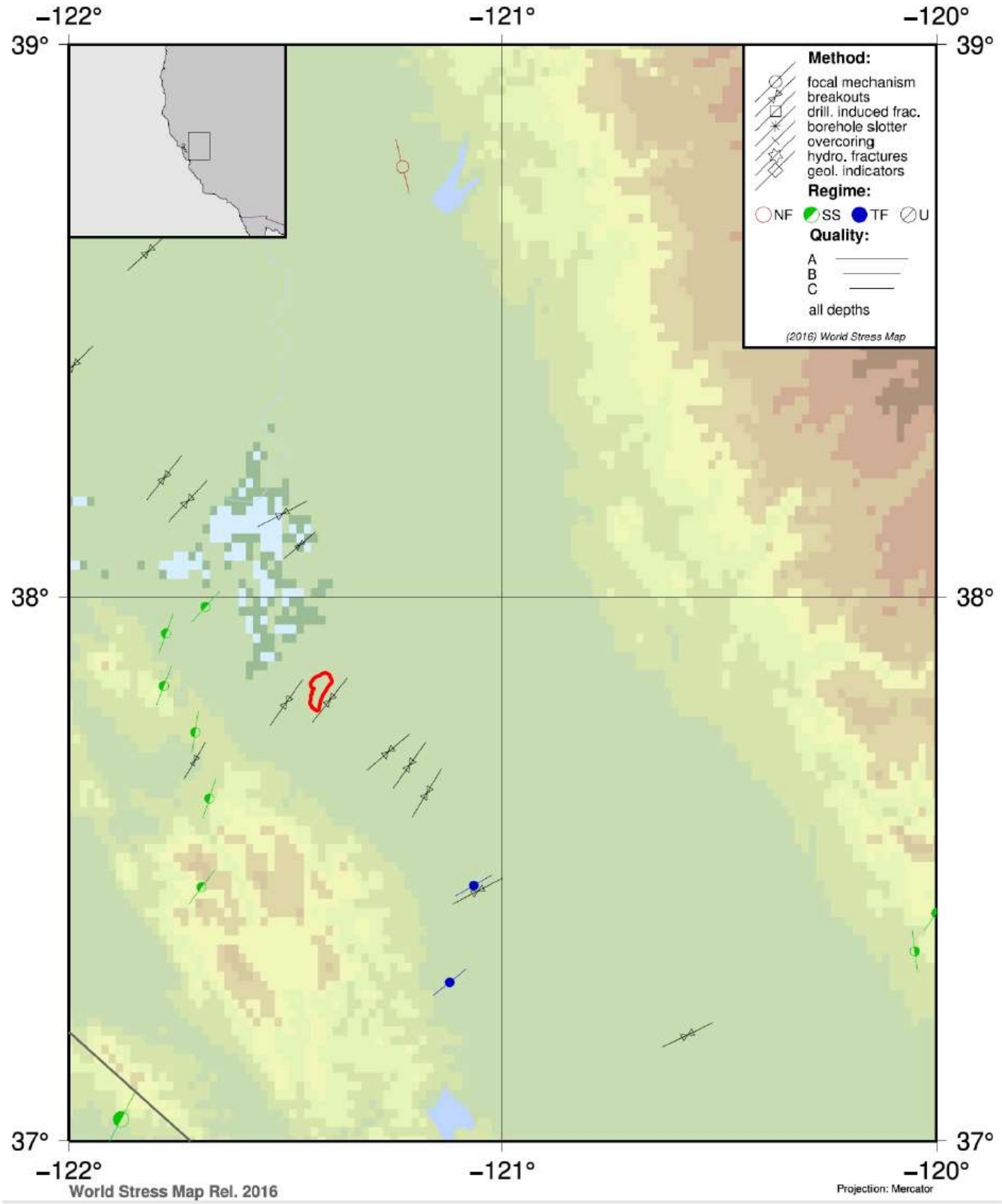

Figure 2.5-3. World Stress Map output showing S_{Hmax} azimuth indicators and earthquake faulting styles in the Sacramento Basin (Heidbach et al., 2016). The red polygon is the project AoR. The background coloring represents topography.

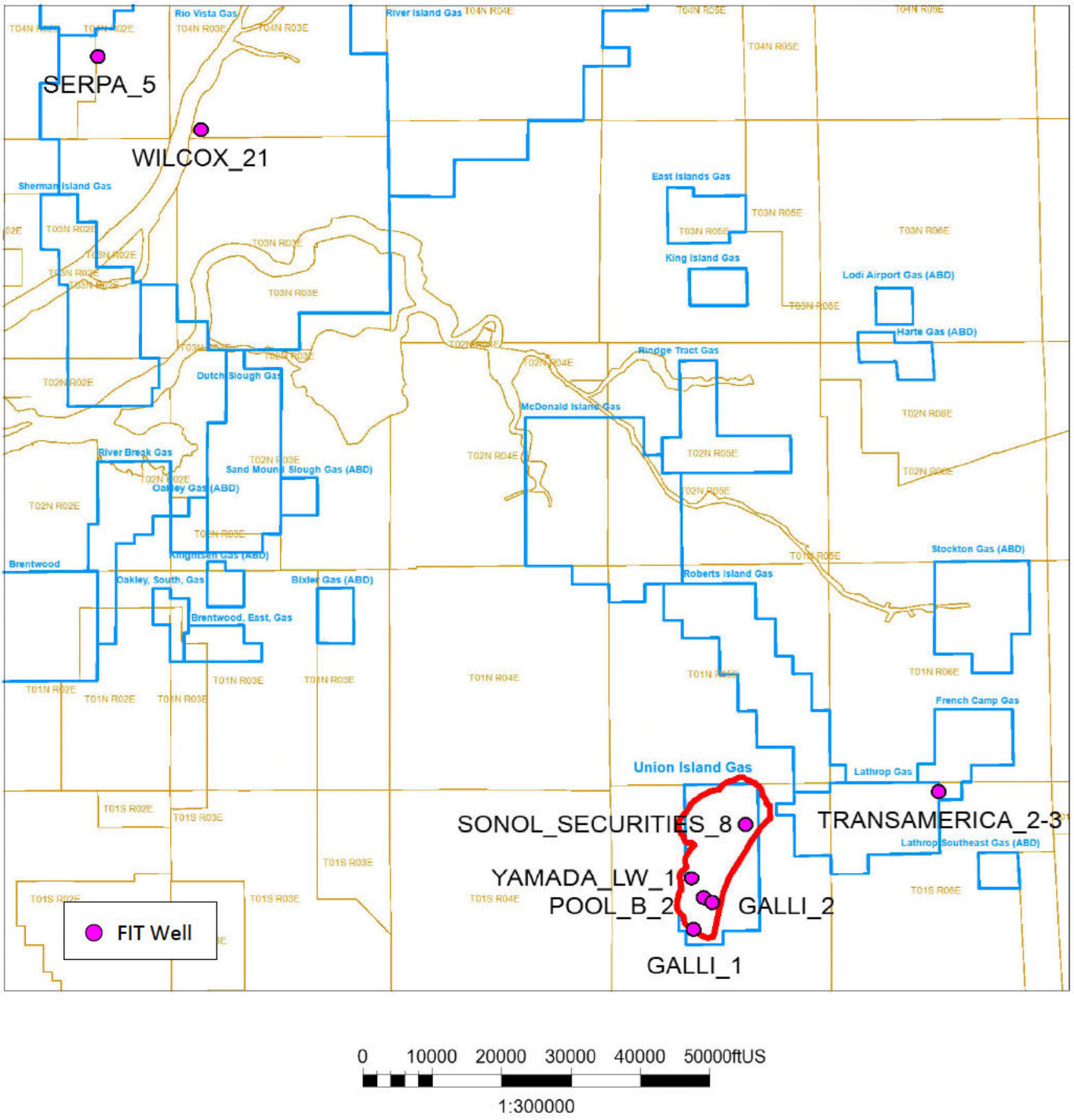

Figure 2.5-4. Location of wells with FIT data.

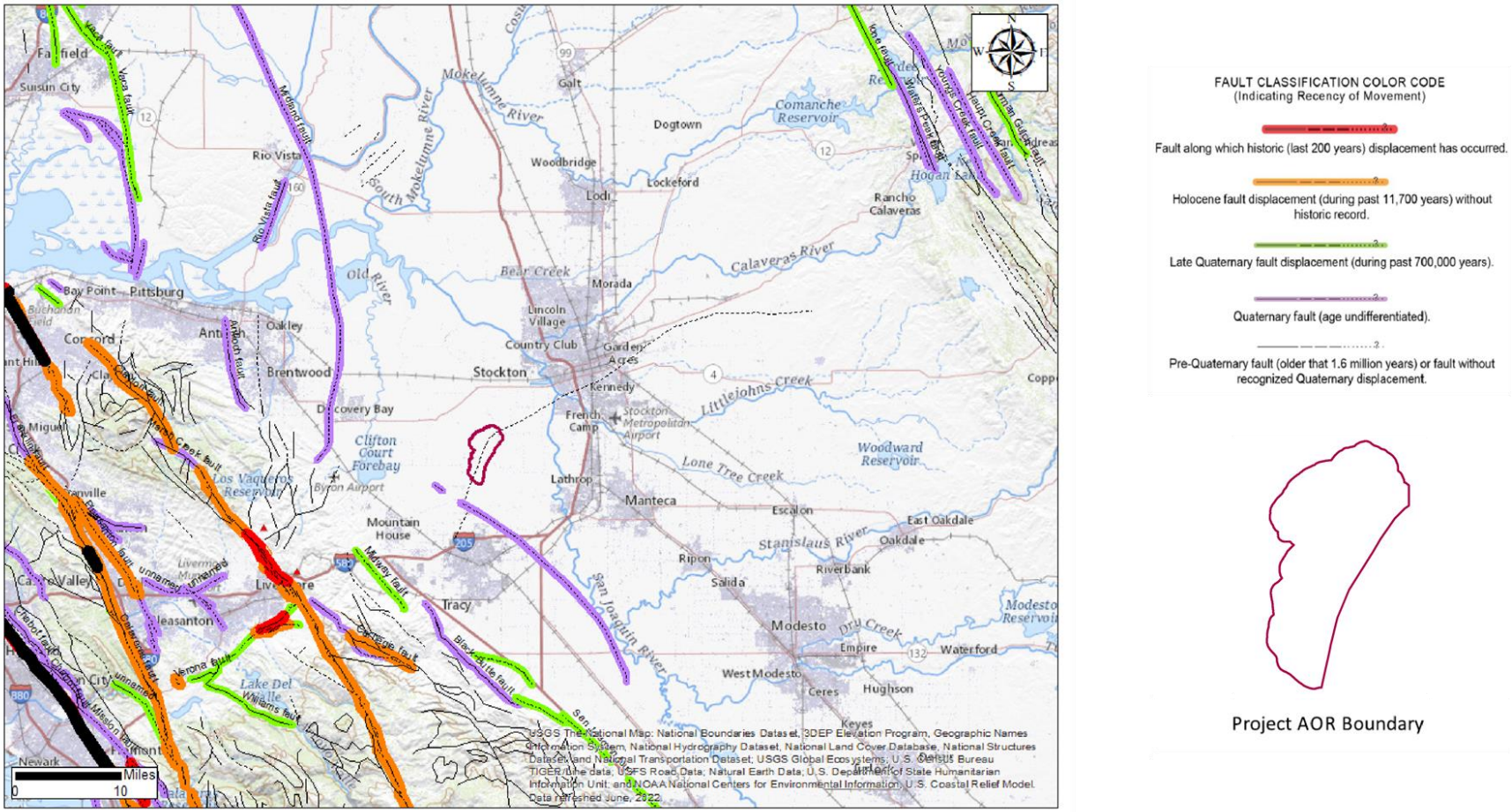

Figure 2.6-1: Fault Activity Map from the California Geologic Survey and United States Geological Survey. The fault trace of the Stockton Fault shown here agrees with the 3D seismic interpretation. The fault trace is not colored indicating it is interpreted as Pre-Quaternary (older than 1.6 million years) by the California Geologic Survey. This is also in agreement with the seismic and well-based interpretation. (https://maps.conservation.ca.gov/cgs/fam/)

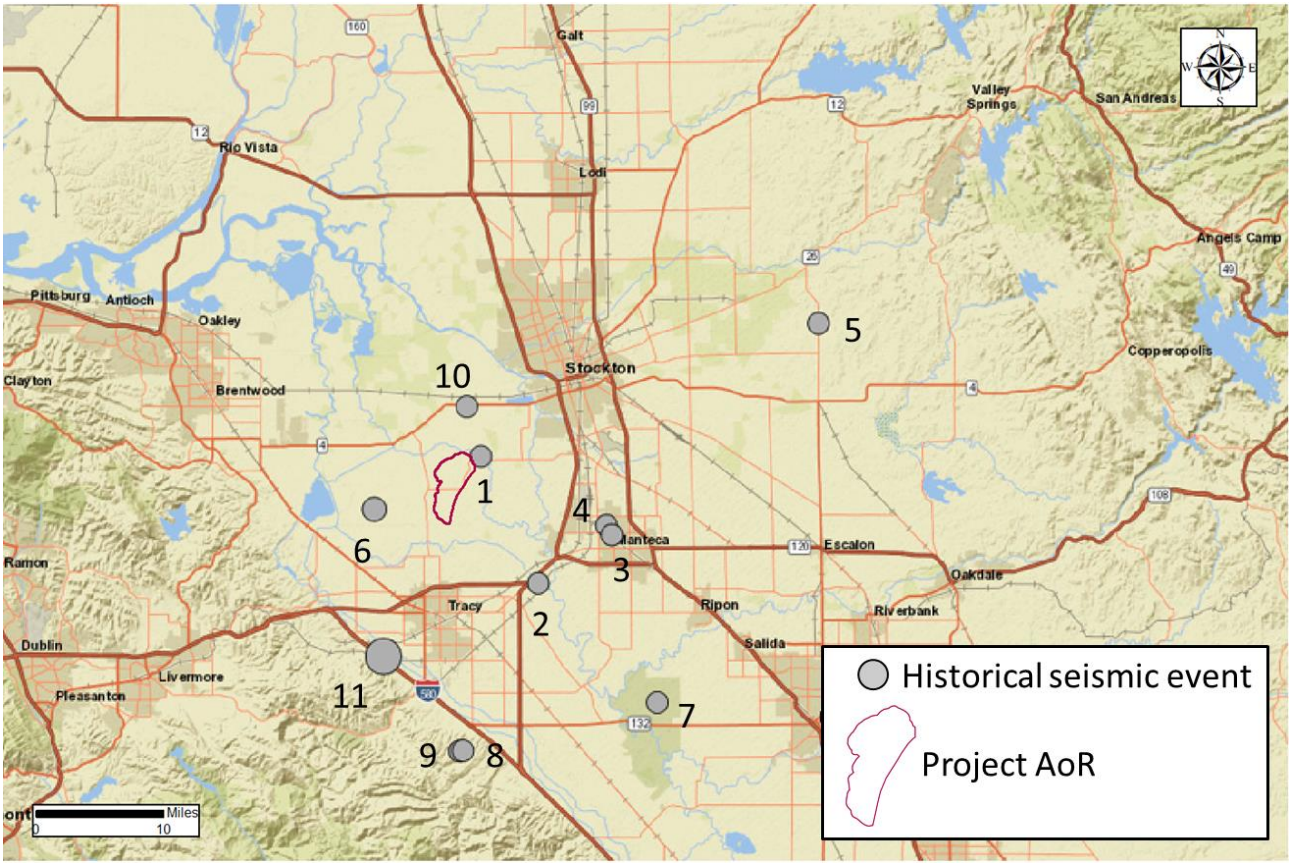

Figure 2.6-2. Image is modified from USGS search results. Data from these events are compiled in **Table 2.6-1** in chronological order associated with events 1 through 11 on the map.

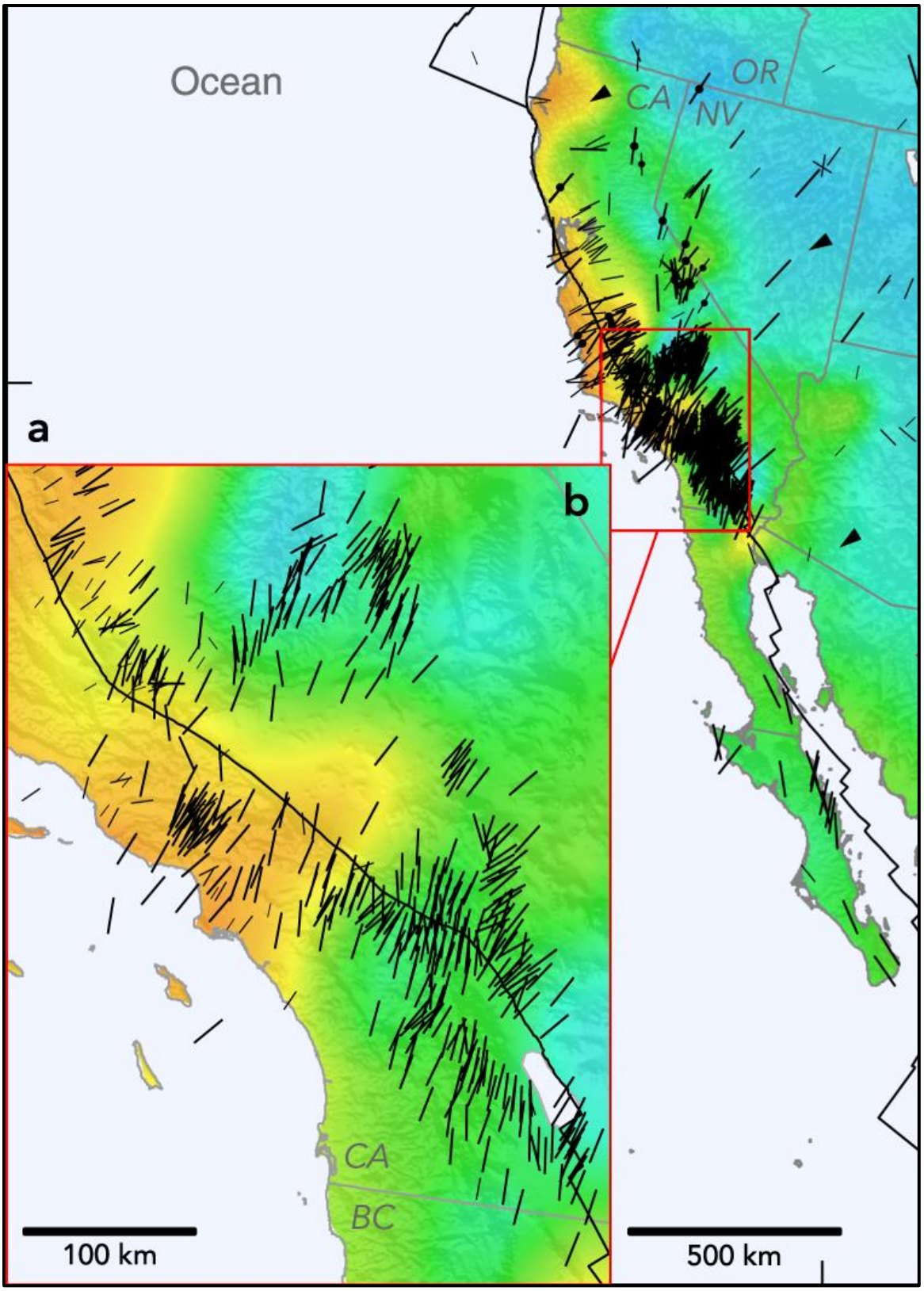

Figure 2.6-3. Image modified from Lund Snee and Zoback (2020) showing relative stress magnitudes across California. Red star indicates CTV II project site area.

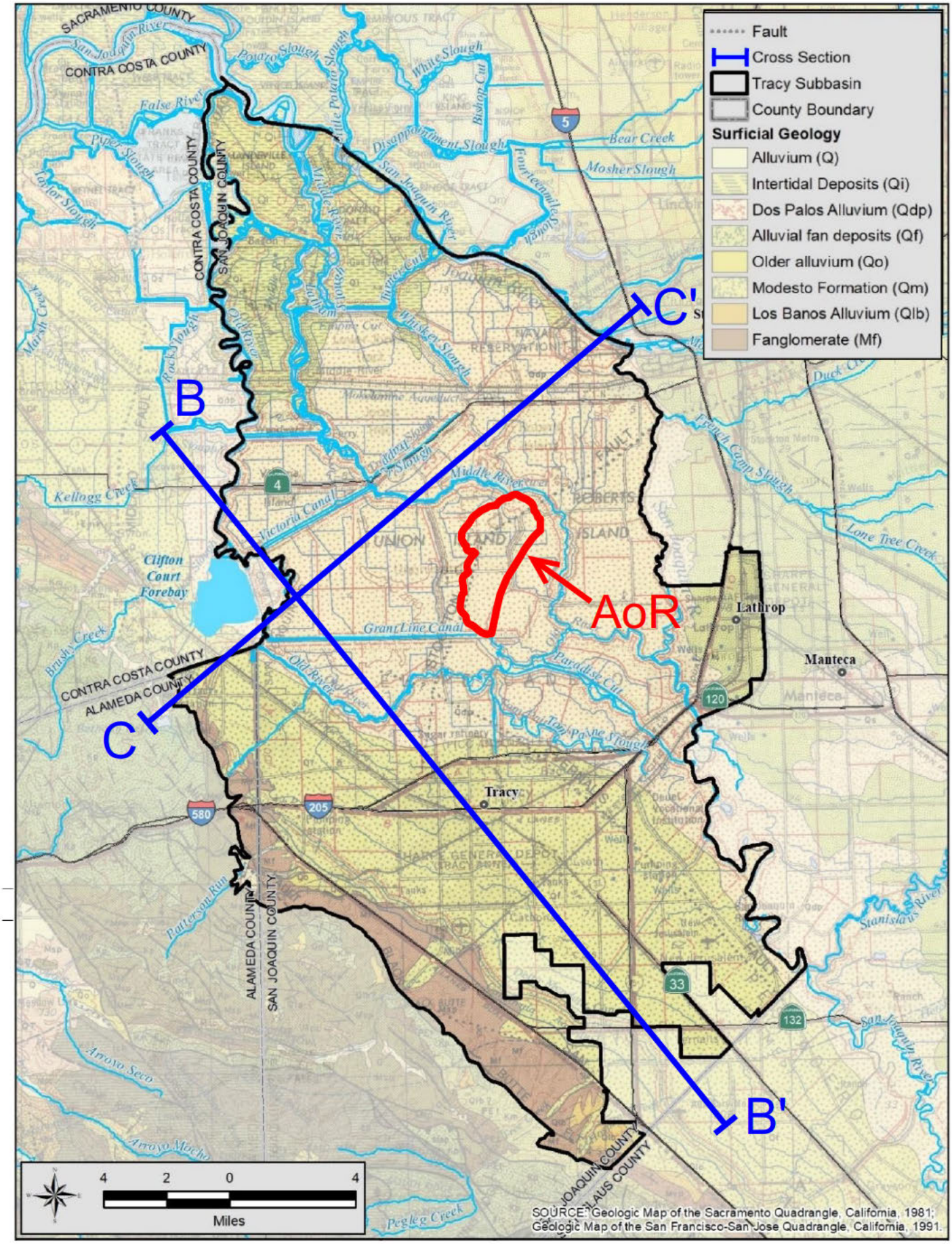

Modified from: GEI Consultants, Inc.; Tracy Subbasin Groundwater Sustainability Plan. November 1, 2021.

Figure 2.7-1 Tracy Subbasin, Surface Geology, and Cross Section Index Map

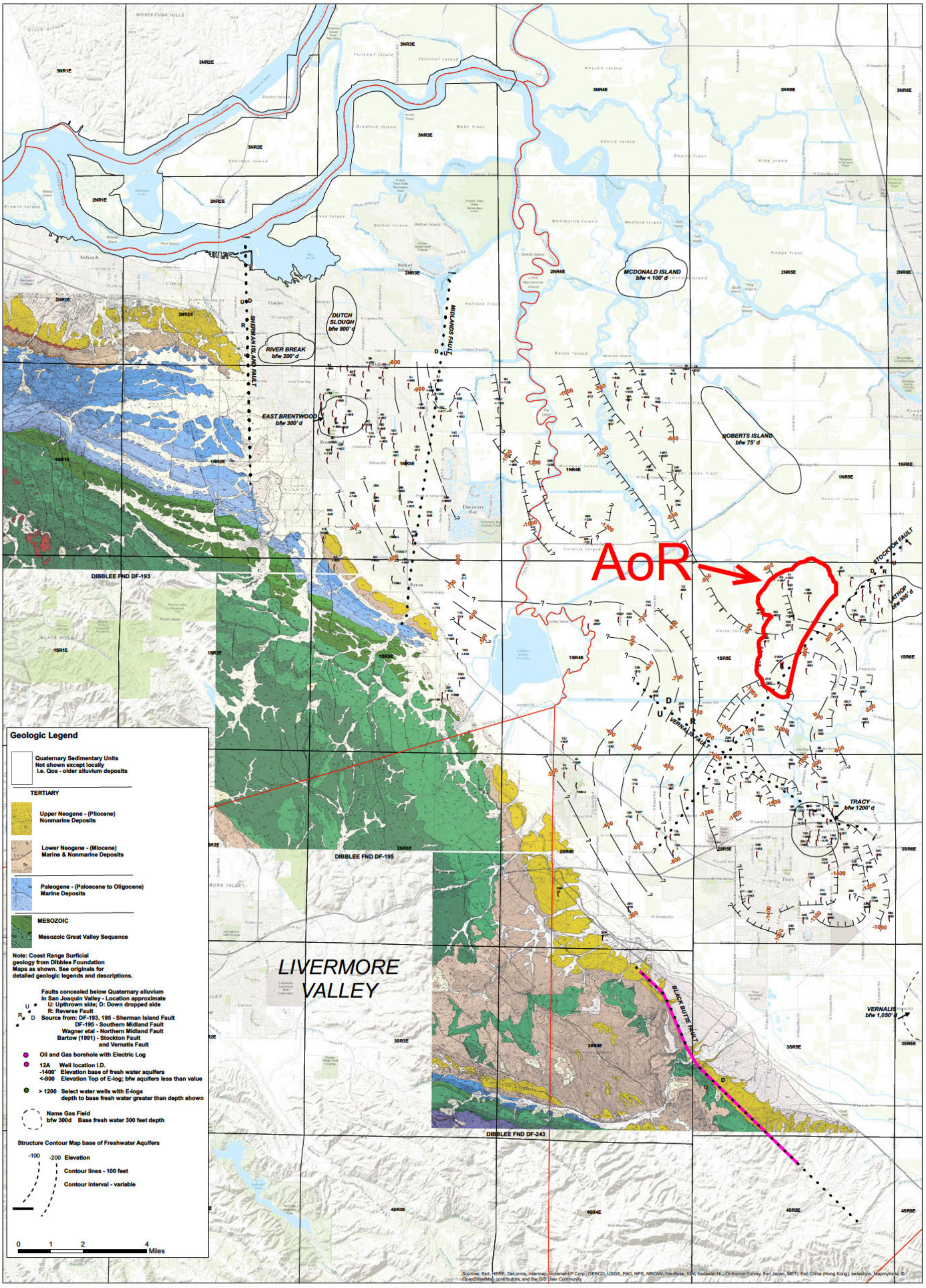

Modified from: Luhdorff & Scalmanini, Consulting Engineers, Inc., An Evaluation of Geologic Conditions, East Contra Costa County, March 29, 2016

Figure 2.7-2 Geologic Map and Base of Fresh Water

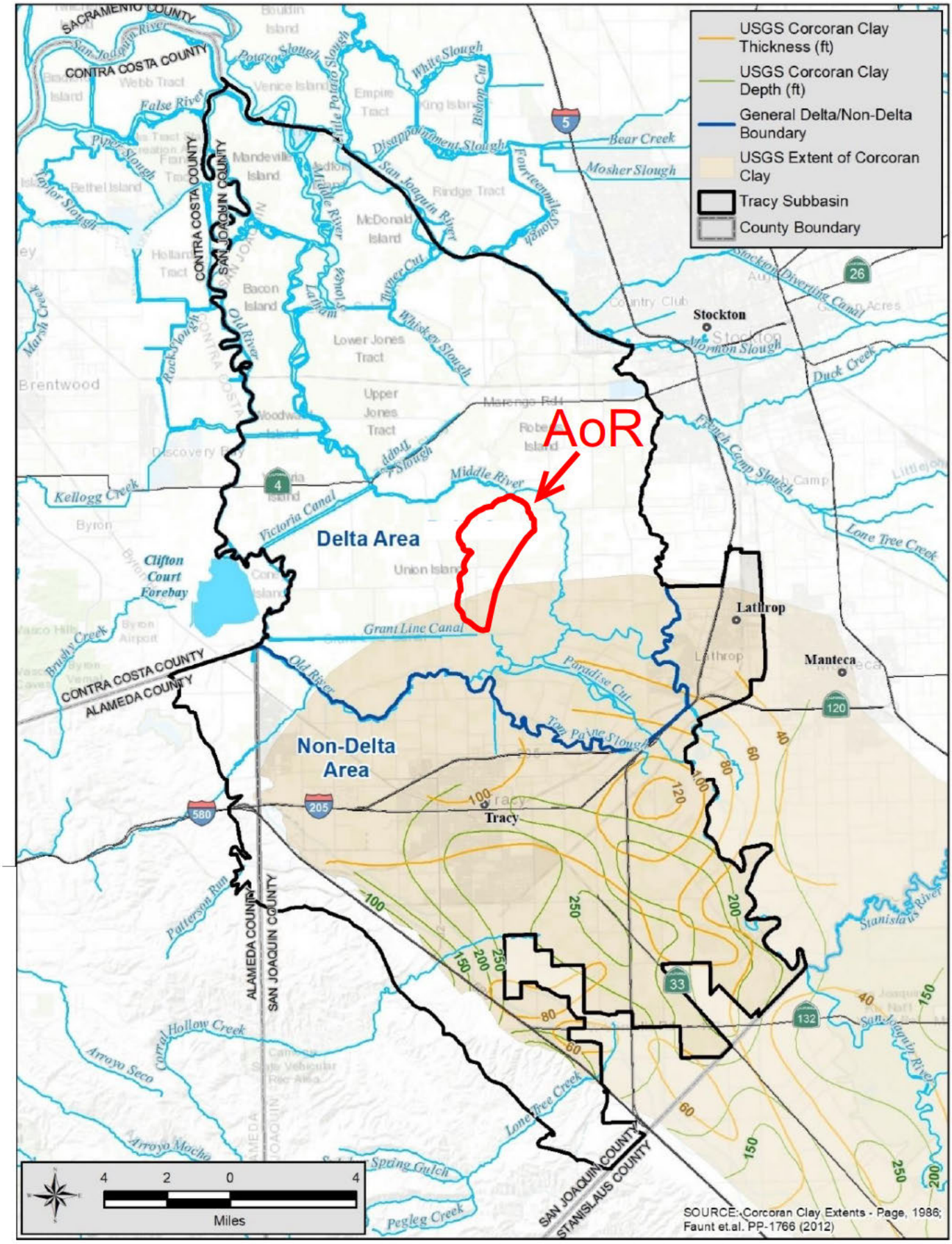

Modified from: GEI Consultants, Inc.; Tracy Subbasin Groundwater Sustainability Plan. November 1, 2021.

Figure 2.7-3 Estimated Corcoran Clay Thickness and Extent

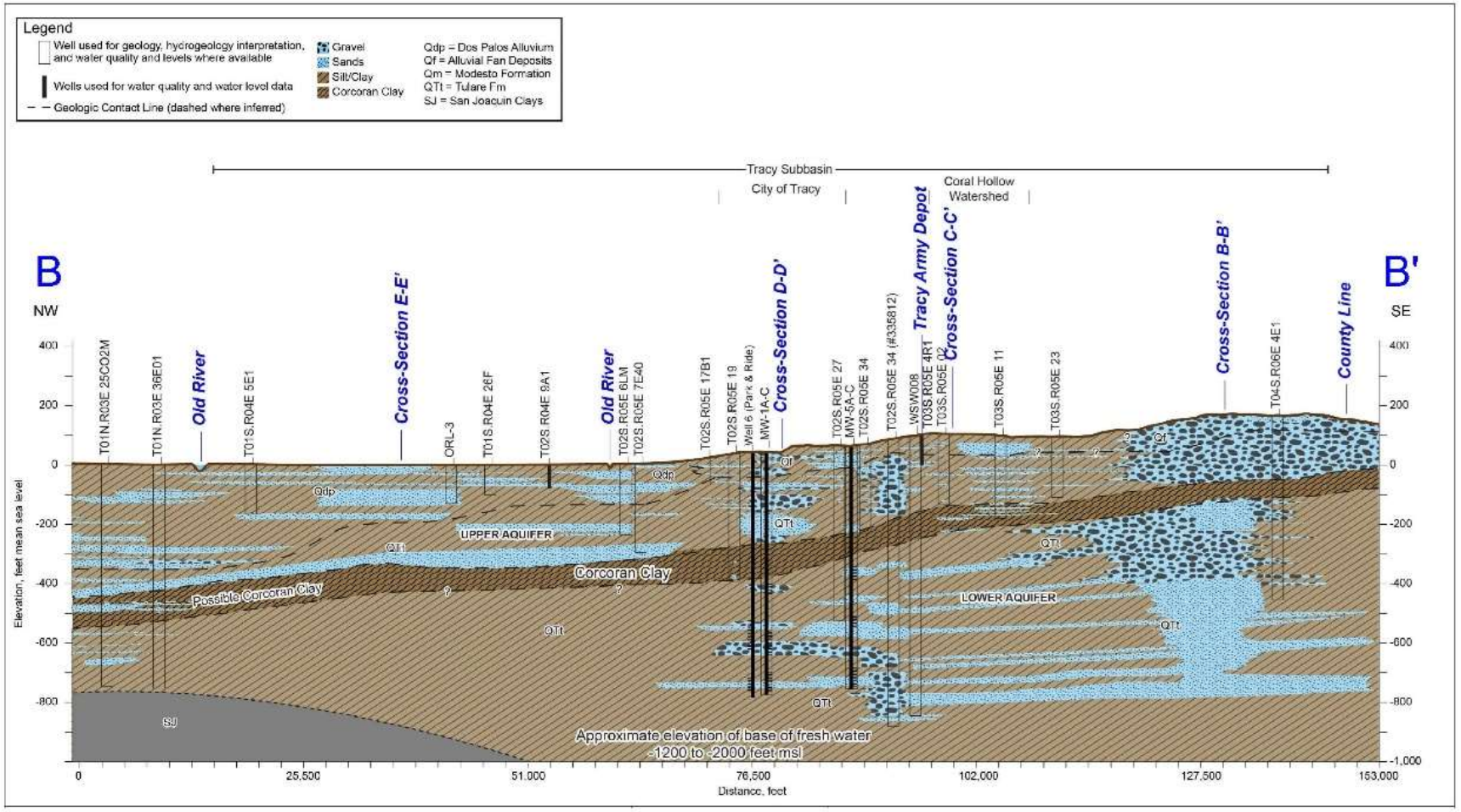

Modified from: GEI Consultants, Inc.; Tracy Subbasin Groundwater Sustainability Plan. November 1, 2021.

Figure 2.7-4. Geologic Cross Section B-B’

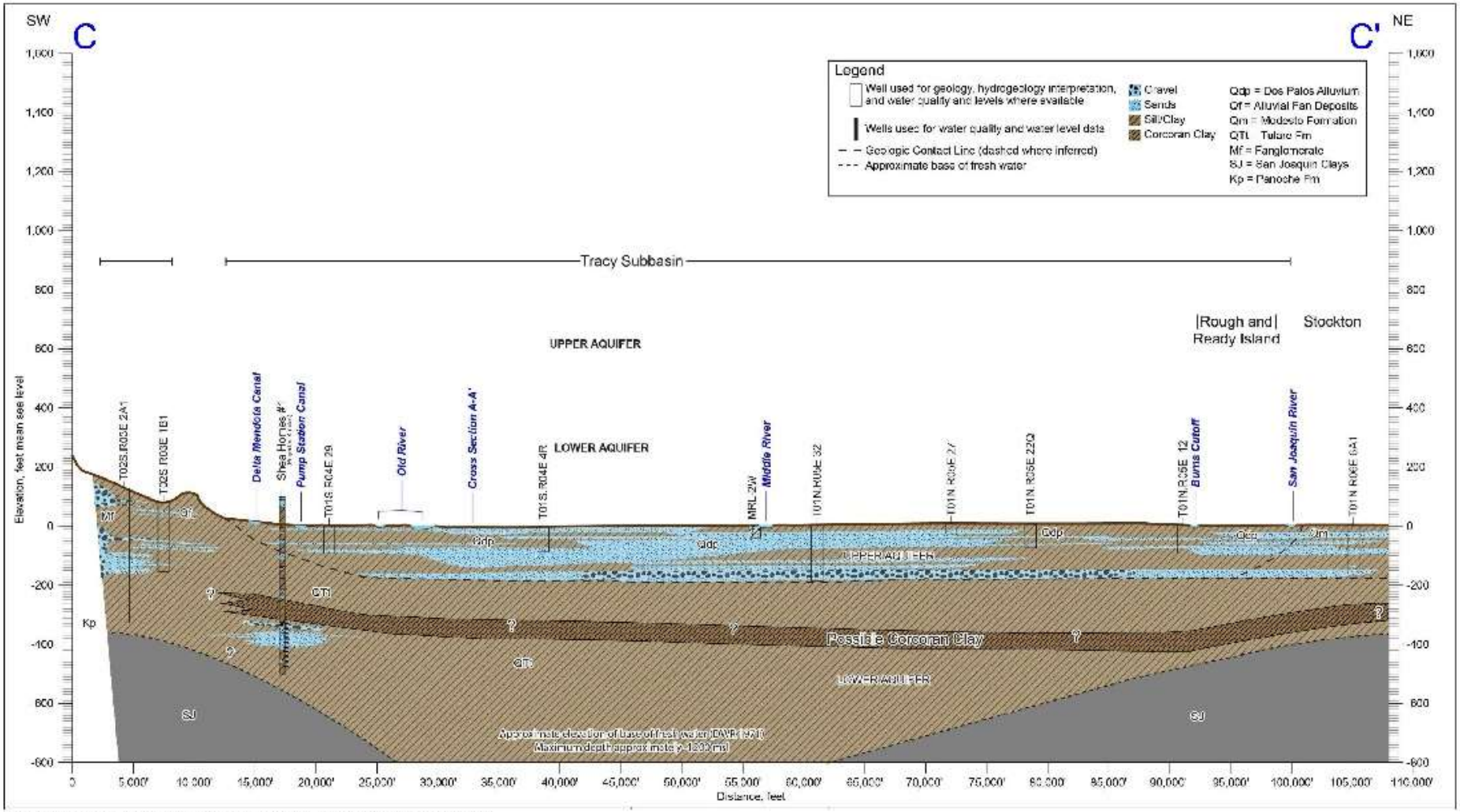

Modified from: GEI Consultants Inc. Tracy Subbasin Groundwater Sustainability Plan. November 1, 2021.

Figure 2.7-5. Geologic Cross Section C-C'

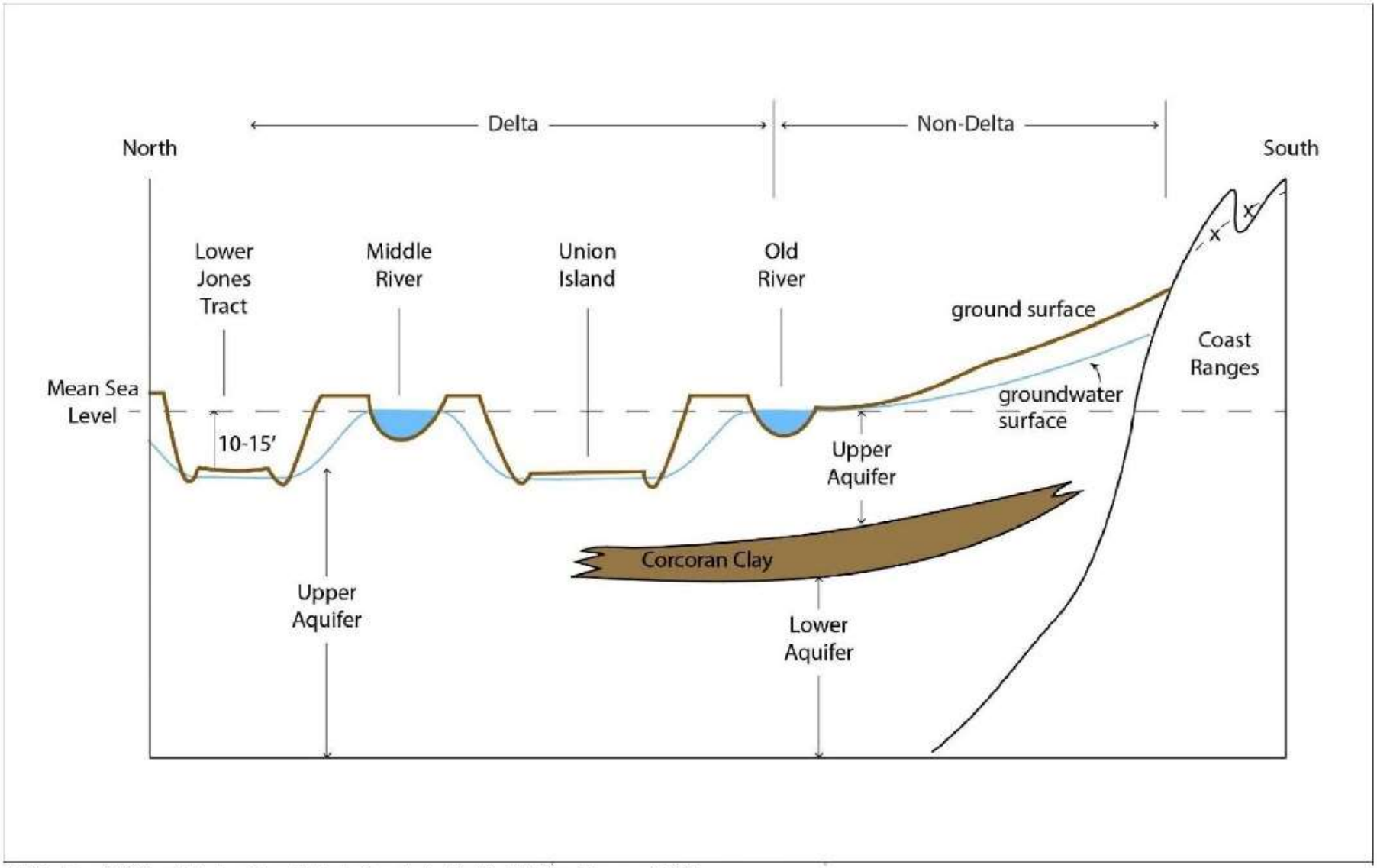

Modified from: GEI Consultants, Inc.; Tracy Subbasin Groundwater Sustainability Plan. November 1, 2021.

Figure 2.7-6. Principal Aquifer Schematic Profile

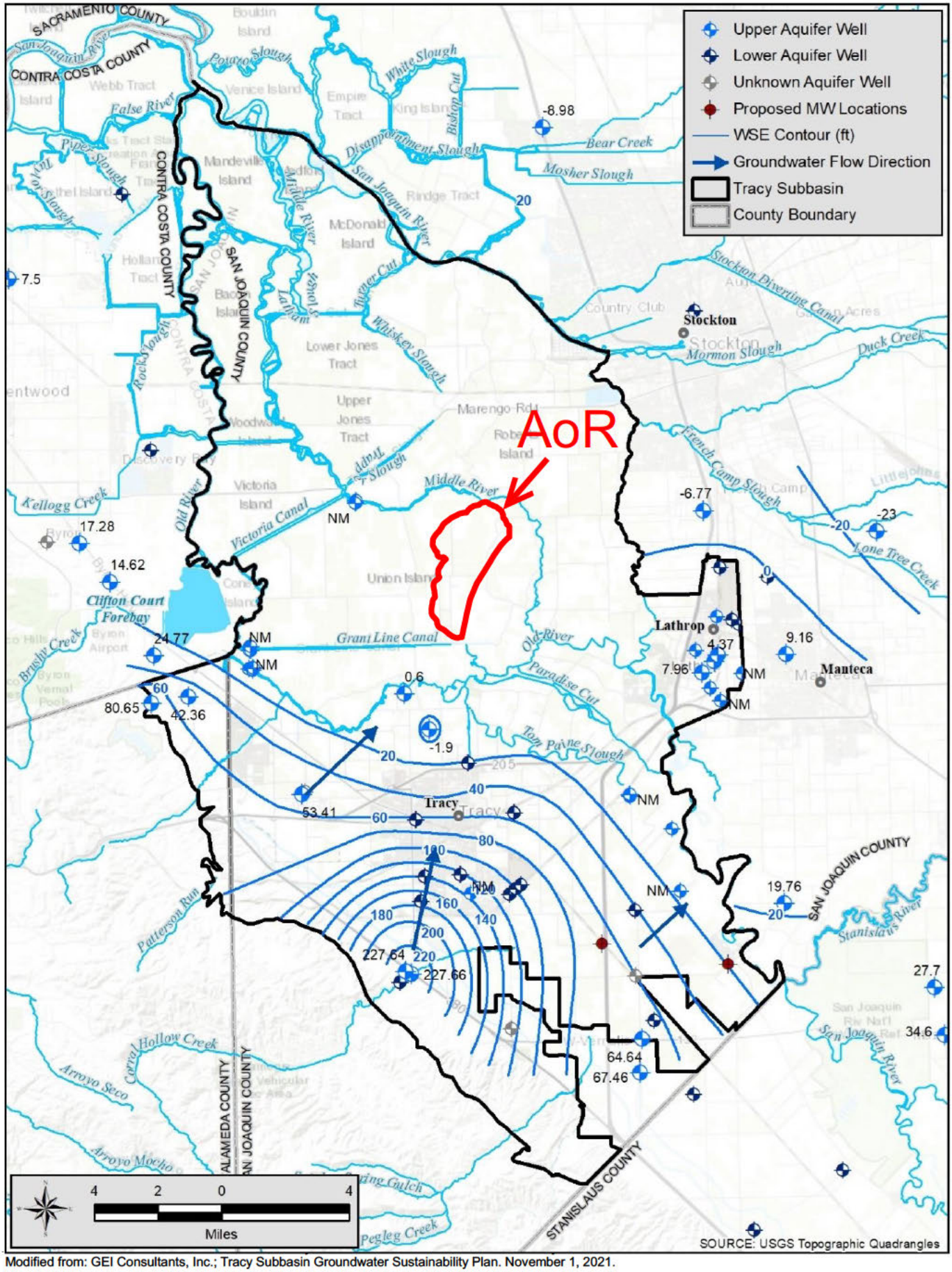

Modified from: GEI Consultants, Inc.; Tracy Subbasin Groundwater Sustainability Plan. November 1, 2021.

Figure 2.7-7 Upper Aquifer Groundwater Elevation- Fall 2019

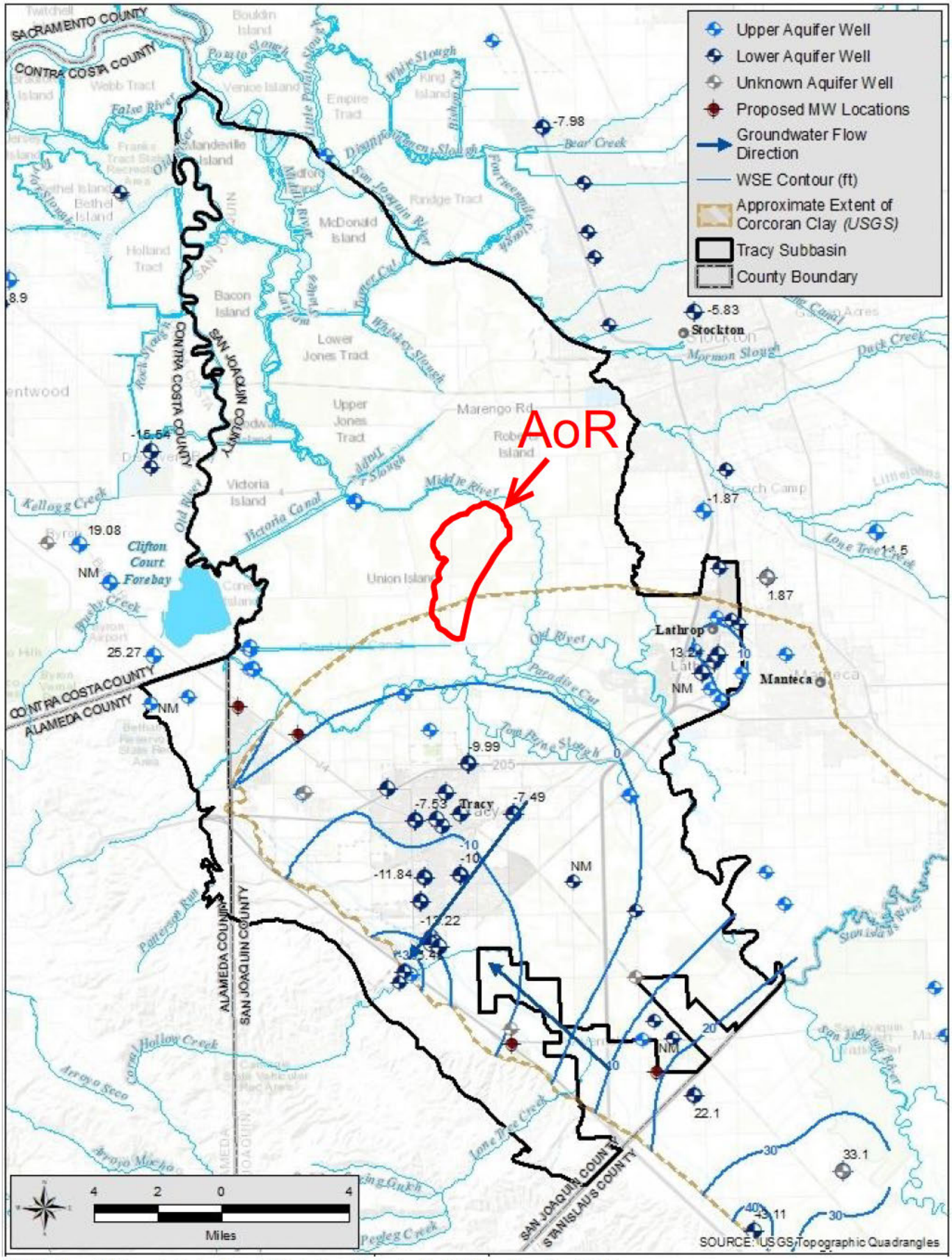

Modified from: GEI Consultants, Inc.; Tracy Subbasin Groundwater Sustainability Plan. November 1, 2021.

Figure 2.7-8 Lower Aquifer Groundwater Elevation- Spring 2019

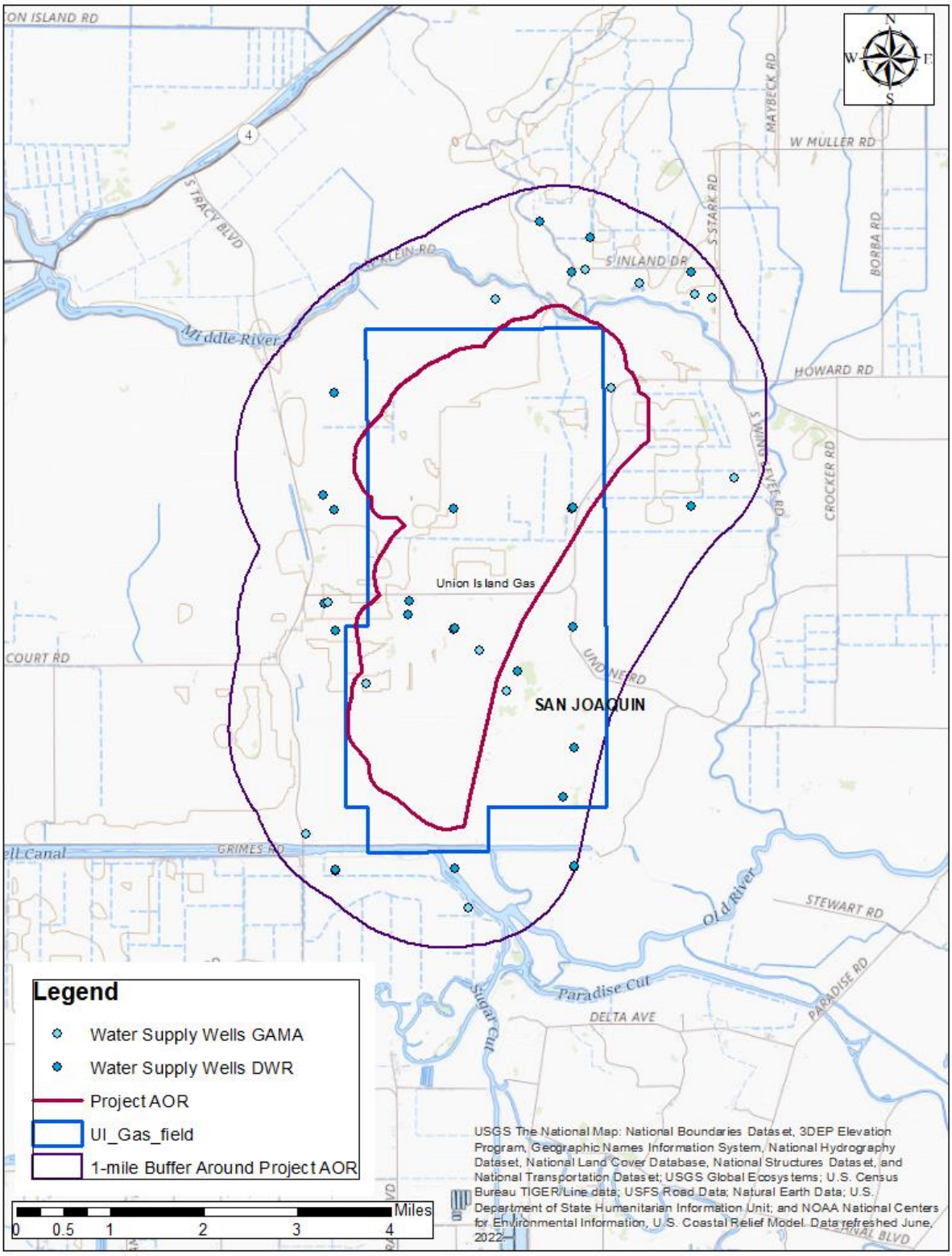

Figure 2.7-9. Water Well Location Map

BAKER HUGHES

Pacific Coast Area Laboratory
3901 Fanucchi Way
Shafter, CA. 93263

Report Date: 2/13/2015

Complete Water Analysis Report SSP v.8

Customer:	CALIFORNIA RESOURCES PROD CORP NORTH	**Sample Point Name**	Produced Water Tank
District:	West Kern	**Sample ID:**	201506004560
Sales Rep:	Christopher Haines	**Sample Date:**	1/19/2015
Lease:	Sonol	**Log Out Date:**	2/13/2015
Site Type:	Well Sites	**Analyst:**	SR/IL
Sample Point Description:	WATER TANK		

CALIFORNIA RESOURCES PROD CORP NORTH, Sonol, Produced Water Tank

Field Data

Initial Temperature (°F):	250
Final Temperature (°F):	85
Initial Pressure (psi):	100
Final Pressure (psi):	15

pH:

pH at time of sampling:	7.4

Alkalinity by Titration:	mg/L	meq/L
Bicarbonate (HCO_3^-):	1120.0	18.4
Carbonate (CO_3^{2-}):	ND	
Hydroxide (OH^-):	ND	

aqueous CO_2 (ppm):	0.0
aqueous H_2S (ppm):	0.0
aqueous O_2 (ppb):	ND
Calculated TDS (mg/L):	15595
Density/Specific Gravity (g/cm³):	1.0082
Measured Density/Specific Gravity	ND
Conductivity (mmhos):	25.3
Resistivity:	ND
MCF/D:	No Data
BOPD:	No Data
BWPD:	No Data

Analysis of Sample

Anions:	mg/L	meq/L
Chloride (Cl^-):	8243.7	232.5
Sulfate (SO_4^{2-}):	4.9	0.1
Borate (H_3BO_3):	ND	
Fluoride (F^-):	ND	
Bromide (Br^-):	ND	
Nitrite (NO_2^-):	ND	
Nitrate (NO_3^-):	ND	
Phosphate (PO_4^{3-}):	ND	
Silica (SiO_2):	66.0	

Organic Acids:	mg/L	meq/L
Formic Acid:	ND	
Acetic Acid:	ND	
Propionic Acid:	ND	
Butyric Acid:	ND	
Valeric Acid:	ND	

Anion/Cation Ratio:	0.93

Cations:	mg/L	meq/L
Sodium (Na^+):	5966.5	259.6
Potassium (K^+):	85.3	2.2
Magnesium (Mg^{2+}):	29.8	2.4
Calcium (Ca^{2+}):	118.0	5.9
Strontium (Sr^{2+}):	23.0	0.5
Barium (Ba^{2+}):	2.0	0.0
Iron (Fe^{2+}):	2.1	0.1
Manganese (Mn^{2+}):	0.1	0.0
Lead (Pb^{2+}):	ND	
Zinc (Zn^{2+}):	ND	
Aluminum (Al^{3+}):	ND	
Chromium (Cr^{3+}):	ND	
Cobalt (Co^{2+}):	ND	
Copper (Cu^{2+}):	ND	
Molybdenum (Mo^{2+}):	ND	
Nickel (Ni^{2+}):	ND	
Tin (Sn^{2+}):	ND	
Titanium (Ti^{2+}):	ND	
Vanadium (V^{2+}):	ND	
Zirconium (Zr^{2+}):	ND	
Total Hardness:	445	N/A

ND = Not Determined

Conditions		Barite ($BaSO_4$)		Calcite ($CaCO_3$)		Gypsum ($CaSO_4 \cdot 2H_2O$)		Anhydrite ($CaSO_4$)	
Temp	Press.	Index	Amt (ptb)	Index	Amt (ptb)	Index	Amt (ptb)	Index	Amt (ptb)
85°F	15 psi	-0.59	0.000	0.63	55.186	-3.46	0.000	-3.68	0.000
103°F	24 psi	-0.73	0.000	0.69	59.171	-3.46	0.000	-3.60	0.000
122°F	34 psi	-0.85	0.000	0.79	65.093	-3.45	0.000	-3.51	0.000
140°F	43 psi	-0.94	0.000	0.90	71.259	-3.43	0.000	-3.41	0.000
158°F	53 psi	-1.02	0.000	1.01	77.066	-3.41	0.000	-3.29	0.000
177°F	62 psi	-1.08	0.000	1.14	82.259	-3.38	0.000	-3.17	0.000
195°F	72 psi	-1.13	0.000	1.26	86.736	-3.35	0.000	-3.05	0.000
213°F	81 psi	-1.16	0.000	1.40	90.704	-3.32	0.000	-2.91	0.000
232°F	91 psi	-1.18	0.000	1.55	93.917	-3.28	0.000	-2.77	0.000
250°F	100 psi	-1.19	0.000	1.69	96.409	-3.24	0.000	-2.63	0.000

Conditions		Celestite ($SrSO_4$)		Halite (NaCl)		Iron Sulfide (FeS)		Iron Carbonate ($FeCO_3$)	
Temp	Press.	Index	Amt (ptb)	Index	Amt (ptb)	Index	Amt (ptb)	Index	Amt (ptb)
85°F	15 psi	-2.50	0.000	-3.10	0.000	-8.70	0.000	0.72	1.247
103°F	24 psi	-2.50	0.000	-3.12	0.000	-8.78	0.000	0.84	1.318
122°F	34 psi	-2.48	0.000	-3.13	0.000	-8.79	0.000	0.98	1.382
140°F	43 psi	-2.46	0.000	-3.14	0.000	-8.78	0.000	1.13	1.429
158°F	53 psi	-2.42	0.000	-3.14	0.000	-8.75	0.000	1.27	1.462
177°F	62 psi	-2.37	0.000	-3.14	0.000	-8.70	0.000	1.41	1.485
195°F	72 psi	-2.32	0.000	-3.13	0.000	-8.64	0.000	1.54	1.501
213°F	81 psi	-2.26	0.000	-3.12	0.000	-8.55	0.000	1.67	1.513
232°F	91 psi	-2.19	0.000	-3.11	0.000	-8.46	0.000	1.80	1.522
250°F	100 psi	-2.11	0.000	-3.10	0.000	-8.36	0.000	1.92	1.528

Note 1: When assessing the severity of the scale problem, both the saturation index (SI) and amount of scale must be considered
Note 2: Precipitation of each scale is considered separately. Total scale will be less than the sum of the amounts of the eight (8) scales.
Note 3: Saturation Index predictions on this sheet use pH and alkalinity; $\%CO_2$ is not included in the calculations.

Calculate

ScaleSoftPitzer™ SSP2010

Comments: _____

Figure 2.8-1. Water geochemistry for Sonol_Securities_4 well.

Dick Brown's Technical Service

Gas & Oilfield Measurement and Control Specialist
Design - Installation - Service

Company: CRC
Location: Sonol #5
Meter ID:
Analysis Time: 03/01/2022 15:14 Sample Type: Spot
Flowing Temp.: 80 Deg. F Flowing Pressure: 15 psig

Comp	UnNorm %	Normal %	Liquids (USgal/MCF)	Ideal (Btu/SCF)	Rel. Density
Propane	0.07668	0.07727	0.02131	1.94427	0.00118
Hydrogen Sulfide	0.00000	0.00000	0.00000	0.00000	0.00000
IsoButane	0.01738	0.01751	0.00574	0.56938	0.00035
Butane	0.02022	0.02038	0.00644	0.66485	0.00041
NeoPentane	0.00000	0.00000	0.00000	0.00000	0.00000
IsoPentane	0.01515	0.01526	0.00559	0.61062	0.00038
Pentane	0.01556	0.01568	0.00569	0.62846	0.00039
Hexane+	0.06383	0.06432	0.00000	0.00000	0.00000
Nitrogen	13.19429	13.29594	0.00000	0.00000	0.12861
Methane	84.99076	85.64405	0.00000	865.00488	0.47444
CarbonDioxide	0.20376	0.20533	0.00000	0.00000	0.00312
Ethane	0.63934	0.64426	0.17262	11.40145	0.00669
Hexane	0.00000	0.06432	0.02649	3.05896	0.00191
Heptane+	0.00000	0.00000	0.00000	0.00000	0.00000
Heptane	0.00000	0.00000	0.00000	0.00000	0.00000
Octane	0.00000	0.00000	0.00000	0.00000	0.00000
Nonane+	0.00000	0.00000	0.00000	0.00000	0.00000
Nonane	0.00000	0.00000	0.00000	0.00000	0.00000
Decane	0.00000	0.00000	0.00000	0.00000	0.00000
Undecane	0.00000	0.00000	0.00000	0.00000	0.00000
Dodecane	0.00000	0.00000	0.00000	0.00000	0.00000
Ethane-	0.00000	0.00000	0.00000	0.00000	0.00000
Propane +	0.00000	0.00000	0.00000	0.00000	0.00000
Total	99.23697	100.00000	0.24387	883.88293	0.61831

Inferior Wobbe 1109.2899 (Btu/SCF) Superior Wobbe 1128.8501 (Btu/SCF)
Compressibility 0.9983 Density 0.0473 (lbm/ft3)
Real Rel. Density 0.6183 Ideal CV 883.8829 (Btu/SCF)
Wet CV 872.2740 (Btu/SCF) Dry CV 887.4617 (Btu/SCF)
Contract Temp. 60.0000 (deg F) Contract Press. 14.7300 (psia)
Number of Cycles 2 Connected Stream 1
Atmospheric Pressure 14.73

Figure 2.8.2. Gas chromatography for the Sonol_Securities_5 well.

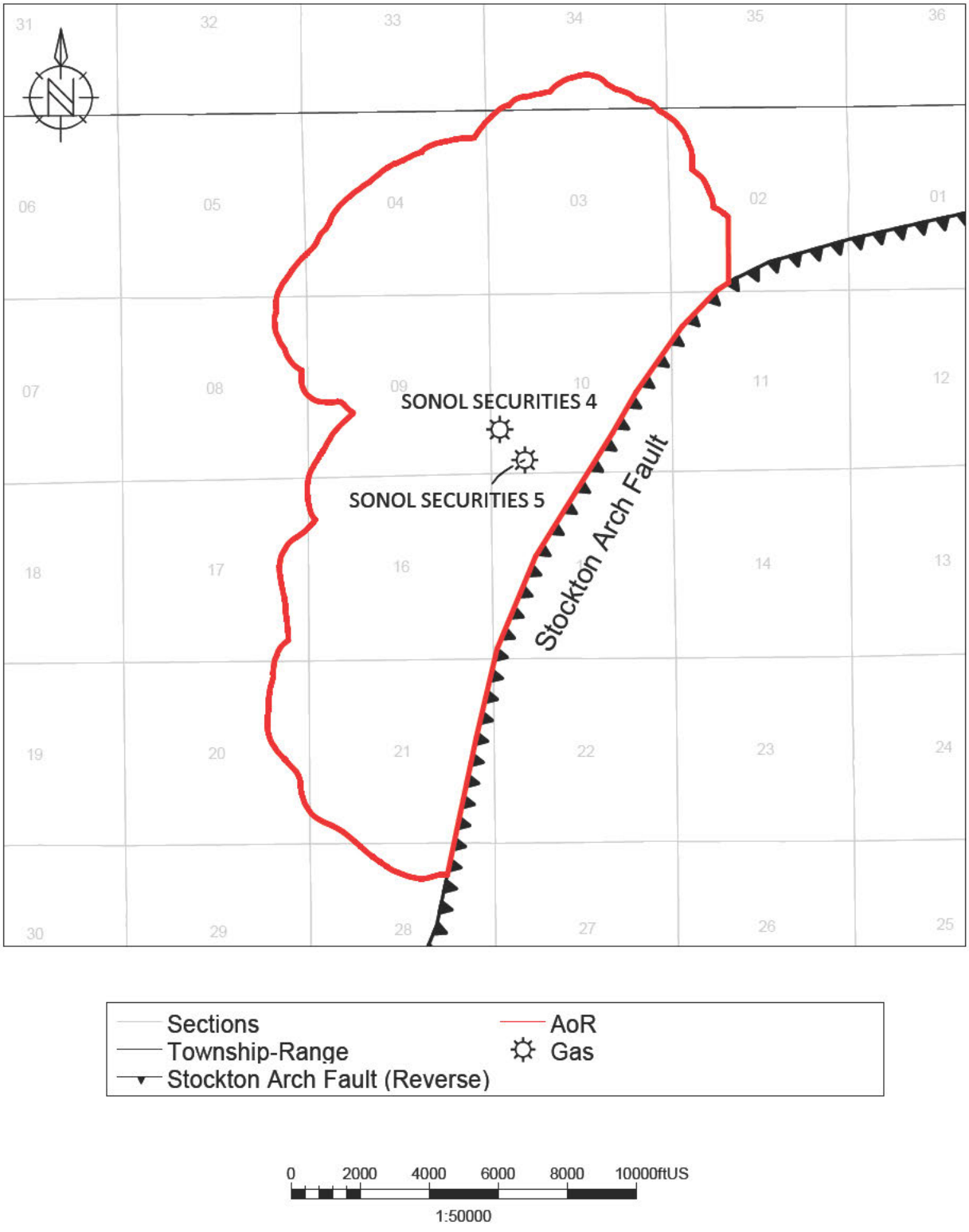

Figure 2.8-3. Location of wells with geochemistry data.

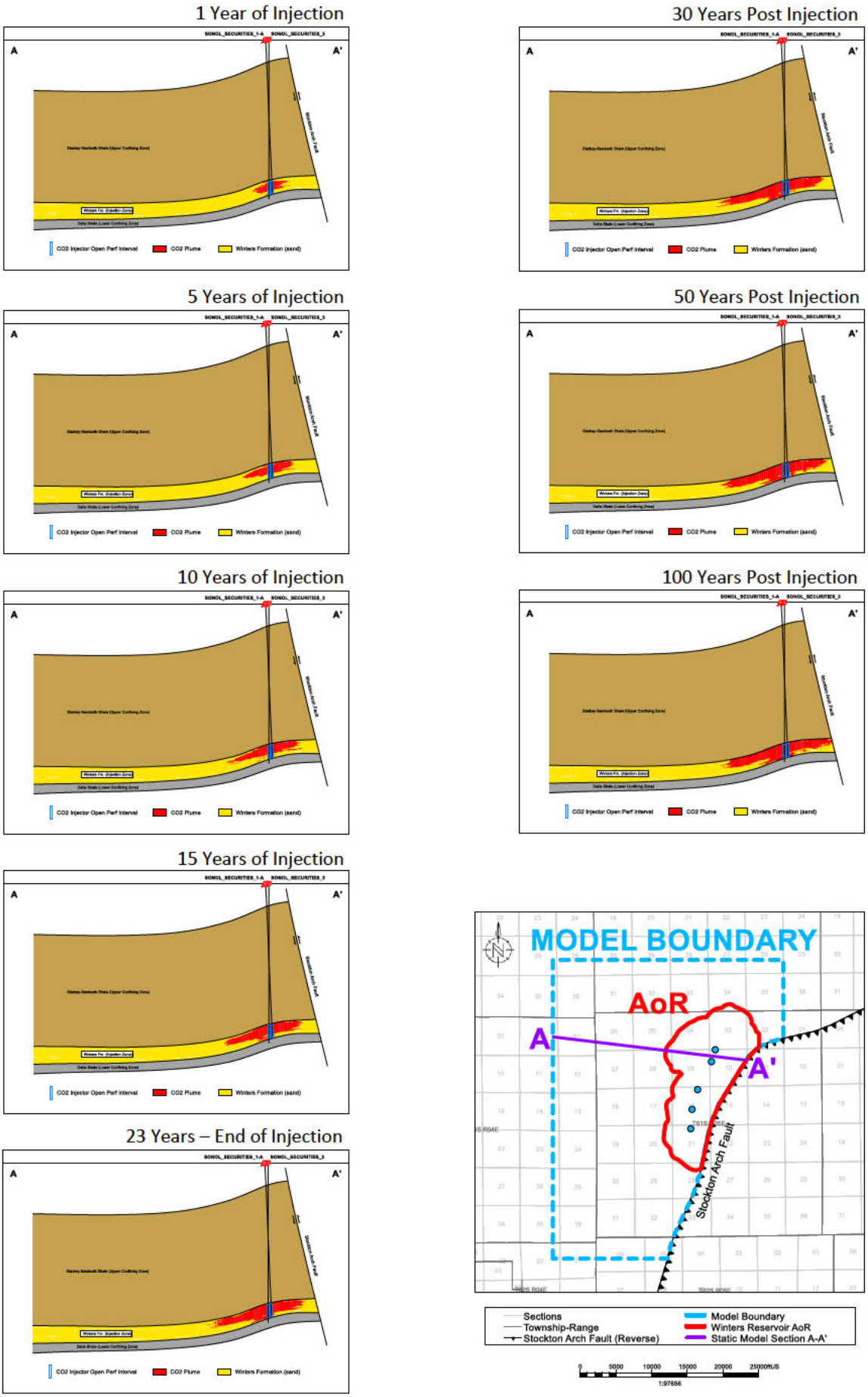

Figure 2.10-1A. Section showing proximity of CO2 (Injectate 1) to the Stockton Arch Fault and lateral dispersion of CO2 throughout time and confinement under the overlying Starkey-Sawtooth through time for the five injector modeled Base scenario. As the sections show, plume growth over time is driven by the reservoir anticlinal structure, and is thus representative of the plume growth at all injector locations.

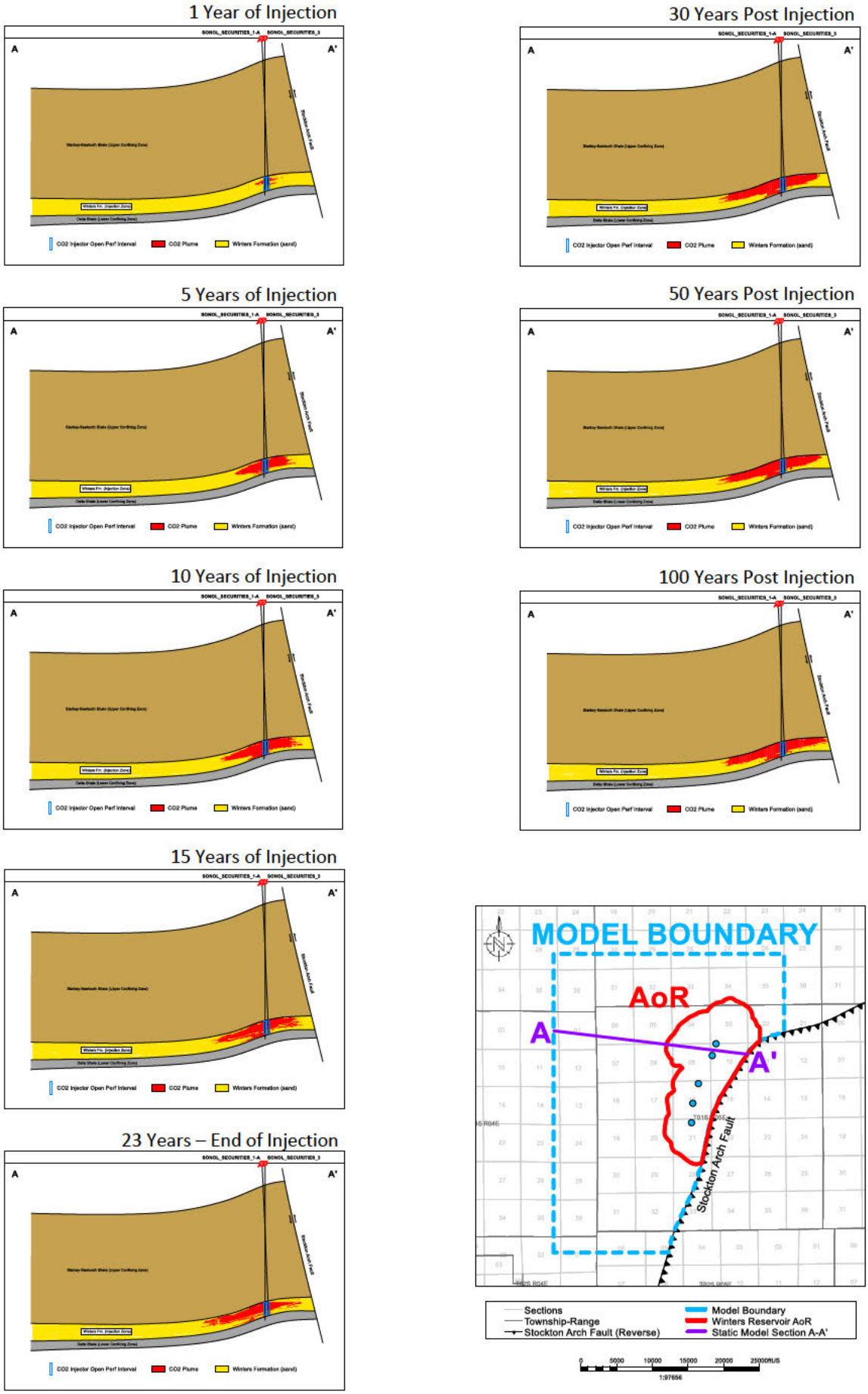

Figure 2.10-1B. Section showing proximity of CO2 (Injectate 2) to the Stockton Arch Fault and lateral dispersion of CO2 throughout time and confinement under the overlying Starkey-Sawtooth through time for the five injector modeled Base scenario. As the sections show, plume growth over time is driven by the reservoir anticlinal structure, and is thus representative of the plume growth at all injector locations.

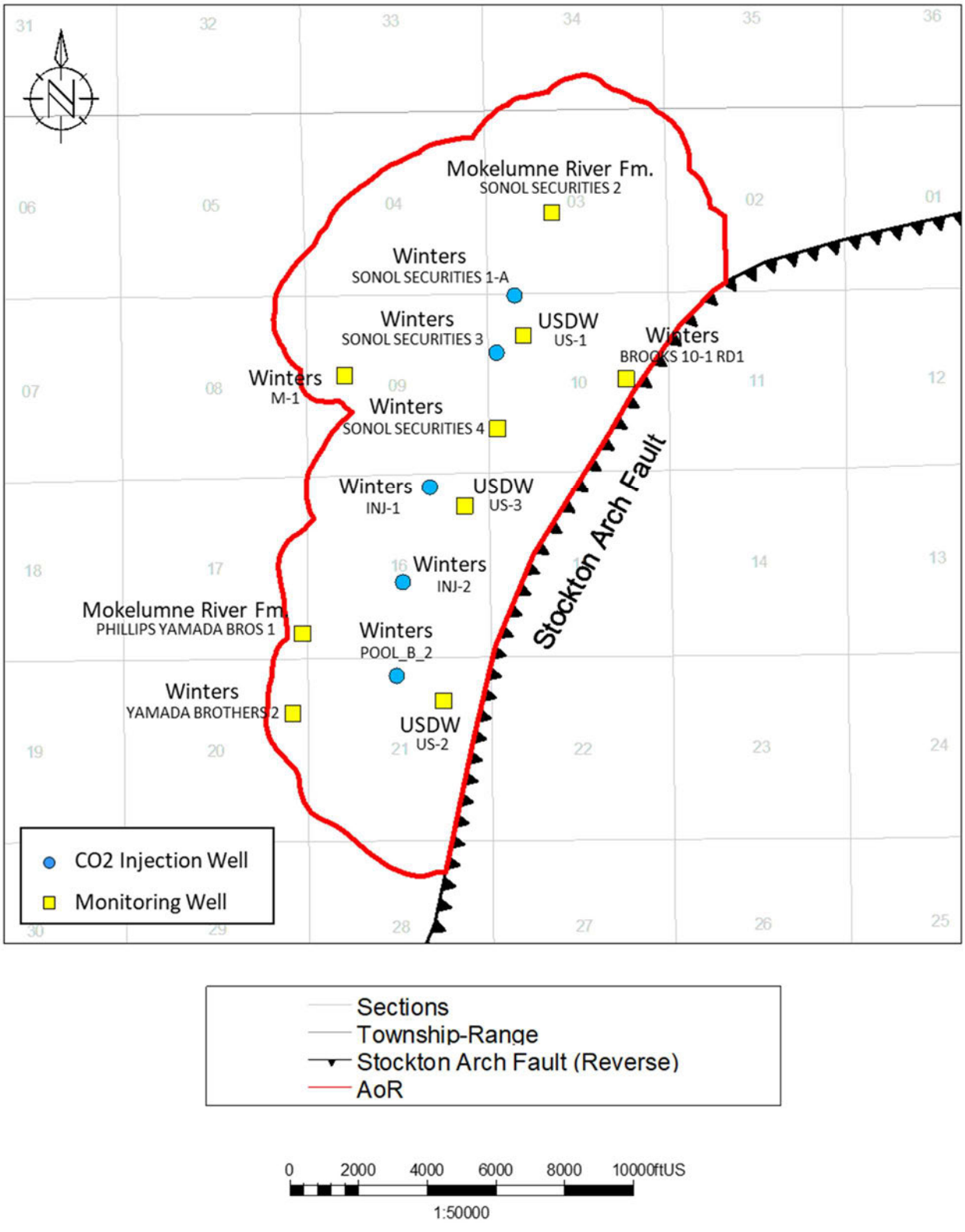

Figure 5.1. Map showing the location of injection wells and monitoring wells

NARRATIVE - TABLES

Table 2.4-1: Formation mineralogy from X-ray diffraction in GP_Dohrmann_1_RD1 and XRD and Fourier transform infrared spectroscopy (FTIR) in the Speckman_Decarli_1 well. Well locations shown in Figure 2.4-1.

Well	Zone	Depth (ft)	Quartz	Plagioclase	K-Feldspar	Calcite	Dolomite	Siderite	Barite	Glauconite	Pyrite	Kaolinite	Chlorite	Illite & Mica	Smectite	MXL I/S	Total Clay
Speckman_Decarli_1	H&TShale	8828.0	23.0	21.0	9.0	3.0	0.0			0.0	1.0	12.0	5.0			26.0	43.0
Speckman_Decarli_1	H&TShale	8830.0	30.0	17.0	11.0	0.0	0.0			0.0	4.0	3.4	14.4	6.1	14.1		38.0
Speckman_Decarli_1	H&TShale	8909.0	20.0	20.0	13.0	0.0	0.0			2.0	2.0	5.0	3.0			35.0	43.0
Speckman_Decarli_1	H&TShale	8937.0	20.0	12.0	8.0	0.0	0.0			0.0	2.0	14.0	6.0			38.0	58.0
Speckman_Decarli_1	H&TShale	8939.0	24.0	18.0	11.0	1.0	0.0			0.0	3.0	3.0	15.5	7.7	16.8		43.0
Speckman_Decarli_1	H&TShale	8940.0	23.0	29.0	12.0	0.0	0.0			0.0	0.0	4.0	5.0			27.0	36.0
Speckman_Decarli_1	H&TShale	8942.0	23.0	15.0	10.0	0.0	0.0			0.0	2.0	12.0	5.0			33.0	50.0
Speckman_Decarli_1	H&TShale	9439.0	20.0	14.0	9.0	0.0	0.0			0.0	1.0	0.0	5.0			51.0	56.0
Speckman_Decarli_1	H&TShale	9441.0	21.0	19.0	12.0	2.0	0.0			0.0	3.0	0.0	0.0			43.0	43.0
GP_Dohrmann_1_RD1	Winters	9755.1	64.0	9.0	2.0		1.0	11.0				5.0			8.0		13.0
GP_Dohrmann_1_RD1	Winters	9758.5	70.0	12.0	4.0		1.0	2.0				5.0			6.0		11.0
GP_Dohrmann_1_RD1	Winters	9762.5	28.0	8.0	3.0		1.0	1.0			1.0	21.0	2.0	2.0	33.0		58.0
GP_Dohrmann_1_RD1	Delta Shale	10073.5	69.0	13.0	5.0		1.0	1.0				3.0	1.0	1.0	6.0		11.0
GP_Dohrmann_1_RD1	Delta Shale	10077.5	30.0	7.0	2.0	1.0		3.0			1.0	17.0	5.0	2.0	32.0		56.0
GP_Dohrmann_1_RD1	Delta Shale	10082.5	70.0	13.0	3.0		1.0	1.0				3.0	2.0	2.0	5.0		12.0
GP_Dohrmann_1_RD1	Delta Shale	10090.5	51.0	8.0	2.0		1.0				2.0	8.0	4.0	3.0	21.0		36.0
GP_Dohrmann_1_RD1	Delta Shale	10096.2	72.0	13.0	3.0		1.0		1.0			3.0	1.0	2.0	4.0		10.0
GP_Dohrmann_1_RD1	Delta Shale	10070.5	69.0	14.0	4.0		1.0	1.0				4.0	1.0		6.0		11.0

Table 2.4-2: Starkey-Sawtooth Shale and Winters Formation gross thickness and depth within the AoR.

Zone	Property	Low	High	Mean
Upper Confining Zone *Starkey-Sawtooth Shale*	Thickness (feet)	2,158	2,637	2,288
	Depth (feet TVD)	7,208	7,776	7,457
Reservoir *Winters Formation Sandstone*	Thickness (feet)	120	365	256
	Depth (feet TVD)	9,492	9,995	9,713

Table 2.6-1. Data from USGS earthquake catalog for faults in the region of CTV II.

Date	Latitude	Longitude	Depth (km)	Magnitude	Last Updated	Location
10/15/2010	37.88	-121.39	14.6	3.1	1/23/2017	9 km WSW of Taft Mosswood, California
2/10/1992	37.77	-121.32	14.6	3.1	2/9/2016	8 km SSW of Lathrop, California
2/4/1991	37.81	-121.24	7.7	3.1	12/18/2016	2 km NW of Manteca, California
2/3/1991	37.82	-121.24	9.4	3.1	12/18/2016	2 km E of Lathrop, California
1/27/1980	38	-121	6	3.3	4/2/2016	8 km ESE of Linden, California
8/6/1979	37.83	-121.51	6	4.3	4/1/2016	6 km NNE of Mountain House, California
2/2/1979	37.66	-121.19	18	3.5	4/1/2016	10 km WSW of Salida, California
10/6/1976	37.61	-121.41	2.9	3.3	12/15/2016	13 km S of Tracy, California
9/5/1976	37.61	-121.41	6.5	3.5	12/15/2016	13 km S of Tracy, California
2/2/1944	37.93	-121.4	6	3.8	1/28/2016	7 km SW of Country Club, California
7/15/1866	37.7	-121.5		6	1/30/2021	Southwest of Stockton, California

Table 2.7-1: Water Supply Well Information

Data Source	WCR Number	Wells from GAMA	Legacy Log Number	Planned Use or Former Use	LAT (DWR)	LONG (DWR)	LAT & LONG Accuracy (DWR)	LAT (GAMA)	LONG (GAMA)	T	R	S	APN	Date Work Ended	Total Completed Depth	Top of Perforated Interval	Bottom of Perforated Interval	Static Water Level
DWR	WCR1953-000314	NA	39-1016	Water Supply Domestic	37.89012	-121.4081	Centroid of Section	NA	NA	01N	05E	34	NA	9/2/1953	32	22	25	NA
DWR	WCR2013-001675	NA	e0200322	Monitoring	37.89444	-121.4053		NA	NA	01N	05E	34	131-310-3	10/28/2013	85	70	80	
DWR	WCR0079890	NA			37.89012	-121.4081	Centroid of Section	NA	NA	01N	05E	34	NA	NA	NA	NA	NA	NA
DWR	WCR2013-001674	NA	e0200320	Monitoring	37.89639	-121.4131		NA	NA	01N	05E	34	131-310-2	10/30/2013	45	35	40	NA
DWR	WCR2013-001673	NA	e0200318	Monitoring	37.89639	-121.4131		NA	NA	01N	05E	34	131-310-2	10/27/2013	90	75	85	NA
DWR	WCR0256937	NA			37.89022	-121.3897	Centroid of Section	NA	NA	01N	05E	35	NA	NA	NA	NA	NA	NA
DWR	WCR1950-000581	NA	39-1018	Water Supply Domestic	37.89022	-121.3897	Centroid of Section	NA	NA	01N	05E	35	NA	6/27/1950	60	40	45	NA
DWR	WCR2001-002697	NA	736784	Water Supply Domestic	37.89022	-121.3897	Centroid of Section	NA	NA	01N	05E	35	131-320-2	10/11/2001	45	33	43	12
DWR	WCR2008-000742	NA	944033	Water Supply Domestic	37.89022	-121.3897	Centroid of Section	NA	NA	01N	05E	35	NA	9/15/2008	52	30	50	10
DWR	WCR2008-000743	NA	944034	Other Unused	37.89022	-121.3897	Centroid of Section	NA	NA	01N	05E	35	NA	9/14/2008	NA	NA	NA	NA
DWR	WCR1950-000580	NA	39-1017	Water Supply Domestic	37.89022	-121.3897	Centroid of Section	NA	NA	01N	05E	35	NA	6/14/1950	62	NA	NA	NA
DWR	WCR1974-000848	NA	98960	Water Supply Domestic	37.87549	-121.4449	Centroid of Section	NA	NA	01S	05E	5	NA	3/5/1974	70	57	67	NA
DWR	WCR0192144	NA			37.87549	-121.4449	Centroid of Section	NA	NA	01S	05E	5	NA	NA	NA	NA	NA	NA
DWR	WCR0259899	NA			37.86116	-121.4448	Centroid of Section	NA	NA	01S	05E	8	NA	NA	NA	NA	NA	NA
DWR	WCR2020-000218	NA		Water Supply Domestic	37.86301	-121.4466		NA	NA	01S	05E	8	19328022	12/12/2019	300	260	300	NA
DWR	WCR1956-000052	NA	21463	Water Supply Domestic	37.86116	-121.4448	Centroid of Section	NA	NA	01S	05E	8	NA	6/6/1956	32	NA	NA	NA
DWR	WCR1953-000317	NA	39-1173	Water Supply Domestic	37.86132	-121.4263	Centroid of Section	NA	NA	01S	05E	9	NA	4/30/1953	35	NA	NA	NA
DWR	WCR0244683	NA			37.86132	-121.4263	Centroid of Section	NA	NA	01S	05E	9	NA	NA	NA	NA	NA	NA
DWR	WCR0059123	NA	64879	Water Supply Domestic	37.86149	-121.408	Centroid of Section	NA	NA	01S	05E	10	NA	4/28/1987	60	40	60	NA
DWR	WCR2004-003467	NA	926292	Water Supply Domestic	37.86149	-121.408	Centroid of Section	NA	NA	01S	05E	10	NA	7/1/2004	55	41	51	9
DWR	WCR1991-010920	NA	433872	Water Supply Domestic	37.86139	-121.4081		NA	NA	01S	05E	10	189-210-19	9/29/1991	106	78	98	NA
DWR	WCR0218619	NA			37.86149	-121.408	Centroid of Section	NA	NA	01S	05E	10	NA	NA	NA	NA	NA	NA
DWR	WCR1987-008304	NA	64879	Water Supply Domestic	37.86149	-121.408	Centroid of Section	NA	NA	01S	05E	10	NA	4/28/1987	97	NA	NA	NA
DWR	WCR1992-009665	NA	488363	Water Supply Domestic	37.86165	-121.3896	Centroid of Section	NA	NA	01S	05E	11	189-220-11	9/23/1992	80	45	65	NA
DWR	WCR0274319	NA			37.86165	-121.3896	Centroid of Section	NA	NA	01S	05E	11	NA	NA	NA	NA	NA	NA
DWR	WCR1953-000319	NA	39-1175	Water Supply Domestic	37.86165	-121.3896	Centroid of Section	NA	NA	01S	05E	11	NA	6/1/1953	49	46	49	NA
DWR	WCR1994-005899	NA	569345	Water Supply Domestic	37.84694	-121.4079	Centroid of Section	NA	NA	01S	05E	15	189-160-9	5/30/1994	187	115	125	
DWR	WCR1952-000293	NA	39-1177	Other Unused	37.84694	-121.4079		NA	NA	01S	05E	15	NA	5/16/1952	NA	NA	NA	NA
DWR	WCR1983-001903	NA	243982	Water Supply Domestic	37.84694	-121.4079	Centroid of Section	NA	NA	01S	05E	15	NA	6/6/1983	110	NA	NA	NA
DWR	WCR2008-000103	NA	940591	Water Supply Irrigation - Agriculture	37.84694	-121.4079	Centroid of Section	NA	NA	01S	05E	15	NA	1/13/2008	85	60	80	NA
DWR	WCR0034671	NA			37.84694	-121.4079	Centroid of Section	NA	NA	01S	05E	15	NA	NA	NA	NA	NA	NA
DWR	WCR2020-006687	NA		Water Supply Domestic	37.84149	-121.4165		NA	NA	01S	05E	15	189-160-20	5/19/2020	100	80	100	12
DWR	WCR0079944	NA			37.84674	-121.4263	Centroid of Section	NA	NA	01S	05E	16	NA	NA	NA	NA	NA	NA
DWR	WCR1987-005878	NA	251137	Water Supply Irrigation - Agriculture	37.84674	-121.4263	Centroid of Section	NA	NA	01S	05E	16	NA	6/2/1987	98	NA	NA	NA
DWR	WCR1975-000098	NA	111941	Water Supply Domestic	37.84674	-121.4263	Centroid of Section	NA	NA	01S	05E	16	NA	12/1/1975	482	258	278	NA
DWR	WCR1988-007184	NA	284293	Water Supply Domestic	37.84667	-121.4264		NA	NA	01S	05E	16	NA	9/15/1988	230	NA	NA	NA
DWR	WCR2006-003520	NA	e0938241	Water Supply Domestic	37.84674	-121.4263	Centroid of Section	NA	NA	01S	05E	16	NA	11/7/2006	50	30	40	7
DWR	WCR1951-000470	NA	39-1178	Water Supply Domestic	37.84674	-121.4263	Centroid of Section	NA	NA	01S	05E	16	NA	3/20/1951	36	33	36	
DWR	WCR0020139	NA	938241	Water Supply Domestic	37.8484	-121.4335	>50 FT	NA	NA	01S	05E	16	NA	11/7/2006	40	30	40	7
DWR	WCR2020-010134	NA		Water Supply Domestic	37.85004	-121.4333	Unknown	NA	NA	01S	05E	16	189-160-140	7/21/2020	80	60	80	10
DWR	WCR1952-000294	NA	39-1179	Water Supply Domestic	37.84674	-121.4263	Centroid of Section	NA	NA	01S	05E	16	NA	10/10/1952	43	24	28	NA
DWR	WCR1954-000381	NA	21451	Water Supply Domestic	37.84674	-121.4263	Centroid of Section	NA	NA	01S	05E	16	NA	5/20/1954	39	36	39	NA
DWR	WCR1978-001522	NA	128682	Water Supply Domestic	37.84654	-121.4448	Centroid of Section	NA	NA	01S	05E	17	NA	5/18/1978	98	48	98	NA
DWR	WCR1993-006062	NA	495202	Water Supply Industrial	37.84654	-121.4448	Centroid of Section	NA	NA	01S	05E	17	NA	8/11/1993	250	130	175	NA
DWR	WCR2016-015880	NA	E0299807		37.84972	-121.4464	Unknown	NA	NA	01S	05E	17	18917005	2/4/2016	NA	NA	NA	NA
DWR	WCR1984-002263	NA	178094	Water Supply Public	37.84654	-121.4448	Centroid of Section	NA	NA	01S	05E	17	NA	7/19/1984	90	23	73	NA
DWR	WCR0316821	NA			37.84654	-121.4448	Centroid of Section	NA	NA	01S	05E	17	NA	NA	NA	NA	NA	NA
DWR	WCR1953-000321	NA	39-1180	Water Supply Domestic	37.84654	-121.4448	Centroid of Section	NA	NA	01S	05E	17	NA	4/28/1953	28	25	28	NA
DWR	WCR2016-015881	NA	E0299805		37.84972	-121.4464	Unknown	NA	NA	01S	05E	17	18917005	2/4/2016	NA	NA	NA	NA
DWR	WCR2022-009653	NA		Water Supply Domestic	37.82617	-121.4096	>50 Ft	NA	NA	01S	05E	22	189-200-060	3/24/2022	60	40	60	10
DWR	WCR1999-006661	NA	814148	Water Supply Irrigation - Agriculture	37.83219	-121.4078	Centroid of Section	NA	NA	01S	05E	22	189-200-6	1/12/1999	160	120	160	NA
DWR	WCR0089724	NA			37.81768	-121.4078	Centroid of Section	NA	NA	01S	05E	27	NA	NA	NA	NA	NA	NA
DWR	WCR1979-000974	NA	86184	Water Supply Domestic	37.81768	-121.4078	Centroid of Section	NA	NA	01S	05E	27	NA	7/1/1979	97	36	46	
DWR	WCR1952-000295	NA	39-1181	Water Supply Domestic	37.81768	-121.4078	Centroid of Section	NA	NA	01S	05E	27	NA	5/23/1952	85	74	78	NA
DWR	WCR1990-012688	NA	370320	Water Supply Domestic	37.81778	-121.4078		NA	NA	01S	05E	27	189-230-17	6/27/1990	184	NA	NA	NA
DWR	WCR1776-000538	NA	39-1182		37.81747	-121.4261	Centroid of Section	NA	NA	01S	05E	28	NA	NA	79	NA	NA	NA
DWR	WCR0045687	NA			37.81747	-121.4261	Centroid of Section	NA	NA	01S	05E	28	NA	NA	NA	NA	NA	NA
DWR	WCR1981-000061	NA	77028	Water Supply Domestic	37.81725	-121.4446	Centroid of Section	NA	NA	01S	05E	29	NA	7/2/1981	80	NA	NA	NA
DWR	WCR0118174	NA			37.81725	-121.4446	Centroid of Section	NA	NA	01S	05E	29	NA	NA	NA	NA	NA	NA
DWR	WCR1986-007552	NA	61498	Water Supply Domestic	37.81725	-121.4446	Centroid of Section	NA	NA	01S	05E	29	NA	6/1/1986	90	NA	NA	NA
DWR	WCR1999-002585	NA	715079	Water Supply Domestic	37.81725	-121.4446	Centroid of Section	NA	NA	01S	05E	29	NA	9/15/1999	67	40	60	10
DWR	WCR0173869	NA	61498	Water Supply Domestic	37.81725	-121.4446	Centroid of Section	NA	NA	01S	05E	29	NA	NA	90	55	85	10
DWR	WCR1999-002586	NA	715080	Water Supply Domestic	37.81725	-121.4446	Centroid of Section	NA	NA	01S	05E	29	NA	9/15/1999	77	60	70	12
DWR	WCR1990-012755	NA	370466	Water Supply Domestic	37.81722	-121.4447		NA	NA	01S	05E	29	189-120-13	11/4/1990	400	NA	NA	NA
DWR	WCR1985-001635	NA	150861	Water Supply Domestic	37.81725	-121.4446	Centroid of Section	NA	NA	01S	05E	29	NA	8/27/1985	172	NA	NA	NA
DWR	NA	01N05E34H001M	NA	NA	NA	NA	NA	37.8904	-121.406	01N	05E	34	NA	NA	NA	NA	NA	NA
DWR	NA	01N05E34M001M	NA	NA	NA	NA	NA	37.8868	-121.42	01N	05E	34	NA	NA	NA	NA	NA	NA

Data Source	WCR Number	Wells from GAMA	Legacy Log Number	Planned Use or Former Use	LAT (DWR)	LONG (DWR)	LAT & LONG Accuracy (DWR)	LAT (GAMA)	LONG (GAMA)	T	R	S	APN	Date Work Ended	Total Completed Depth	Top of Perforated Interval	Bottom of Perforated Interval	Static Water Level
WB_ILRP	NA	AGW080021029-TRT-JRWELL	NA	NA	NA	NA	NA	37.8888092835394	-121.397746823405	01N	05E	35	NA	NA	NA	NA	NA	NA
WB_ILRP	NA	AGW080018185-BALMATWELL	NA	NA	NA	NA	NA	37.887410206647	-121.389043828814	01N	05E	35	NA	NA	NA	NA	NA	NA
WB_ILRP	NA	AGW080021028-TRT-DDWELL	NA	NA	NA	NA	NA	37.8870142726623	-121.386370550753	01N	05E	35	NA	NA	NA	NA	NA	NA
DWR	NA	01S05E02E002M	NA	NA	NA	NA	NA	37.876	-121.402	01S	05E	2	NA	NA	NA	NA	NA	NA
DWR	NA	01S05E12D001M	NA	NA	NA	NA	NA	37.8651	-121.383	01S	05E	12	NA	NA	NA	NA	NA	NA
WB_ILRP	NA	AGW080018610-RANCHWELL1	NA	NA	NA	NA	NA	37.8440993607178	-121.422379008358	01S	05E	16	NA	NA	NA	NA	NA	NA
DDW	NA	CA3900713_001_001	NA	NA	NA	NA	NA	37.84	-121.44	01S	05E	17	NA	NA	NA	NA	NA	NA
DDW	NA	CA3900583_001_001	NA	NA	NA	NA	NA	37.84	-121.44	01S	05E	17	NA	NA	NA	NA	NA	NA
USGS_NWIS	NA	375000121260001	NA	NA	NA	NA	NA	37.8499722	-121.4457778	01S	05E	17	NA	NA	NA	NA	NA	NA
GAMA_USGS	NA	TRCY-07	NA	NA	NA	NA	NA	37.84997222	-121.44577778	01S	05E	17	NA	NA	NA	NA	NA	NA
WB_ILRP	NA	AGW080020866-PACKNGSHED	NA	NA	NA	NA	NA	37.8391188886566	-121.418215944341	01S	05E	22	NA	NA	NA	NA	NA	NA
DPR	NA	77958	NA	NA	NA	NA	NA	37.812639	-121.424143	01S	05E	28	NA	NA	NA	NA	NA	NA
WB_CLEANUP	NA	T0607700643-DW1	NA	NA	NA	NA	NA	37.8216318	-121.4491863	01S	05E	29	NA	NA	NA	NA	NA	NA

Notes:

1= all depths are based on feet below ground surface
WCR= Department of Water Resources Well Completion Report
LAT= Latitude
LONG= Longiutde
T= Township
R= Range
S= Section
APN= Assessor Parcel Number
NA= Data is not available or not applicable
GAMA= State Water Board's GAMA website

Table 2.8-1: Formation fluid properties

Formation Fluid Property	Formation Water	Formation Gas
Density, g/cm^3	1.0082	0.00076
Viscosity, cp	1.26	0.029
TDS, ppm	~15,000	NA

Table 7.1. Injectate compositions

Component	Injectate 1	Injectate 2
	Mass%	Mass%
CO2	99.213%	99.884%
H2	0.051%	0.006%
N2	0.643%	0.001%
H2O	0.021%	0.000%
CO	0.029%	0.001%
Ar	0.031%	0.000%
O2	0.004%	0.000%
SO2+SO3	0.003%	0.000%
H2S	0.001%	0.014%
CH4	0.004%	0.039%
NOx	0.002%	0.000%
NH3	0.000%	0.000%
C2H6	0.000%	0.053%
Ethylene	0.000%	0.002%
Total	**100.00%**	**100.00%**

Table 7.2. Simplified 4 component composition for Injectate 1

Injectate 1	
Component	**mass%**
CO2	99.213%
N2	0.643%
SO2+SO3	0.003%
H2S	0.001%

Injectate 2	
Component	**mass%**
CO2	99.884%
CH4	0.039%
C2H6	0.053%
H2S	0.014%

Table 7.3. Injectate properties range over project life at downhole conditions for Injectate 1 and Injectate 2

Injectate property at downhole conditions	Injectate 1	Injectate 2
Viscosity, cp	0.022 – 0.054	0.022 – 0.056
Density, lb/ft^3	9.1 - 40.6	9.1 – 41.5
Compressibility factor, Z	0.81 - 0.67	0.80 – 0.66